

~~2~~
4-19-79

LA-7663-MS

Informal Report

MASTER

**Summary Documentation of LASL
Nuclear Data Evaluations for ENDF/B-V**

University of California



LOS ALAMOS SCIENTIFIC LABORATORY

Post Office Box 1663 Los Alamos, New Mexico 87545

DISTRIBUTION OF THIS DOCUMENT IS UNLIMITED

LA-7663-MS
Informal Report

Special Distribution
Issued: January 1979

Summary Documentation of LASL
Nuclear Data Evaluations for ENDF/B-V

Compiled by
P. G. Young

NOTICE—

This report was prepared as an account of work sponsored by the United States Government. Neither the United States nor the United States Department of Energy, nor any of their employees, nor any of their contractors, subcontractors, or their employees, makes any warranty, express or implied, or assumes any legal liability or responsibility for the accuracy, completeness or usefulness of any information, apparatus, product or process disclosed, or represents that its use would not infringe privately owned rights.

LASL

DISTRIBUTION OF THIS DOCUMENT IS UNLIMITED

ley

SUMMARY DOCUMENTATION OF LASL
NUCLEAR DATA EVALUATIONS FOR ENDF/B-V

Compiled by

P. G. Young

ABSTRACT

Summaries are presented of nuclear data evaluations performed at Los Alamos Scientific Laboratory (LASL) that will comprise part of Version V of the Evaluated Nuclear Data File, ENDF/B. A total of 18 general purpose evaluations of neutron-induced data are summarized, together with 6 summaries directed specifically at covariance data evaluations. The general purpose evaluation summaries cover the following isotopes: ^{1-3}H , $^3,^4\text{He}$, $^6,^7\text{Li}$, ^{10}B , $^{14,15}\text{N}$, ^{16}O , ^{27}Al , $^{182,183,184,186}\text{W}$, ^{233}U , and ^{242}Pu . The covariance data summaries are given for ^1H , ^6Li , ^{10}B , ^{14}N , ^{16}O , and ^{27}Al .

I. INTRODUCTION

The utilization of new versions of the Evaluated Nuclear Data File, ENDF/B, which is issued through Brookhaven National Laboratory (BNL), is greatly enhanced by the availability on a timely basis of appropriate supporting documentation. Because comprehensive reports describing new evaluations are sometimes delayed in time, it has been the practice of BNL to collect shorter, summary documents from contributing evaluators and to provide this information for each new version of ENDF/B. The purpose of the present report is to provide the summary documents for evaluations performed at Los Alamos Scientific Laboratory (LASL) that will be a part of Version V of ENDF/B. This report only summarizes evaluations of general purpose or covariance files to which LASL evaluators made recent and/or significant contributions. The summaries do not cover LASL work on such special purpose files as fission-product yields, activation cross sections, gas production, etc.

II. CONTENT OF SUMMARIES

A. General Purpose Files

Summary documentation for the general purpose file evaluations is given in Appendix A. These evaluations generally cover all neutron and gamma-ray production cross sections, angular distributions, and energy distributions for

incident neutron energies in the range 10^{-5} eV to 20 MeV and may or may not include covariance data. Summaries are given for the following isotopes: ^{1-3}H , $^{3,4}\text{He}$, $^{6,7}\text{Li}$, ^{10}B , $^{14,15}\text{N}$, ^{16}O , ^{27}Al , $^{182,183,184,186}\text{W}$, ^{233}U , and ^{242}Pu .

Each of the summary documents includes a section summarizing the extent of modification of the evaluation for Version V, followed by a more detailed section that describes the major entries in each ENDF/B file for the various reaction types (MT numbers). In all cases the latter section is based upon the descriptive data in File 1 of the evaluation. For those isotopes that include neutron cross section standards, an additional section is given that summarizes the standards data in more detail. Graphical comparisons of evaluated and experimental data are included in several of the summaries.

B. Covariance Files

Additional documentation is provided in Appendix B for the covariance data (ENDF/B File 33) evaluations of ^1H , ^6Li , ^{10}B , ^{14}N , ^{16}O , and ^{27}Al . The covariance summaries provide details as to the content and limitations of the correlated error data, together with brief descriptions of the methodology used for each of the error evaluations.

ACKNOWLEDGMENTS

It is a pleasure to thank H. M. Holleman for her help in interpreting the ENDF/B narrative descriptions and in typing the summaries.

I also wish to acknowledge the various evaluators for their efforts in providing detailed narrative files, which made the present task straightforward.

APPENDIX A

**Summary Documentation of LASL Nuclear
Data Evaluations for the General Purpose
Files of ENDF/B-V**

SUMMARY DOCUMENTATION FOR ^1H

by

L. Stewart, R. J. LaBauve, and P. G. Young
Los Alamos Scientific Laboratory
Los Alamos, New Mexico

I. SUMMARY

The ^1H evaluation for ENDF/B-V (MAT 1301) is basically the same as the Version IV evaluation. Changes include the addition of correlated error data in MF=33 and different interpolation rules for MT=1 and 2 in MF=3. The evaluation covers the energy range 10^{-5} eV to 20 MeV, and documentation is provided in LA-4574 (1971) and LA-6518-MS (1976).

II. STANDARDS DATA

The $^1\text{H}(n,n)^1\text{H}$ elastic scattering cross section and angular distribution (MF=3, 4; MT=2) are standards in the energy region 1 keV - 20 MeV.

The extensive theoretical analysis of fast-neutron measurements by Hopkins and Breit¹ was used to generate the scattering cross section and angular distributions of the neutrons for the ENDF/B-V file.² The code and the Yale phase shifts³ were obtained from Hopkins⁴ in order to obtain the data on a fine-energy grid. Pointwise angular distributions were produced to improve the precision over that obtained from the published Legendre coefficients.* The phase shifts were also used to extend the energy range down below 200 keV as represented in the original paper.¹

At 100 eV, the elastic cross section calculated from the phase shifts is 20.449 barns, in excellent agreement with the thermal value of 20.442 derived by Davis and Barschall.⁵ Therefore, for the present evaluation, the free-atom scattering cross section is assumed to be constant below 100 eV and equal to the value calculated from the Yale phase shifts at 100 eV giving a thermal cross section of 20.449 b.

Total cross-section measurements are compared with the evaluation in Fig. 1 for the energy range from 10 eV to 0.5 MeV. Similarly, Figs. 2 and 3 compare the evaluation with measured data from 0.5 to 20 MeV. The agreement with the earlier experiments shown in Fig. 2 is quite good over the entire energy range. The 1969 data of Schwartz⁶ included in Fig. 3, however, lie slightly below the evaluation over most of the energy range even though agreement with the 1972 results of Clement⁷ is quite acceptable.

* For $E_n = 30$ MeV, the difference in the 180° cross section is $\sim 1\%$ as calculated from the Legendre coefficients³ compared to that calculated from the phase shifts.

Unfortunately, few absolute values of the angular dependence of the neutrons (or recoil protons) exist and even the relative measurements are often restricted to less than half of the angular range. The experiment of Oda⁸ at 3.1 MeV is not atypical of the earlier distributions which, as shown in Fig. 4, does not agree with the phase-shift predictions. Near 14 MeV, the T(d,n) neutron source has been employed in many experiments to determine the angular distributions. A composite of these measurements is compared with ENDF/B-V in Fig. 5A. Note that most of the experiments are in reasonable agreement on a relative scale, but 10% discrepancies frequently appear among the data sets. The measurements of Cambou⁹ average more than 5% lower than the predicted curve and differences of 5% or more are occasionally apparent among the data of a single set. Figure 5B shows the measurements of Calonsky¹⁰ at 17.9 MeV compared with the evaluation. Again, the agreement on an absolute basis is quite poor.

Elastic scattering angular distributions at 0.1, 5, 10, 20, and 30 MeV are provided in Ref. 11 as Legendre expansion coefficients. Using the Hopkins-Breit phase-shift program and the Yale phase shifts, additional and intermediate energy points were calculated for the present evaluation.² As shown in Figs. 5-16 of Ref. 2, the angular distributions are neither isotropic below 10 MeV nor symmetric about 90° above 10 MeV as assumed in earlier evaluations. In this evaluation, the angular distribution at 100 keV is assumed to be isotropic since the calculated 180°/0° ratio is very nearly unity, that is, 1.0011. At 500 keV, this ratio approaches 1.005. Therefore, the pointwise normalized probabilities as a function of the center-of-mass scattering angle are provided at the following energies: 10⁻⁵ eV (isotropic), 100 keV (isotropic), 500 keV, and at 1-MeV intervals from 1 to 20 MeV.

Certainly the Hopkins-Breit phase shifts reproduce reasonably well the measured angular distributions near 14 MeV. It is important, however, that experiments be made at two or three energies which would, hopefully, further corroborate this analysis. Near 14 MeV, the energy-dependent total cross section is presently assumed to be known to ~ 1% and the angular distribution to ~ 2-3%. At lower energies where the angular distributions approach isotropy, the error estimate on the angular distribution is less than 1%.

It should be pointed out that errors involved in using hydrogen as a standard depend upon the experimental techniques employed and therefore may be significantly larger than the errors placed on the standard cross section. The elastic angular distribution measurements of neutrons scattered by hydrogen, which are available today, seem to indicate that $\sigma(\theta)$ is difficult to measure with the precision ascribed to the reference standard. If this is the case, then the magnitude of the errors in the $\sigma(\theta)$ measurements might be indicative of error assignments which should be made on hydrogen flux monitors. That is, it is difficult to assume that hydrogen scattering can be implemented as a standard with much higher precision than it can be measured. Even though better agreement with many past measurements can be reached by renormalizing the absolute scales, such action may not always be warranted.

At this time, no attempt has been made to estimate the effect of errors on the energy scale in ENDF/B. It is clear, however, that a small energy shift would produce a large change in the cross section, especially at low energies. For example, a 50-keV shift in energy near 1 MeV would produce a change in the standard cross section of approximately 2½%. Therefore, precise determination of the incident neutron energy and the energy spread could be very important in employing hydrogen as a cross-section standard, depending upon the experimental technique.

III. ENDF/B-V FILES

File 1. General Information

MT=451. Descriptive data.

File 2. Resonance Parameters

MT=151. Effective scattering radius = 1.27565×10^{-12} cm.

Resonance parameters not given.

File 3. Neutron Cross Sections

MT=1. Total Cross Sections

The total cross sections are obtained by adding the elastic scattering and radiative capture cross sections at all energies, 1.0E-05 eV to 20 MeV.

MT=2. Elastic Scattering

Standard - see discussion in Sec. II.

MT=102. Radiative Capture

These cross sections are taken from the publication of A. Horsley where a value of 332 mb was adopted for the thermal value. See Ref. 51.

MT=251. Average Value of Cosine of Scattering Angle In Lab System from 1.0E-05 Ev to 20 MeV. (Provided by BNL).

MT=252. Average Logarithmic Energy Change Per Collision, from 1.0E-05 eV to 20 MeV. (Provided by BNL).

MT=253. Gamma, from 1.0E-05 eV to 20 MeV. (Provided by BNL).

File 4. Neutron Angular Distributions

MT=2. Neutron elastic scattering angular distributions in the center of mass system, given as normalized pointwise probabilities. See Sec. II above.

File 7. Thermal Neutron Scattering Law Data

MT=4. 0.00001 to 5 eV free gas sigma = 20.449 barns.

File 12. Gamma Ray Multiplicities

MT=102. Radiative Capture Multiplicities.

Multiplicity is unity at all neutron energies. LP=2 is now implemented; therefore, all gamma energies must be calculated.

File 14. Gamma Ray Angular Distributions

MT=102. Radiative capture angular distribution

Assumed isotropic at all neutron energies.

File 33. Correlated Errors

MT=1. Covariance matrix derived from MT=2, 102.

MT=2. Covariance data added for the elastic scattering by D. G. Foster, Jr. (Jan. 77).

MT=102. Covariance data for radiative capture added by P. G. Young (Nov. 7, 1978).

REFERENCES

1. J. C. Hopkins and G. Breit, "The H(n,n)H Scattering Observables Required for High Precision Fast-Neutron Measurements," Nuclear Data A 9, 137 (1971) and private communication prior to publication (1970).
2. L. Stewart, R. J. LaBauve, and P. G. Young, "Evaluated Nuclear Data for Hydrogen in the ENDF/B-II Format," LA-4574 (1971). Neither the cross sections nor the angular distributions have been changed since Version II except to add one more significant figure to the total cross section.
3. R. E. Seamon, K. A. Friedman, G. Breit, R. D. Haracz, J. M. Holt, and A. Prakash, Phys. Rev. 165, 1579 (1968).
4. J. C. Hopkins, private communication to L. Stewart (1970).
5. J. C. Davis and H. H. Barschall, "Adjustment in the n-p Singlet Effective Range," Phys. Lett. 27B, 636 (1968).
6. R. B. Schwartz, R. A. Schrack, and H. T. Heaton, "A Search for Structure in the n-p Scattering Cross Section," Phys. Lett. 30, 36 (1969).
7. J. M. Clement, P. Stoler, C. A. Goulding, and R. W. Fairchild, "Hydrogen and Deuterium Total Neutron Cross Sections in the MeV Region," Nucl. Phys. a 183, 51 (1972).
8. Y. Oda, J. Sanada, and S. Yamabe, "On the Angular Distribution of 3.1-MeV Neutrons Scattered by Protons," Phys. Rev. 80, 469 (1950).
9. F. Cambou, "Amelioration des Methods de Spectrometrie des Neutrons Rapides," Thesis - U. of Paris, CEA-N-2002 (1961).
10. A. Galonsky and J. P. Judish, "Angular Distribution of n-p Scattering at 17.9 MeV," Phys. Rev. 100, 121 (1955).
11. "ENDF/B Summary Documentation," ENDF-201, Compiled by D. Garber, (October 1975).

12. E. Melkonian, "Slow Neutron Velocity Spectrometer Studies of O₂, N₂, A, H₂, H₂O, and Seven Hydrocarbons," Phys. Rev. 76, 1950 (1949).
13. D. H. Frisch, "The Total Cross Sections of Carbon and Hydrogen for Neutrons of Energies from 35 to 490 keV," Phys. Rev. 70, 589 (1946).
14. W. D. Allen and A. T. G. Ferguson, "The n-p Cross Section in the Range 60-550 keV," Proc. Phys. Soc. (London) 68, 1077 (1955).
15. E. Bretscher and E. B. Martin, "Determination of the Collision Cross-Section of H, Deuterium, C and O for Fast Neutrons," Helv. Phys. Acta 23, 15 (1950).
16. C. E. Engleke, R. E. Benenson, E. Melkonian, and J. M. Lebowitz, "Precision Measurements of the n-p Total Cross Section at 0.4926 and 3.205 MeV," Phys. Rev. 129, 324 (1963).
17. C. L. Bailey, W. E. Bennett, T. Bergstrahl, R. G. Nuckolls, H. T. Richards, and J. H. Williams, "The Neutron-Proton and Neutron-Carbon Scattering Cross Sections for Fast Neutrons," Phys. Rev. 70, 583 (1946).
18. E. E. Lampi, G. Frier, and J. H. Williams, "Total Cross Section of Carbon and Hydrogen for Fast Neutrons," Phys. Rev. 76, 188 (1949).
19. W. E. Good and G. Scharff-Goldhaber, "Total Cross Sections for 900-keV Neutrons," Phys. Rev. 59, 917 (1941).
20. S. Bashkin, B. Petree, F. P. Mooring, and R. E. Peterson, "Dependence of Neutron Cross Sections on Mass Number," Phys. Rev. 77, 748 (1950).
21. R. E. Fields, R. L. Becker, and R. K. Adair, "Measurement of the Neutron-Proton Cross Section at 1.0 and 2.5 MeV," Phys. Rev. 94, 389 (1954).
22. C. L. Storrs and D. H. Frisch, "Scattering of 1.32 MeV Neutrons by Protons," Phys. Rev. 95, 1252 (1954).
23. D. G. Foster, Jr. and D. W. Glasgow, "Neutron Total Cross Sections, 2.5-15 MeV, Part 1 (Experimental)," Nucl. Instr. and Methods, 36, 1 (1967).
24. R. E. Fields, "The Total Neutron-Proton Scattering Cross Section at 2.5 MeV," Phys. Rev. 89, 908 (1953).
25. G. Ambrosina and A. Sorriaux, "Total Cross Section Efficiency for Carbon, Gluorine and Vanadium," Comptes Rendus 260, 3045 (1965).
26. W. H. Zinn, S. Seely, and V. W. Cohen, "Collision Cross SEctions for D-D Neutrons," Phys. Rev. 56, 260 (1939).
27. N. Nereson and S. Darden, "Average Neutron Total Cross Sections in the 3- to 12- MeV Region," Phys. Rev. 94, 1678 (1954).
28. E. M. Hafner, W. F. Hornyak, C. E. Falk, G. Snow, and T. Coor, "The Total n-p Scattering Cross Section at 4.75 MeV," Phys. Rev. 89, 204 (1953).

29. W. Sleator, Jr., "Collision Cross Sections of Carbon and Hydrogen for Fast Neutrons," *Phys. Rev.* 72, 207 (1947).
30. A. Bratenahl, J. M. Peterson, and J. P. Stoering, "Neutron Total Cross Sections in the 7- to 14-MeV Region," UCRL-4980 (1957).
31. A. H. Lasday, "Total Neutron Cross Sections of Several Nuclei at 14 MeV," *Phys. Rev.* 81, 139 (1951).
32. L. S. Goodman, "Total Cross Sections for 14-MeV Neutrons," *Phys. Rev.* 88, 686 (1952).
33. H. L. Poss, E. O. Salant, and L. C. L. Yuan, "Total Cross Sections of Carbon and Hydrogen for 14-MeV Neutrons," *Phys. Rev.* 85, 703 (1951).
34. M. Tanaka, N. Koori, and S. Shirato, "Differential Cross Sections for Neutron-Proton Scattering at 14.1 MeV," *J. Phys. Soc. (Japan)* 28, 11 (1970).
35. M. E. Battat, R. O. Bondelid, J. H. Coon, L. Cranberg, R. B. Day, F. Edeskuty, A. H. Frentrop, R. L. Henkel, R. L. Mills, R. A. Nobles, J. E. Perry, D. D. Phillips, T. R. Roberts, and S. G. Sydoriak, "Total Neutron Cross Sections of the Hydrogen and Helium Isotopes," *Nucl. Phys.* 12, 291 (1959).
36. J. C. Allred, A. H. Armstrong, and L. Rosen, "The Interaction of 14-MeV Neutrons with Protons and Deuterons," *Phys. Rev.* 91, 90 (1953).
37. C. F. Cook and T. W. Bonner, "Scattering of Fast Neutrons in Light Nuclei," *Phys. Rev.* 94, 651 (1954).
38. H. L. Poss, E. O. Salant, G. A. Snow, and L. C. L. Yuan, "Total Cross Sections for 14-MeV Neutrons," *Phys. Rev.* 87, 11 (1952).
39. P. H. Bowen, J. P. Scanlon, G. H. Stafford, and J. J. Thresher, "Neutron Total Cross Sections in the Energy Range 15 to 120 MeV," *Nucl. Phys.* 22, 640 (1961).
40. J. M. Peterson, A. Bratenahl, and J. P. Stoering, "Neutron Total Cross Sections in the 17- to 29-MeV Range," *Phys. Rev.* 120, 521 (1960).
41. D. E. Groce and B. D. Sowerby, "Neutron-Proton Total Cross Sections Near 20, 24, and 28 MeV," *Nucl. Phys.* 83, 199 (1966).
42. M. L. West II, C. M. Jones, and H. B. Willard, "Total Neutron Cross Sections of Hydrogen and Carbon in the 20-30 MeV Region," ORNL-3778, 94 (1965).
43. R. B. Day, R. L. Mills, J. E. Perry, Jr., and F. Schreb, "Total Cross Section for n-p Scattering at 20 MeV," *Phys. Rev.* 114, 209 (1959).
44. R. B. Day and R. L. Henkel, "Neutron Total Cross Sections at 20 MeV," *Phys. Rev.* 92, 358 (1953).

45. M. E. Remley, W. K. Jentschke, and P. G. Kruger, "Neutron-Proton Scattering Using Organic Crystal Scintillation Detectors," Phys. Rev. 89, 1194 (1953).

46. J. D. Seagrave, "Recoil Deuterons and Disintegration Protons from the n-d Interaction, and n-p Scattering at $E_n = 14.1$ MeV," Phys. Rev. 97, 757 (1955).

47. S. Shirato and K. Saitchi, "On The Differential Cross Section for Neutron-Proton Scattering at 14.1 MeV," J. Phys. Soc. (Japan) 36, 331 (1974).

48. T. Nakamura, "Angular Distribution of n-p Scattering at 14.1 MeV," J. Phys. Soc. (Japan) 15, 1359 (1960).

49. A. Suhami and R. Fox, "Neutron-Proton Small Angle Scattering at 14.1 MeV," Phys. Lett. 24, 173 (1967).

50. I. Basar, "Elastic Scattering of 14.4 MeV Neutrons on Hydrogen Isotopes," Few Body Problems Light Nuclei/Nucl. Interactions, Brela, 867 (1967).

51. A. Horsley, "Neutron Cross Sections of Hydrogen in the Energy Range 0.0001 eV-20 MeV," Nucl. Data A2, 243 (1966).

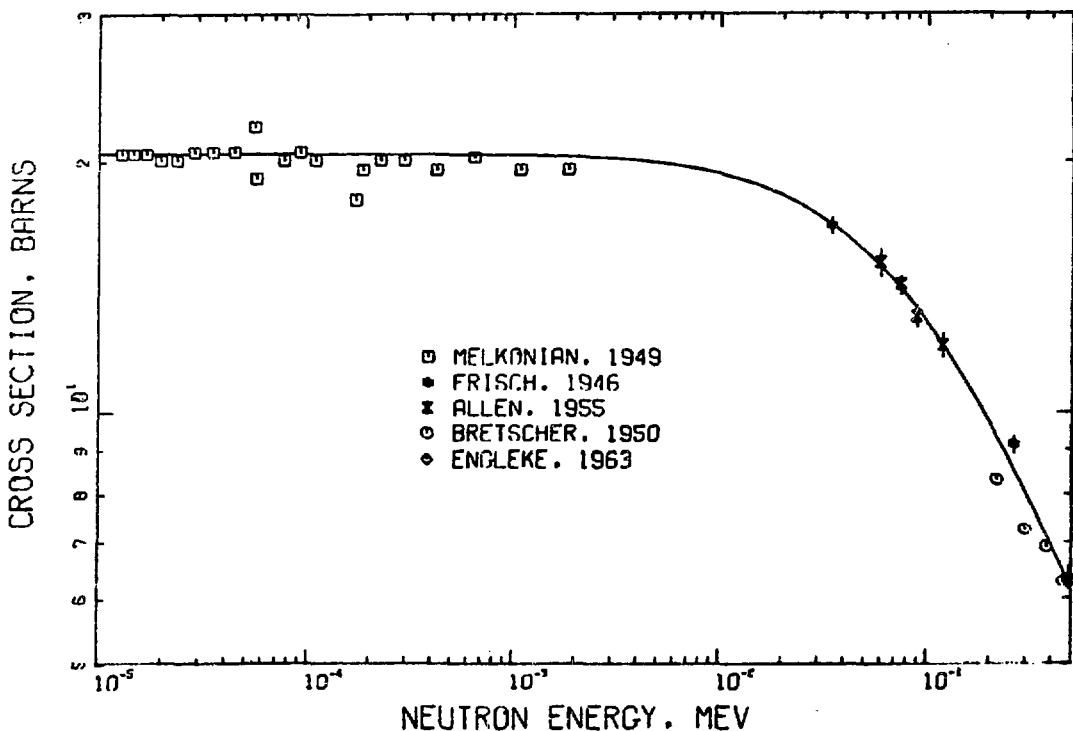


Fig. 1.
Total cross section for hydrogen from 1×10^{-5} eV to 500 keV. The ENDF/B-V evaluation is compared to the measurements of Refs. 12-16.

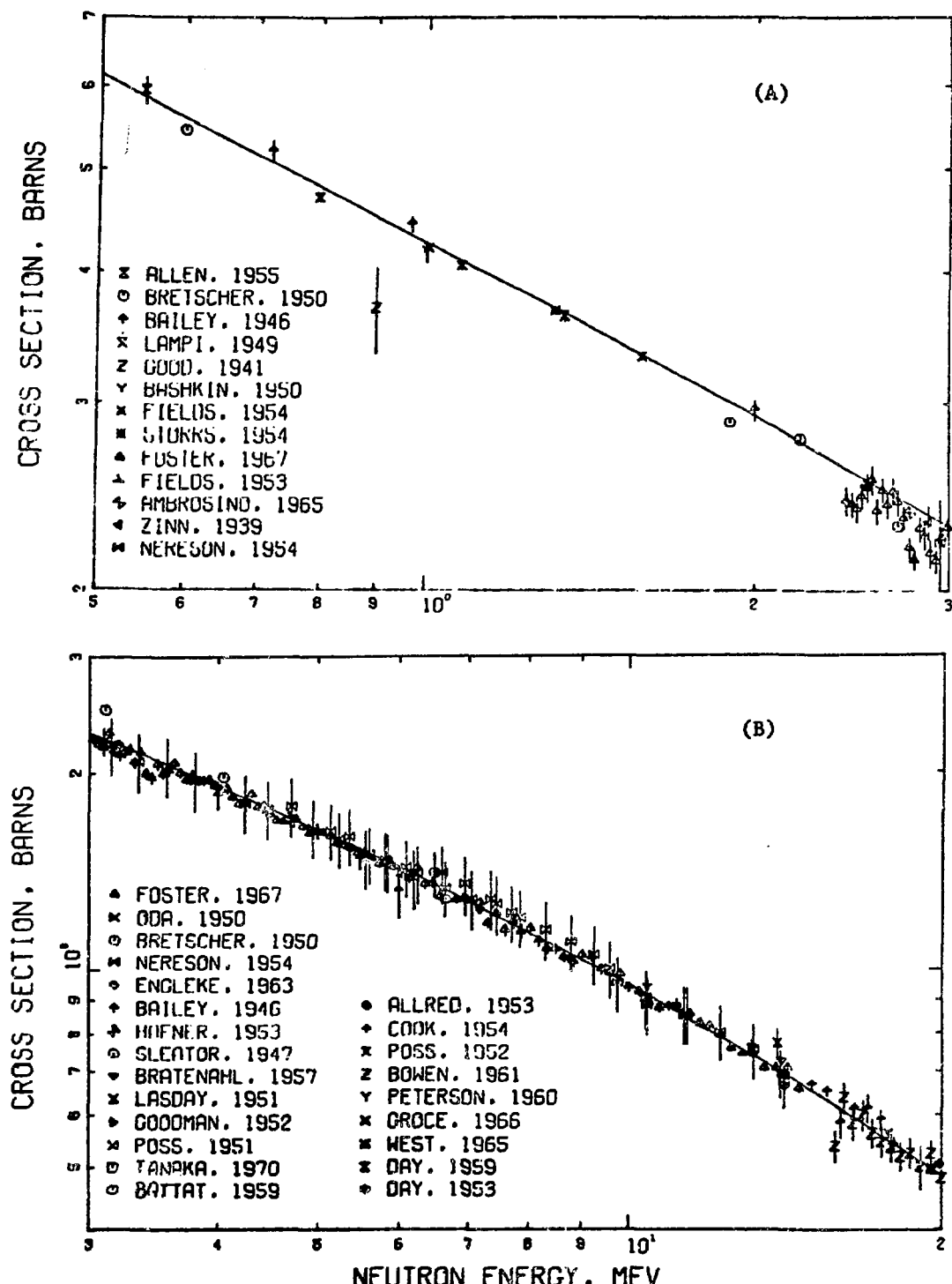


Fig. 2.
Total cross section for hydrogen from 500 keV to 20 MeV. The ENDF/B-V evaluation is compared to measurements reported in Refs. 8, 14-44.

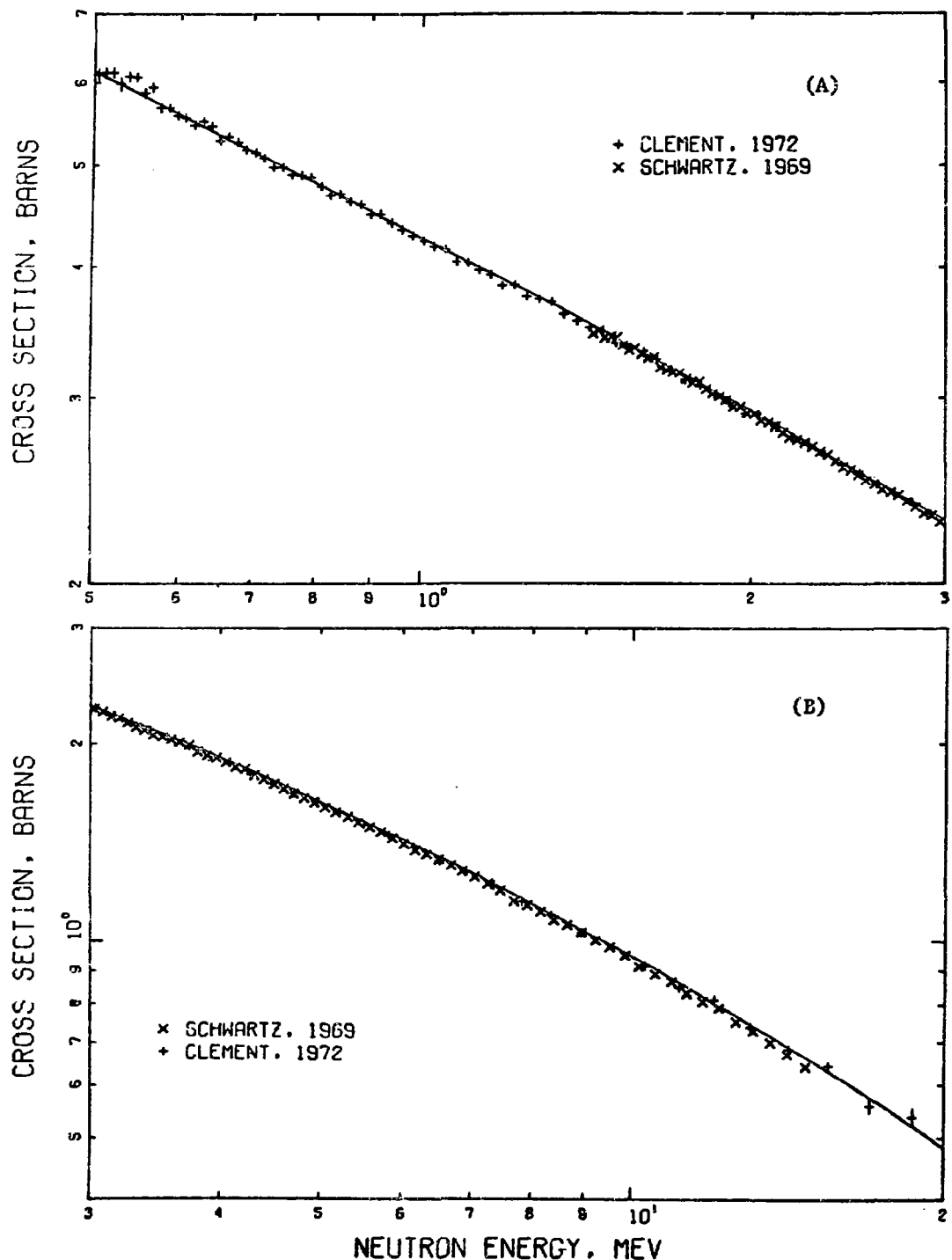


Fig. 3.
Total cross section for hydrogen from 500 keV to 20 MeV. The ENDF/B-V evaluation is compared to measurements reported in Refs. 6 and 7.

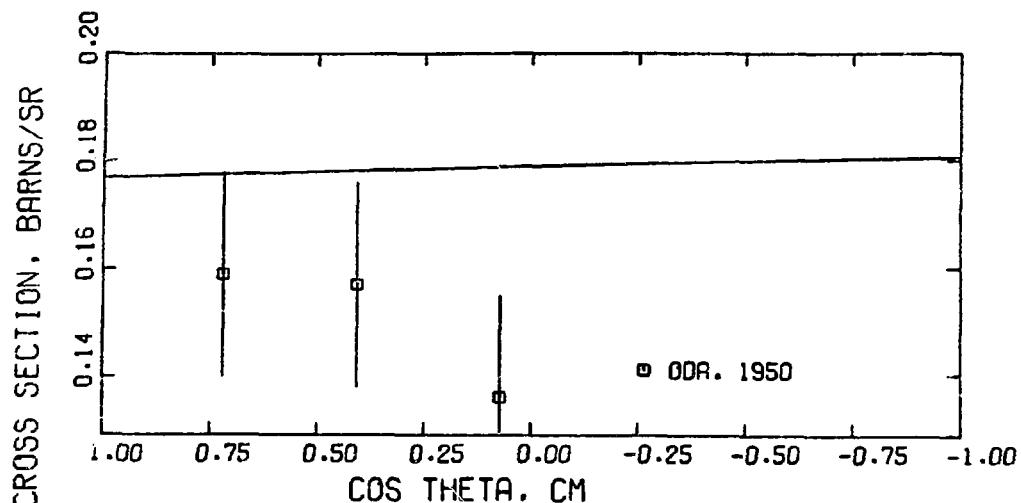


Fig. 4.
Angular distribution of the neutrons elastically scattered from hydrogen at 3.1 MeV. ENDF/B-V is compared with the experimental values of Oda.⁸

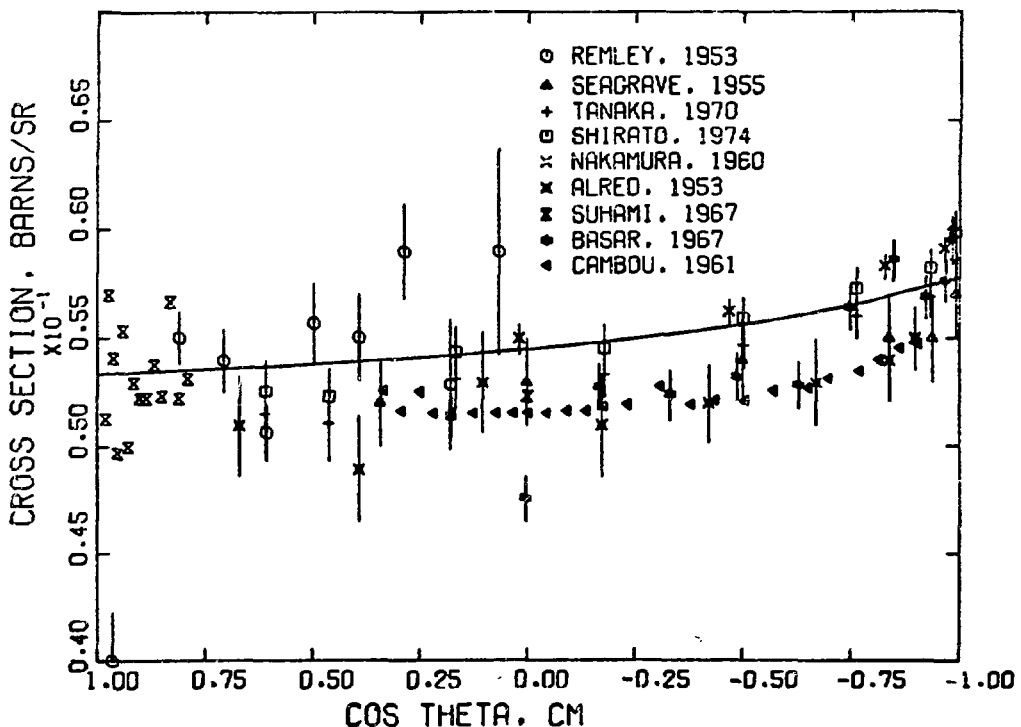


Fig. 5A.
Angular distribution of the neutrons elastically scattered from hydrogen at energies near 14 MeV. The experimental data shown were reported in Refs. 9, 34, 36 and 45-50.

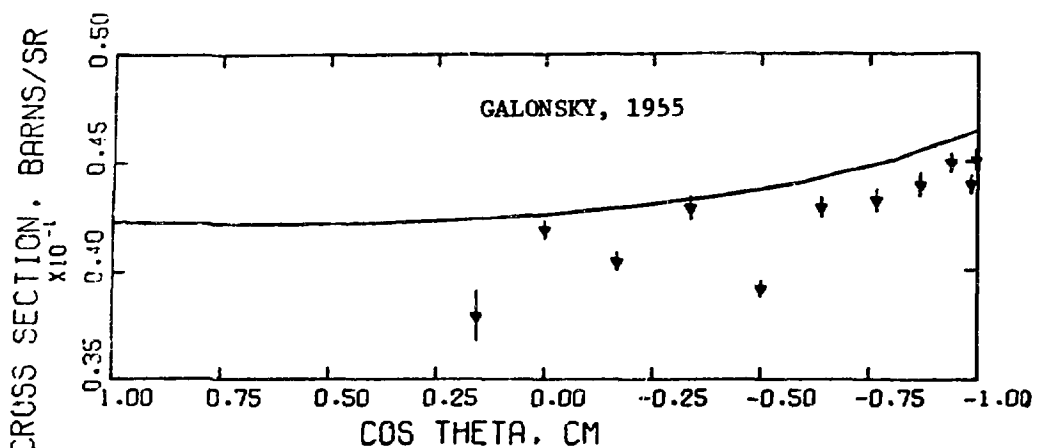


Fig. 5B.
Angular distribution of the neutrons elastically scattered from hydrogen at energies near 17.8 MeV. The experimental data shown were reported in Ref. 10.

SUMMARY DOCUMENTATION FOR ^2H

by

L. Stewart and A. Horsley
Los Alamos Scientific Laboratory
Los Alamos, New Mexico

I. SUMMARY

The ENDF/B-V evaluation (MAT=1302) is entirely different from the Version IV data set and is based upon a revision of an earlier evaluation given in LA-3271 (1968). The main change made to the earlier evaluation was to modify the total and elastic cross sections below 500 keV in order to more closely reflect experimental data from RPI.¹ In addition, Files 8 and 9 have been included to provide tritium production information. The evaluation covers the energy range 10^{-5} eV to 20 MeV.

II. ENDF/B-V FILES

File 1. GENERAL INFORMATION

MT-451. Descriptive data.

File 2. Resonance Parameters

MT=151. Effective scattering radius = 0.51977×10^{-12} cm. Resonance parameters not given.

File 3. Neutron Cross Sections

MT=1. Total Cross Section

All data plotted and compared up to 1967 in LA-3271. Changes incorporated below 1.5 MeV but evaluation does not agree with low-energy experiments at NBS² (which are preliminary) but agrees at higher energies. The Davis data³ show a peculiar drop of a few per cent from 3.5 to 9 MeV but agree above and below these energies.

MT=2. Elastic Cross Sections

Data obtained from integrating n-D and p-D angular distributions. Since the radiative capture is in microbarns, the elastic is

[†]Atomic Weapons Research Establishment, Aldermaston, U.K.

essentially equal to the total cross section below the $n,2n$ threshold and the total minus the $n,2n$ above the threshold. Checks and balances were always made. See LA-3271 for the graphical comparisons.

MT=16. ($n,2n$) Cross Section

Data taken from Holmberg⁴ and from Catron.⁵ See LA-3271. Nothing is known about the cross section above 14 MeV.

MT=102. Radiative Capture Cross Section

The thermal cross section is 506 microbarns which was extrapolated as $1/V$ up to 1 keV. Curve was drawn above this energy to include measurements on the inverse reaction by Bösch.⁶ The 14 MeV value is a factor of 3 lower than Cerineo.⁷ See LA-3271 for graphical results.

File 4. Neutron Angular Distributions

MT=2. Elastic Angular Distributions

Taken from n -D and p -D scattering. Agreement is good with van Oers analysis.⁸ See LA-3271.

MT=16. ($n,2n$) Angular Distributions

Calculated by code of Young⁹ assuming phase space argument, therefore ignoring the observations of the virtual deuteron. See LA-3271 for comparisons with n -D and p -D breakup spectra.

File 5. Neutron Energy Distributions

MT=16. ($n,2n$) Energy Distribution

Discussed under MF=4. Energy distributions calculated assuming pure phase space model.

File 8, 9. Decay Data

MT=102. Decay Information Added For Tritium Production

File 12. Gamma Ray Multiplicities

MT=102. (n,γ) Multiplicity

Assumed a single gamma emitted at all energies. Employed the LP=2 flag to conserve energy.

File 14. Gamma Ray Angular Distributions

MT=102. (n,γ) Angular Distribution

Assumed isotropic.

REFERENCES

1. P. Stoler, N. N. Kaushal, F. Green, E. Harms, and L. Laroze, Phys. Rev. Lett. 29, 1745 (1972).
2. R. B. Schuartz, National Bureau of Standards personal communication (1977).
3. J. C. Davis and H. H. Barschall, Phys. Rev. C3, 1798 (1971).
4. M. Holmberg and J. Hansen, IAEA Conference on Nuclear Data, "Microscopic Cross Sections and Other Data Basis for Nuclear Reactors," Paris, October 17-21, 1966, paper CN-23/18.
5. H. C. Catron, M. D. Goldberg, R. W. Hill, J. M. LeBlanc, J. P. Stoering, C. J. Taylor, and M. A. Williamson, Phys. Rev. 123, 218 (1961).
6. R. Bösch, J. Lang, R. Müller, and Wölfl, Phys. Lett. 8, 120 (1964).
7. M. Cerineo, K. Ilakovac, I. Slaus, and P. Tomas, Phys. Rev. 124, 1947 (1961).
8. W. T. H. van Oers and K. W. Brockman, Jr., Nucl. Phys. 21, 189 (1960).
9. P. G. Young, Los Alamos Scientific Laboratory, personal communication (1977).

SUMMARY DOCUMENTATION FOR ^3H

by

L. Stewart
Los Alamos Scientific Laboratory
Los Alamos, New Mexico

I. SUMMARY

The ENDF/B-V evaluation for ^3H (MAT=1169) is identical to the Version IV evaluation except for the transfer of the decay data from File 1 to File 8. Gamma-ray production data are not included because the radiative capture and (n, n') cross sections are assumed to be negligibly small at all energies. The evaluation covers the energy range 10^{-5} eV to 20 MeV and is documented in LA-3270 (1965).

II. ENDF/B-V FILES

File 1. General Information

MT-451. Descriptive data.

File 2. Resonance Parameters

MT=151. Effective scattering radius = 0.32164×10^{-12} cm. Resonance parameters not given.

File 3. Neutron Cross Sections

MT=1. Total Cross Sections

Total cross sections from 290 keV to 20 MeV from LASL measurements (Ref. 1). Estimated below 290 keV.

MT=2. Elastic Scattering Cross Section

Data taken from measurements (Refs. 2 to 10) up to 1967 on n-T and p-He³ systems. Also, recent measurements on n-T by Seagrave et al. (Ref. 11) and on p-He³ by Morales and Cahill (Ref. 12) and by Hutson et al. (Ref. 13) have been used to update the elastic angular distributions above 15 MeV. (February 1971) (this is the only change made to the evaluation from that described in LA-3270).

MT=16. (n,2n) Cross Section

Only one measurement exists, that of Mather and Pain (Ref. 14) at 14.1 MeV. Estimates of this cross section were therefore made from systematics and the p-He³ reaction studies of Rosen and Leland (Ref. 9) and of Anderson (Ref. 15).

MT=17. (n,3n) Cross Section

No data given since estimates from isospin considerations give essentially zero probabilities. Mather and Pain (Ref. 14) and Cookson (Ref. 16) confirm these estimates.

MT=102. (n, γ) Cross Section (not included)

The measured cross section is less than or equal to 6.7 microbarns at thermal (the sign of the Q-value is uncertain). This cross section is therefore assumed zero at all energies.

MT=251. Average Value of the Scattering Angle in the Laboratory System from 1.0E-05 eV to 20 MeV

MT=252. Average Logarithmic Energy Change Per Collision, From 1.0E-05 eV to 20 MeV

MT=253. Gamma, From 1.0E-05 eV to 20 MeV

File 4. Neutron Angular Distributions

MT=2. Elastic Angular Distributions

These are given in the center-of-mass system as normalized probabilities versus cosine of the scattering angle.

MT=16. (n,2n) Angular Distributions

These are given in the laboratory system as normalized probabilities versus cosine of the scattering angle. See LA-3270 for details on these distribution functions.

File 5. Neutron Energy Distributions

MT=16. (n,2n) Energy Distributions

These are given as normalized probabilities versus energy of the outgoing neutron in the laboratory system. See LA-3270 for details on these distribution functions.

File 8. Decay Data

MT=457. Decay Data Provided by C. Reich (INEL), Based On Chart Of Nuclides, Wapstra's Mass Tables, and Nuclear Data Tables. Placed in ENDF File and Format by BNL and LASL.

Files 12 - 15. Gamma Ray Data (not included)

Only radiative capture produces gamma rays. Since the capture cross section is assumed zero at all energies, these files are purposely left empty.

REFERENCES

1. Los Alamos Physics and Cryogenics Groups, Nucl. Phys. 12, 291 (1959).
2. J. D. Seagrave et al., Phys. Rev. 119, 1981 (1960).
3. J. H. Coon et al., Phys. Rev. 81, 33 (1951).
4. T. B. Clegg et al., Nucl. Phys. 50, 621 (1964).
5. W. Haeberli et al., Phys. Rev. 133, 81178 (1964).
6. J. E. Brolley, Jr., et al., Phys. Rev. 117, 1307 (1960). Data at back angles at which He^3 particles were observed were ignored in this analysis.
7. R. H. Lovberg, Phys. Rev. 103, 1393 (1956).
8. R. A. Vanetsian and E. D. Fedchenko, Sov. J. of Atomic Energy, Trans. 2, 141 (1957), and K. P. Artemov, S. P. Calinin and L. H. Samoilov, JETP 10, 474 (1960). The latter data were not used, since they covered the 5- to 10-MeV energy region and were not available.
9. L. Rosen and W. T. Leland, Wash-1064 (EANDC(US)-79U) (Oct. 1966), p. 99.
10. D. Blanc, F. Cambou, M. Niel, and G. Vedrenne, J. De Physique, Supplement Fasc. 3-4, C1-98 (1966).
11. J. D. Seagrave et al., LA-DC-12954 (1971).
12. J. R. Morales and T. A. Cahill, Bull. Am. Phys. Soc. 14, 554 (1969), and private communication.
13. R. L. Hutson et al., Phys. Rev. 4, C17 (1971).
14. D. S. Mather and L. F. Pain, AWRE 047/69 (1969).
15. John D. Anderson, private communication 1965, and Anderson et al., Phys. Rev. Lett. 15, 66 (1965).

SUMMARY DOCUMENTATION FOR ^3He

by

L. Stewart
Los Alamos Scientific Laboratory
Los Alamos, New Mexico

I. SUMMARY

The ^3He evaluation for ENDF/B-V (MAT=1146) was carried over intact from Version IV. The evaluated data cover the energy range 10^{-5} eV to 20 MeV, and documentation for the standards portion of the data is given in LA-6518-MS (1976).

II. STANDARDS DATA

The $^3\text{He}(n,p)T$ cross section (MF=3; MT=103) is recognized as a standard in the neutron energy range from thermal to 1 MeV. The present evaluation was performed in 1968 and accepted by the CSEWG Standards Subcommittee for the ENDF/B-III file¹ in 1971. No changes have been recommended for this file; therefore, the present evaluation was carried over from both Versions III and IV of ENDF/B.

The thermal cross section of 5327 b was derived from precise measurements by Als-Nielsen and Dietrich² of the total cross section up to an energy of 11 eV. No experimental measurements on the $^3\text{He}(n,p)$ reaction are available below ~ 5 keV, and the cross section was assumed to follow $1/v$ up to 1.7 keV. The evaluation is compared with the available data below 10 keV in Fig. 1. For convenience, the inset includes tabular values of the elastic, (n,p) and total cross sections at a few energies up to 1 keV.

Up to 10 keV, the evaluation is a reasonable representation of the 1966 results of Gibbons and Macklin³ and an average of their cross sections measured in 1963.⁴ These experiments, which extend to 100 keV, are compared with ENDF/B-V in Fig. 2.

From 100 keV to 1 MeV, additional experiments are available. The evaluation is heavily weighted by the data of Refs. 3 and 4 and the cross sections of Perry et al.⁵ as given in Fig. 3. Note that these three measurements are in good agreement among themselves but are higher than the measurements of Batchelor et al.⁶ and of Sayres et al.⁷ On the other hand, Sayres et al. measure an elastic cross section much higher than reported by Seagrave et al.⁸ (noted on the same figure).

In 1970, Costello et al.⁹ measured the (n,p) cross section from 300 keV to 1 MeV and obtained essentially a constant value of 900 mb over this energy range. Agreement of the Costello data with this evaluation above 500 keV is excellent, although from 300 to 400 keV, their measurements are more than 10% lower than ENDF/B-V.

Finally, Lopez et al.¹⁰ measured the relative ratio of the counting rates between ³He and BF₃ proportional counters from 218 eV to 521 keV. To provide a comparison between these two standard cross sections, the Lopez ratios were normalized at 218 eV to the Version IV ratios. Then, by using the present evaluation for the ³He(n,p) cross section to convert the Lopez ratio measurements to ¹⁰B cross sections, reasonable agreement with Version V ¹⁰B(n, α) is obtained. It should be noted, however, that the energy points are too sparse above a few keV to reproduce the structure observed in ¹⁰B.

Although the thermal (n,p) cross section is known to better than 1%, the energy at which this cross section deviates from 1/V is not well established. It should also be emphasized that experiments have not been carried out from 11 eV to a few keV, thereby placing severe restrictions upon the accuracy accompanying the use of the ³He(n,p)T cross-section standard. The 10% error estimates on the ORNL experimental data are directly related to the uncertainties in the analysis of the target samples employed. Certainly, further absolute measurements are needed on this cross-section standard, especially above \sim 100 eV.

III. ENDF/B-V FILES

File 1. General Information

MT=451. Descriptive data.

File 2. Resonance Parameters

MT=151. Scattering length = 0.2821E-12 cm.

File 3. Neutron Cross Sections

MT=1. Total Cross Sections

From 0.00001 eV to 10.8 keV MT1 taken as sum MT2 + MT103. From 10.8 keV to 20.0 MeV MT1 evaluated using experimental data from Ref. 11.

MT=2. Elastic Scattering Cross Sections

From 0.00001 eV to 10.8 keV MT2 taken as constant = 1.0 b. From 10.8 keV to 20.0 MeV MT2=MT1-MT103-MT104 with experimental data from Refs. 7 and 8 as checks. Note that two reactions are missing from the evaluation, namely, (n,n'p) and (n,2n2p). Experimental data at 15 MeV indicate non-zero cross sections for these reactions. In the present evaluation, these reactions are simply absorbed in MT=2.

MT=3. (n,p) Cross Section

Standards reaction - see Sec. II above.

MT=104. (n,d) Cross Sections

Threshold = 4.3614 MeV, Q = -3.2684 MeV. Evaluation from a detailed balance calculation (Ref. 2) and experimental data (Ref. 7).

MT=251. Average Value of Cosine Of Elastic Scattering Angle, Laboratory System.

Obtained from data MF=4, MT=2.

MT=252. Values Of Average Logarithmic Energy Decrement

Obtained from data MF=4, MT=2.

MT=253. Values Of Gamma

Obtained from data MF=4, MT=2.

File 4. Neutron Angular Distributions

MT=2. Angular Distribution Of Secondary Neutrons From Elastic Scattering.

Evaluated from experimental data from Refs. 7, 8, 11-14 covering incident energies as follows:

<u>INCIDENT ENERGY</u>	<u>REFERENCES</u>
1.E-5 eV	(Isotropic)
0.5 MeV	(Isotropic)
1.0 MeV	8
2.0 MeV	8
2.6 MeV	11
3.5 MeV	8
5.0 MeV	11
6.0 MeV	8, 12 (from p+t elastic scattering)
8.0 MeV	7, 12 (from p+t elastic scattering)
14.5 MeV	12, 13 (from p+t elastic scattering)
17.5 MeV	7
20.0 MeV	11 (from p+t elastic scattering)

REFERENCES

1. This evaluation was translated by R. J. LaBauve into the ENDF/B format for Version III.
2. J. Als-Nielsen and O. Dietrich, "Slow Neutron Cross Sections for He³, B, and Au," Phys. Rev. 133, B 925 (1964).
3. J. H. Gibbons and R. L. Macklin, "Total Neutron Yields from Light Elements under Proton and Alpha Bombardment," Phys. Rev. 114, 571 (1959).
4. R. L. Macklin and J. H. Gibbons, Proceedings of the International Conference on the Study of Nuclear Structure with Neutrons, Antwerp, 19-23 July 1965 (North-Holland Publishing Co., 1966), p. 498.
5. J. E. Perry, Jr., E. Haddad, R. L. Henkel, G. A. Jarvis, and R. K. Smith, private communication 1960.

6. R. Batchelor, R. Aves, and T. H. R. Skyrme, "Helium-3 Filled Proportional Counter for Neutron Spectroscopy," *Rev. Sci. Instr.* 26, 1037 (1955).
7. A. R. Sayres, K. W. Jones, and C. S. Wu, "Interaction of Neutrons with He^3 ," *Phys. Rev.* 122, 1853 (1961).
8. J. D. Seagrave, L. Cranberg, and J. E. Simmons, "Elastic Scattering of Fast Neutrons by Tritium and He^3 ," *Phys. Rev.* 119, 1981 (1960).
9. D. G. Costello, S. J. Friesenhahn, and W. M. Lopez, " $^3\text{He}(n,p)\text{T}$ Cross Section from 0.3 to 1.16 MeV," *Nucl. Sci. Eng.* 39, 409 (1970).
10. W. M. Lopez, M. P. Fricke, D. G. Costello, and S. J. Friesenhahn, "Neutron Capture Cross Sections of Tungsten and Rhenium," Gulf General Atomic, Inc. report GA-8835.
11. Los Alamos Physics and Cryogenics Groups, *Nucl. Phys.* 12, 291 (1959).
12. J. E. Brolley, Jr., T. M. Putnam, L. Rosen, and L. Stewart, *Phys. Rev.* 159, 777 (1967).
13. B. Antolkovic, G. Paic, P. Tomas, and R. Rendic, *Phys. Rev.* 159, 777 (1967).
14. L. Rosen and W. Leland, *Private communication* (1967).

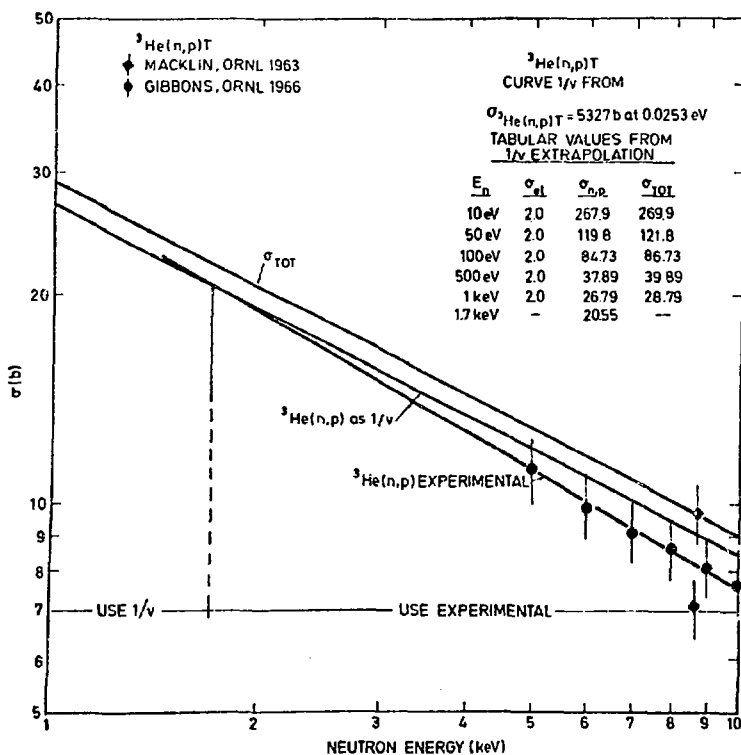


Fig. 1.

The (n,p) and total cross sections for ^3He from 1 to 10 keV. The curve drawn through the experimental points deviates from $1/V$ at 1.7 keV.

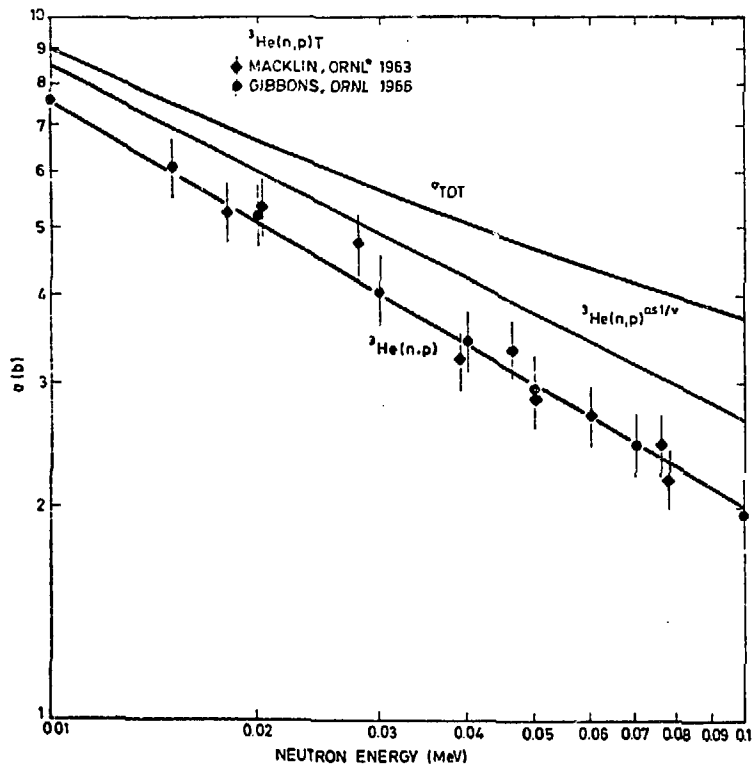


Fig. 2.
The (n,p) and total cross sections for ${}^3\text{He}$ from 10 to 100 keV.

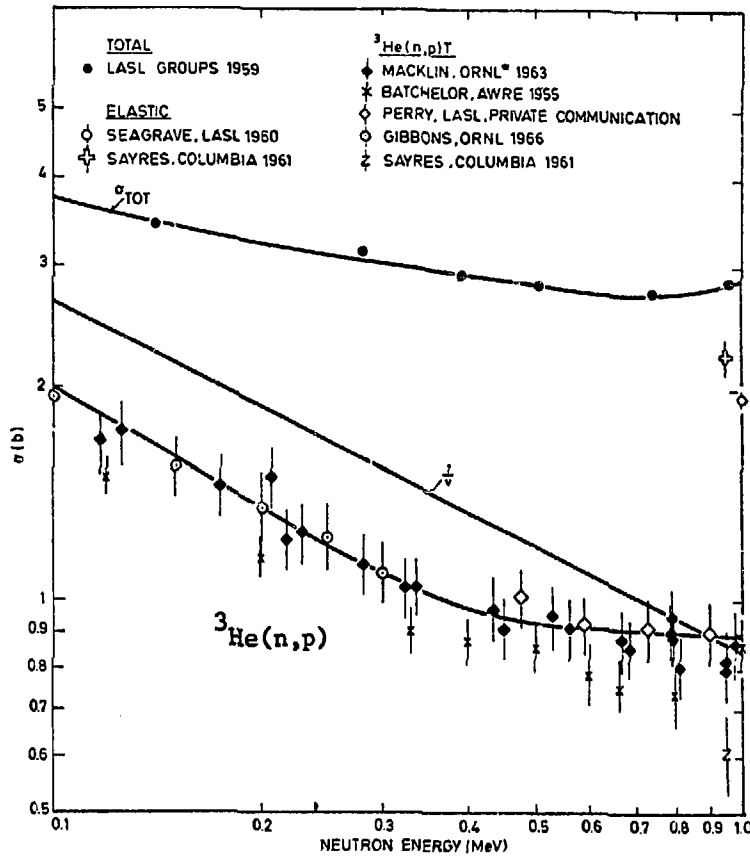


Fig. 3.
The (n,p) , elastic, and total cross sections for ${}^3\text{He}$ from 100 keV to 1 MeV. The Costello data⁹ have been omitted for the sake of clarity.

SUMMARY DOCUMENTATION FOR ${}^4\text{He}$

by

G. M. Hale, R. A. Nisley, and P. G. Young
Los Alamos Scientific Laboratory
Los Alamos, New Mexico

I. SUMMARY

The ENDF/B-V evaluation for ${}^4\text{He}$ (MAT 1270) is the same as Version IV except for minor format changes. The evaluation covers the energy range 10^{-5} eV to 20 MeV and is based at all energies on an extensive R-matrix analysis, which is described in NEANDC (J) 38L (reference Do75). By making use of the charge symmetry of nuclear forces, p- ${}^4\text{He}$ data were included in the analysis along with the available n- ${}^4\text{He}$ measurements of cross sections, angular distributions, and polarizations. Because of the extent of the data base used and the careful analysis it was given, the cross sections and angular distributions are thought to be accurate to about $\pm 2\%$ at all energies. As all gamma-ray production cross sections are essentially zero for ${}^4\text{He}$, gamma ray files (MF=12-16) are deliberately excluded from the evaluation.

II. ENDF/B-V FILES

File 1. General Information

MT=451. Descriptive data.

File 2. Resonance Parameters

MT=151. Effective scattering radius = 0.24579×10^{-12} cm.

Resonance parameters not given.

File 3. Neutron Cross Sections

The 2200 m/s cross sections are as follows:

MT=1 Sigma = 0.75916 b
MT=2 Sigma = 0.75916 b

MT=1. Total Cross Section

See discussion under MT=2 below.

MT=2. Elastic Scattering Cross Section

Although the only reaction possible for neutrons incident on ${}^4\text{He}$ below 20 MeV is elastic scattering, the majority of the $n-{}^4\text{He}$ data is rather imprecise. In order to overcome this problem, an R-matrix analysis was performed with a data set which included not only the $n-{}^4\text{He}$ data but also very precise $p-{}^4\text{He}$ data. All the available $n-{}^4\text{He}$ and $p-{}^4\text{He}$ data below 20 MeV were considered in the analysis. Since the previous evaluation was completed in 1968, several $n-{}^4\text{He}$ elastic scattering measurements have been done. The most significant of these are the low energy neutron cross sections of Rorer (Ro69), the RPI total cross section measurement (Go73), which cover the range $E_n = 0.7-30$ MeV, and the relative angular distributions of Morgan (Mo68). A complete list of references for the $n-{}^4\text{He}$ data used is given below. The $p-{}^4\text{He}$ data was selected to satisfy very stringent statistical criteria and we believe the possible errors of the predicted values for the $p-{}^4\text{He}$ scattering to be less than 1.0%. A simple model for the charge differences between the $n-{}^4\text{He}$ and $p-{}^4\text{He}$ systems was assumed and the $n-{}^4\text{He}$ and $p-{}^4\text{He}$ data sets were simultaneously analyzed. The values of the cross sections and angular distributions contained in Files 3 and 4 are probably accurate to within 2.0%.

Comparisons of the evaluated and experimental total cross section data are given in Figs. 1-4, and the elastic angular distribution data are included in Figs. 5-11. The neutron polarization measurements that were included in the R-matrix analysis are also shown in Figs. 12 and 13.

File 4. Neutron Angular Distributions

MT=2. Elastic Scattering Angular Distributions.

Obtained from the R-matrix analysis described above under MF=3, MT=2. Legendre polynomial representation used in the cm system. See Figs. 5-11 for data.

REFERENCES

Au62 S. M. Austin et al., Phys. Rev. 126, 1532 (1962).
Br72 W. B. Broste et al., Phys. Rev. C5, 761 (1972).
Bu66 F. W. Busser et al., Nucl. Phys. 88, 593 (1966).
Cr72 D. S. Cramer and L. Cranberg, Nucl. Phys. A180, 273 (1972).
Do75 D. C. Dodder, G. M. Hale, R. A. Nisley, K. Witte, and P. G. Young, Proc. of the EANDC Topical Discussion on "Critique of Nuclear Models and Their Validity in the Evaluation of Nuclear Data," Mar. 1974, p. 1. (Published in NEANDC (J) 38L (1975).
Fa63 U. Fasoli and G. Zago, Nuovo Cimento 30, 1169 (1963).
Go73 C. A. Coupling et al., Nucl. Phys. A215, 253 (1973).
Ho66 B. Hoop, Jr. and H. H. Barschall, Nucl. Phys. 83, 65 (1966).
Je66 R. W. Jewell et al., Phys. Rev. 142 687 (1966).

Ma63 T. H. May et al., Nucl. Phys. 45, 17 (1963) (Rev. Mo68 and Sa68).
Mo68 G. L. Morgan and R. L. Walker, Phys. Rev. 168, 1114 (1968).
Ni71 A. Niiler et al., Phys. Rev. C4, 36 (1971) (Rev. 9-72).
Ro69 D. C. Rorer et al., Nucl. Phys. 133, 410 (1969).
Sa68 J. R. Sawers et al., Phys. Rev. 168, 1102 (1968).
Se53 J. D. Seagrave, Phys. Rev. 92, 1222 (1953).
Sh55 D. F. Shaw, Proc. Phys. Soc. (London) 68, 43 (1955).
Sh64 R. E. Shamu and J. G. Jenkins, Phys. Rev. 135, B99 (1964).
Sm54 J. R. Smith, Phys. Rev. 95, 730 (1954).
St70 T. Stammbach et al., Phys. Rev. C2, 434 (1970).
Wh57 R. E. White and F. J. M. Farley, Nucl. Phys. 3, 476 (1957).
Yo63 P. G. Young et al., Aust. J. Phys. 16, 185 (1963).

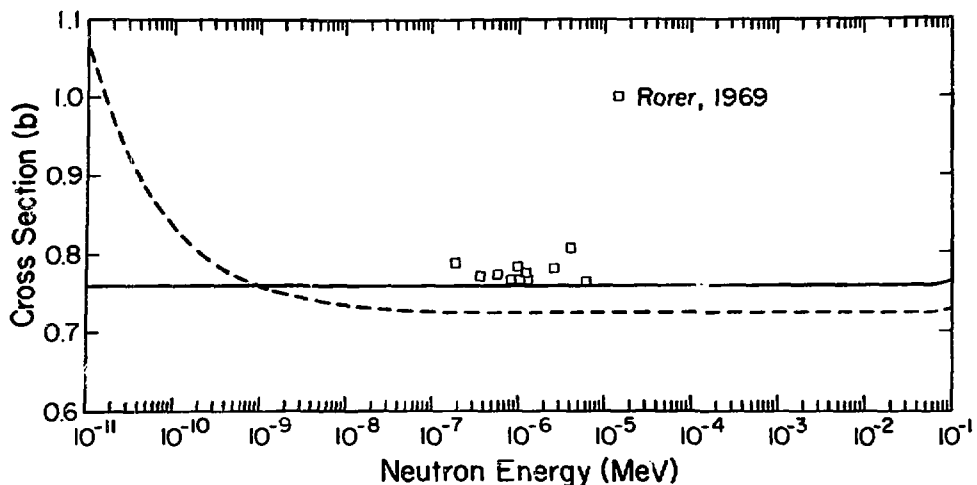


Fig. 1.

Measured and evaluated $n-^2\text{He}$ total cross sections between 10^{-5} eV and 100 keV. The solid curve is ENDF/B-V and the dashed curve is ENDF/B-III.

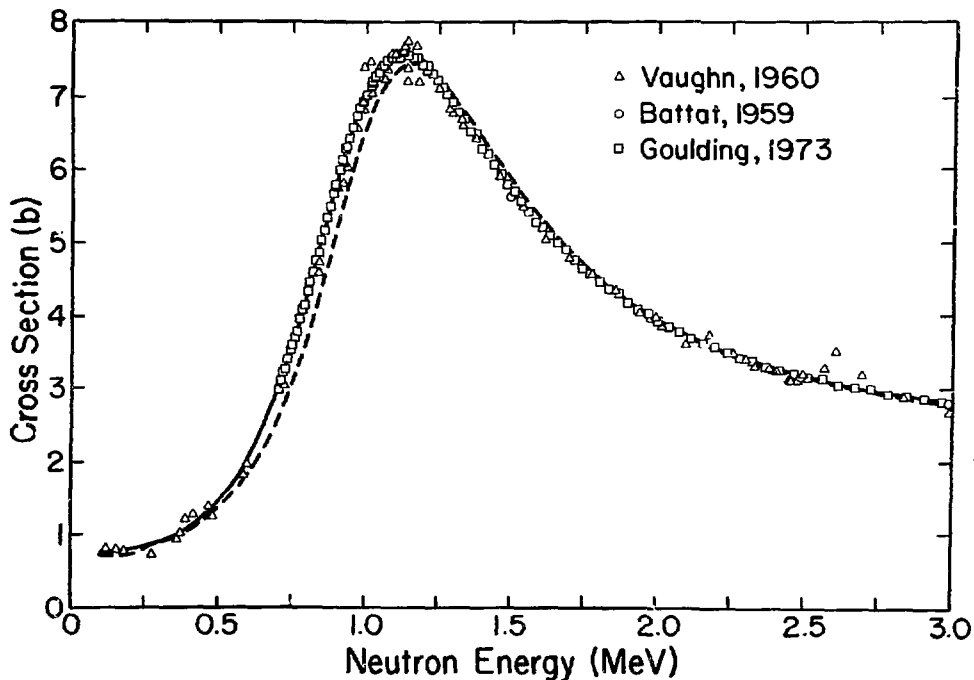


Fig. 2.

Measured and evaluated $n-^4\text{He}$ total cross sections between 0 and 3 MeV. The solid curve is ENDF/B-V and the dashed curve is ENDF/B-III.

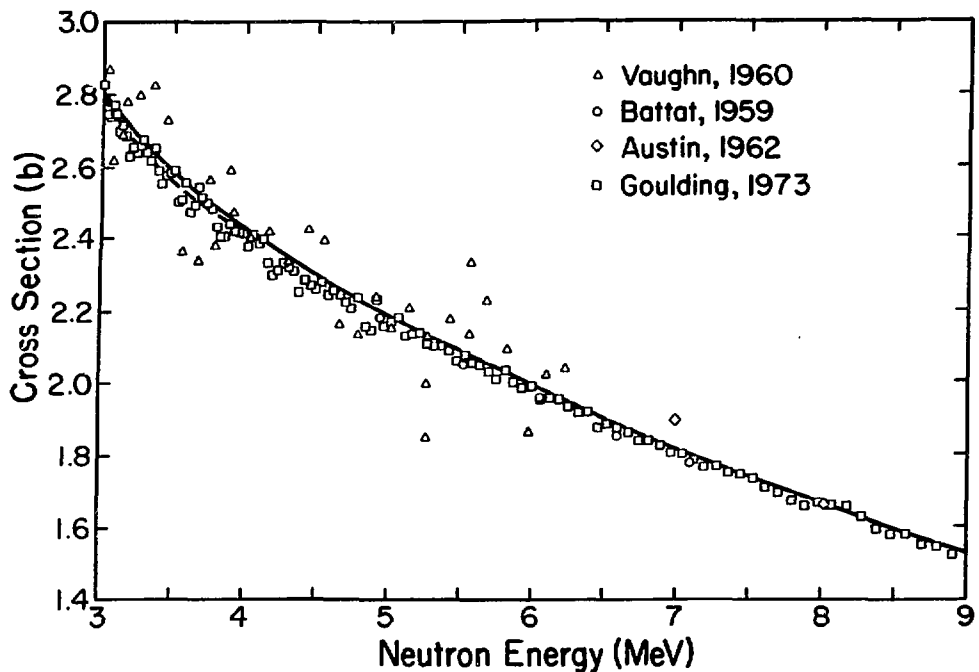


Fig. 3.

Measured and evaluated $n-{}^4\text{He}$ total cross sections between 3 and 9 MeV. The solid curve is ENDF/B-V and the dashed curve is ENDF/B-III.

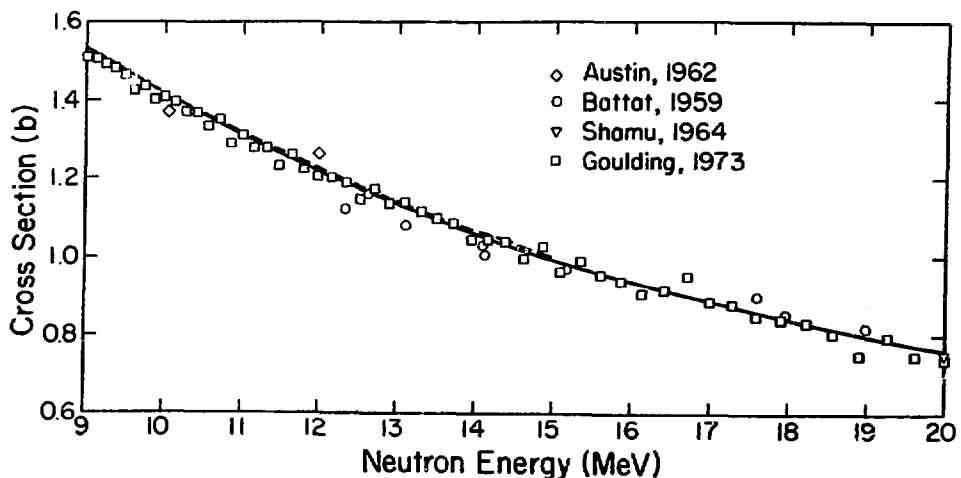


Fig. 4.

Measured and evaluated $n-{}^4\text{He}$ total cross sections between 9 and 20 MeV. The solid curve is ENDF/B-V and the dashed curve is ENDF/B-III.

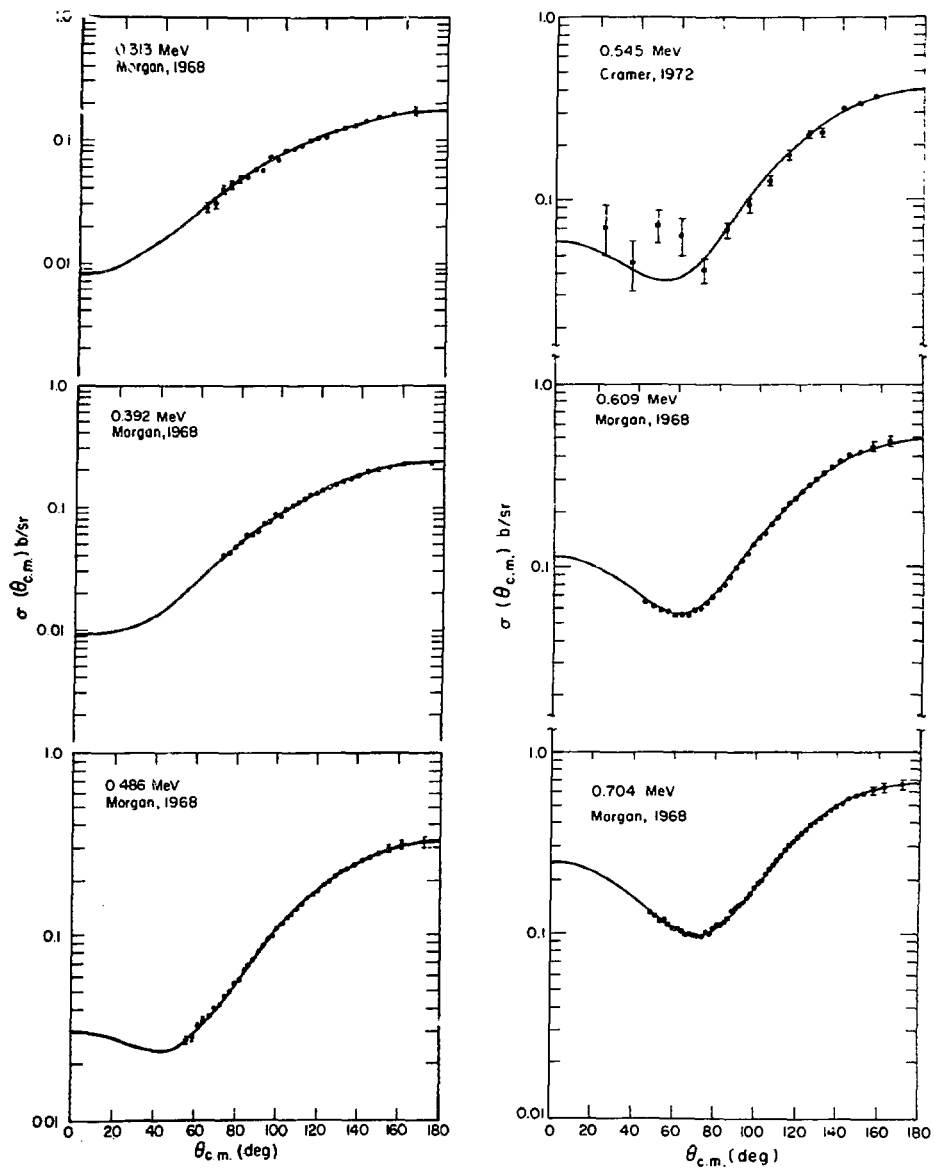


Fig. 5.

Measured and evaluated $n-{}^4He$ differential elastic angular distribution for incident neutron energies between 0.313 and 0.704 MeV.

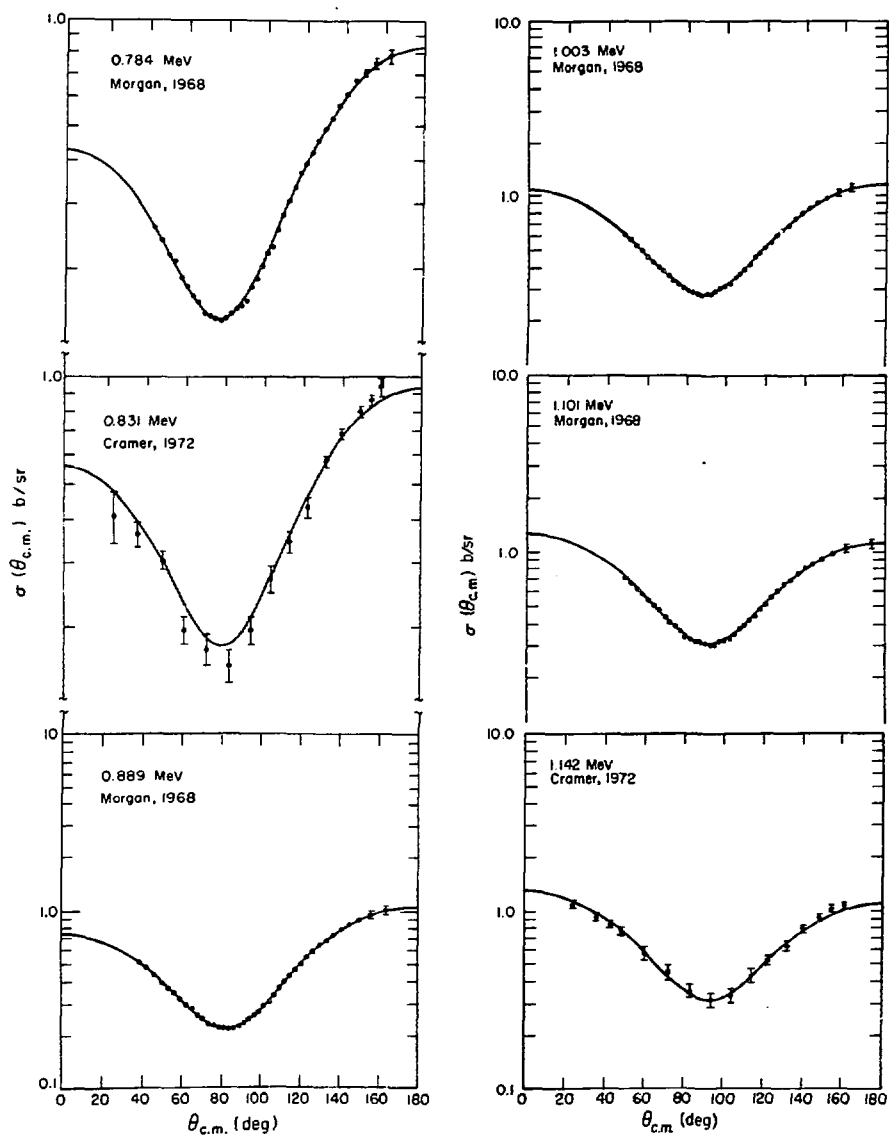


Fig. 6.

Measured and evaluated $n-{}^4\text{He}$ differential elastic angular distribution for incident neutron energies between 0.784 and 1.142 MeV.

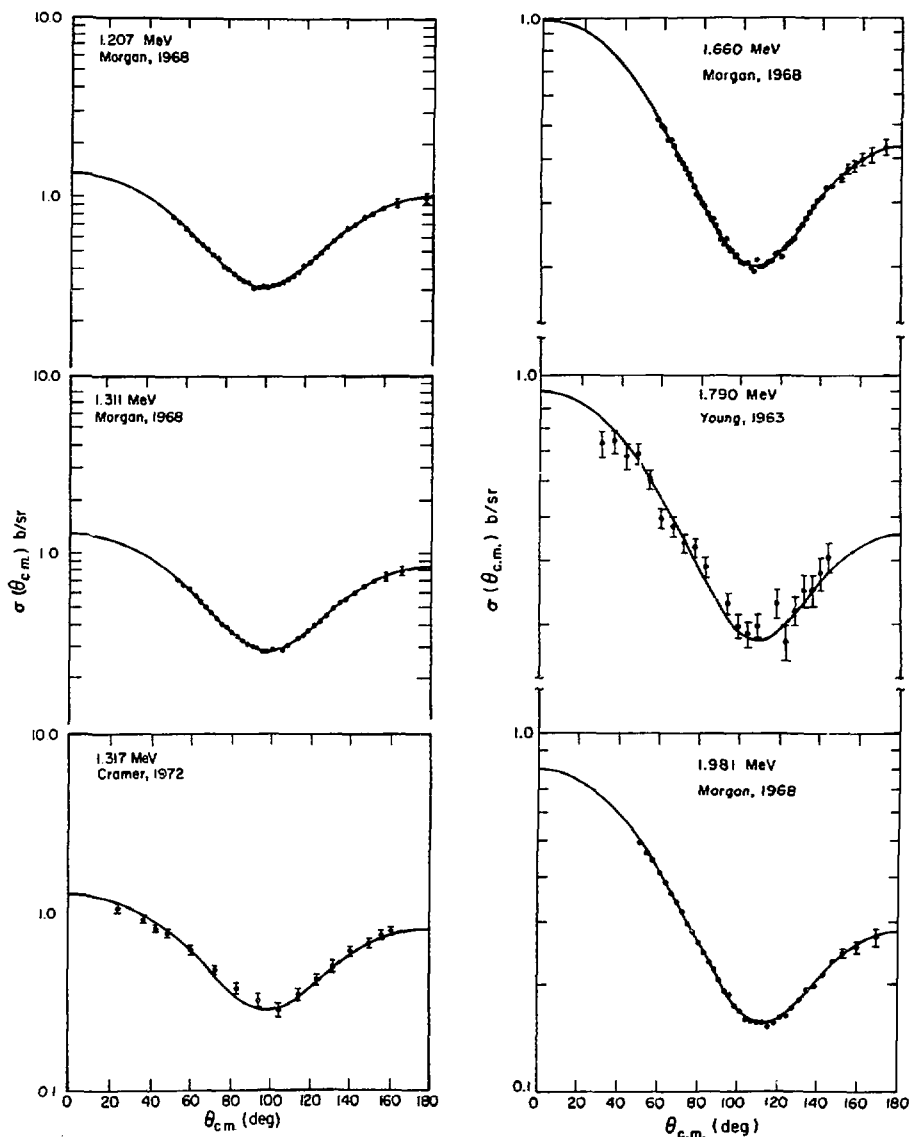


Fig. 7.

Measured and evaluated $n-{}^4He$ differential elastic angular distribution for incident neutron energies between 1.207 and 1.981 MeV.

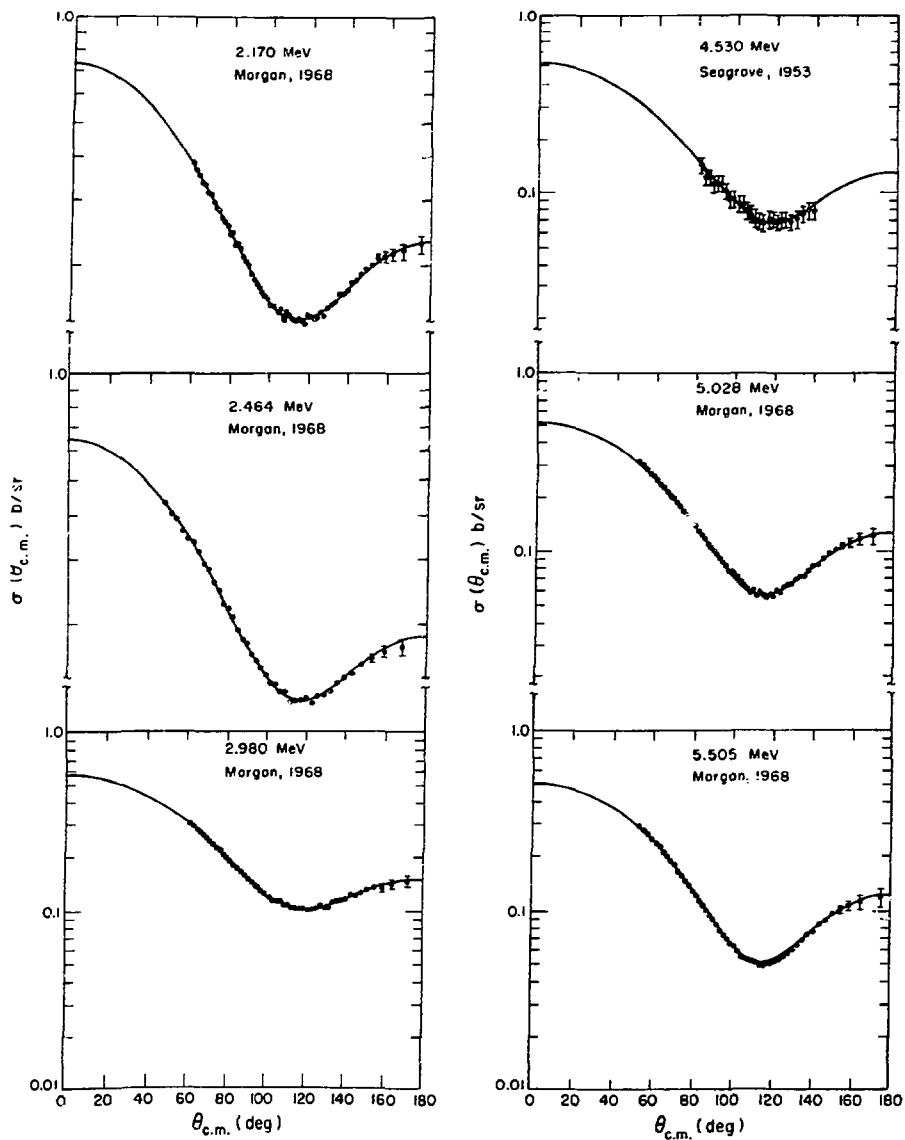


Fig. 8.

Measured and evaluated $n-{}^4He$ differential elastic angular distribution for incident neutron energies between 2.170 and 5.505 MeV.

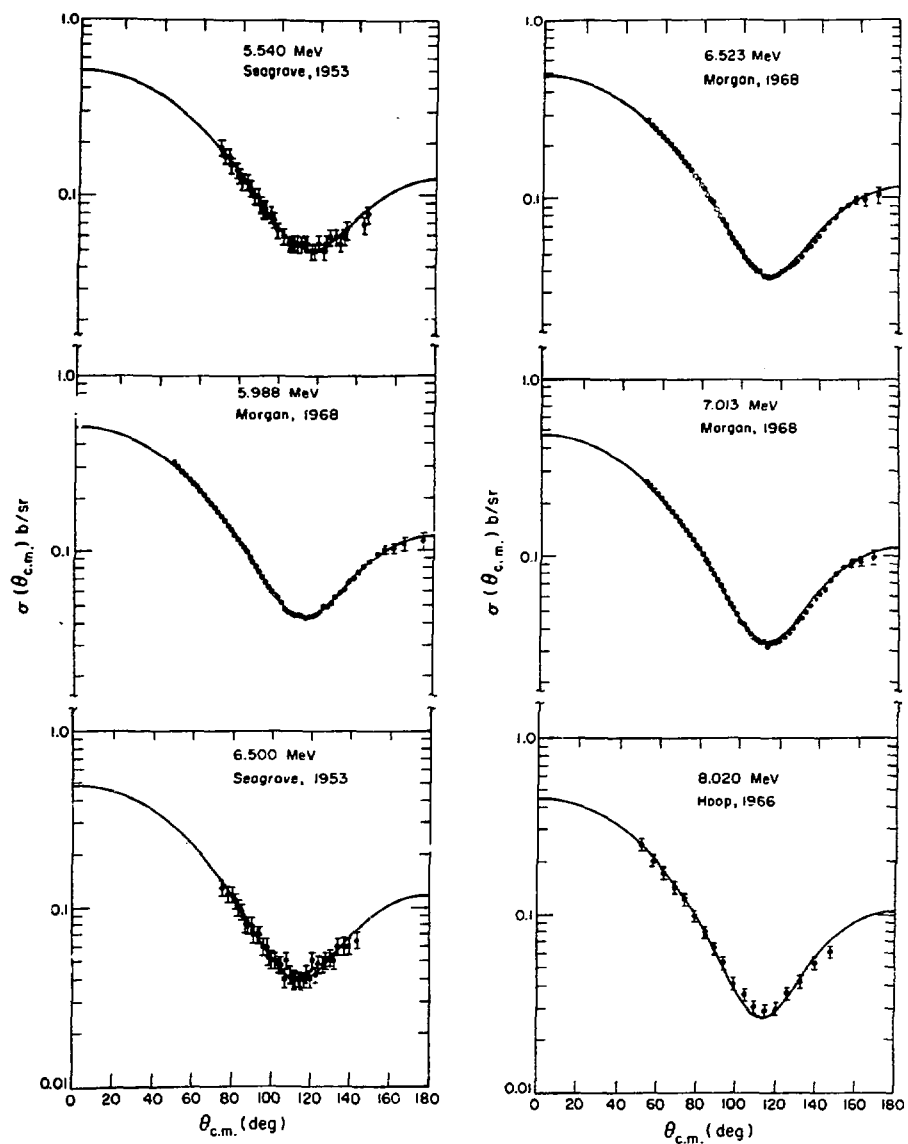


Fig. 9.

Measured and evaluated $n-{}^4He$ differential elastic angular distribution for incident neutron energies between 5.54 and 8.08 MeV.

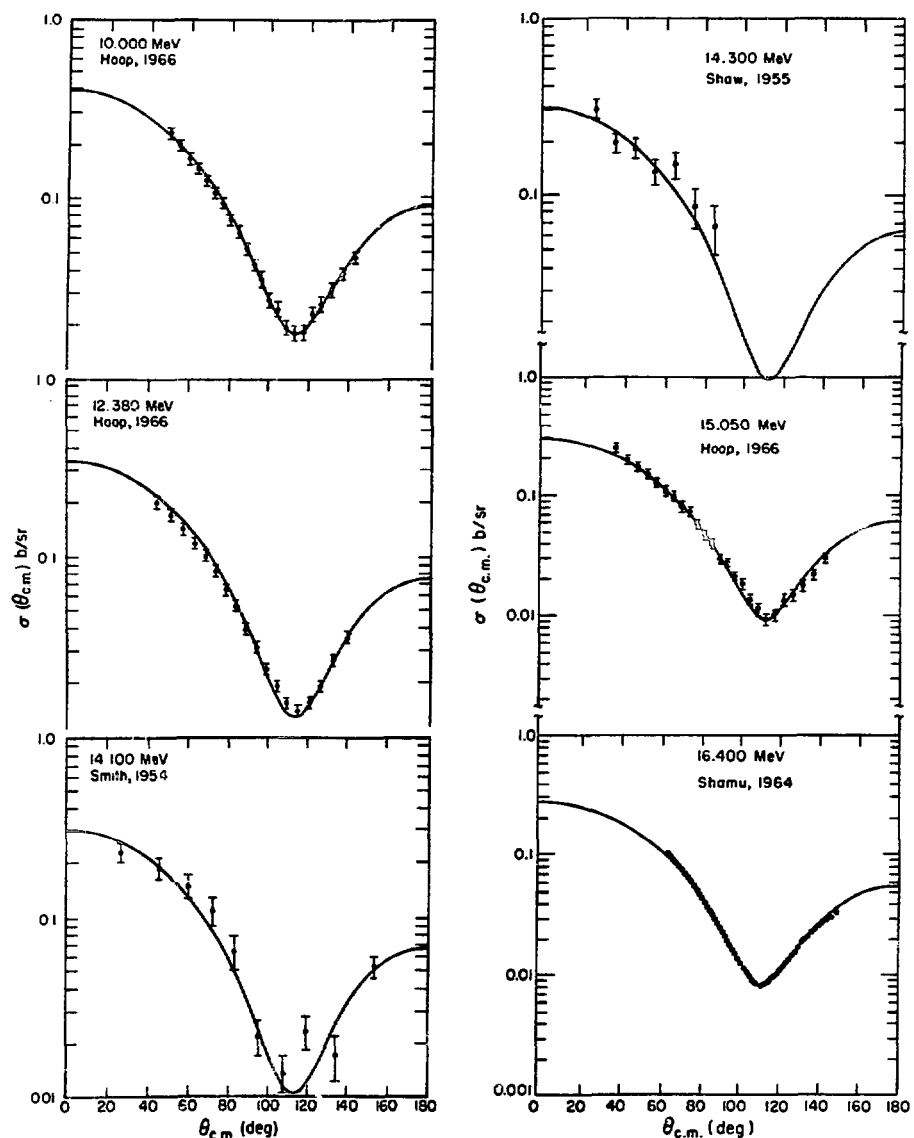


Fig. 10.

Measured and evaluated $n-{}^4\text{He}$ differential elastic angular distribution for incident neutron energies between 10.0 and 16.4 MeV.

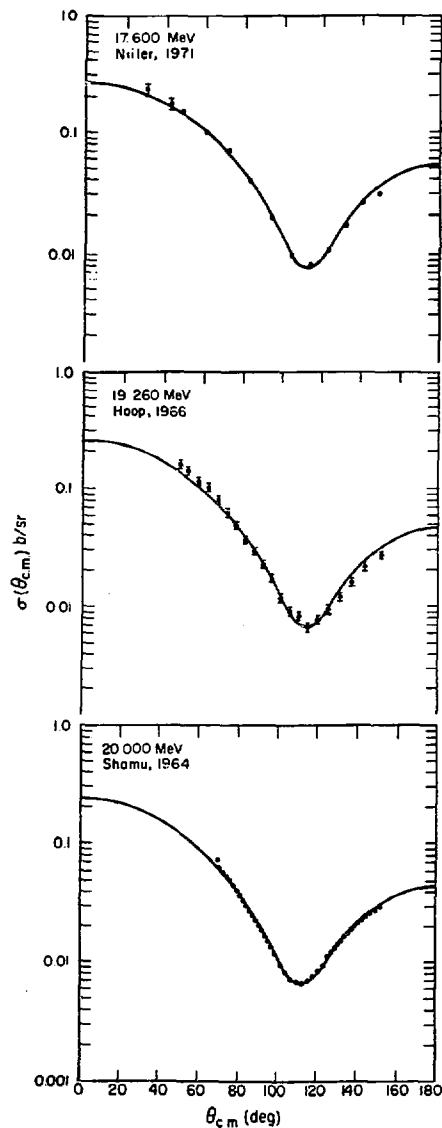


Fig. 11.

Measured and evaluated $n-{}^4He$
differential elastic angular
distribution for incident
neutron energies between
17.6 and 20.0 MeV.

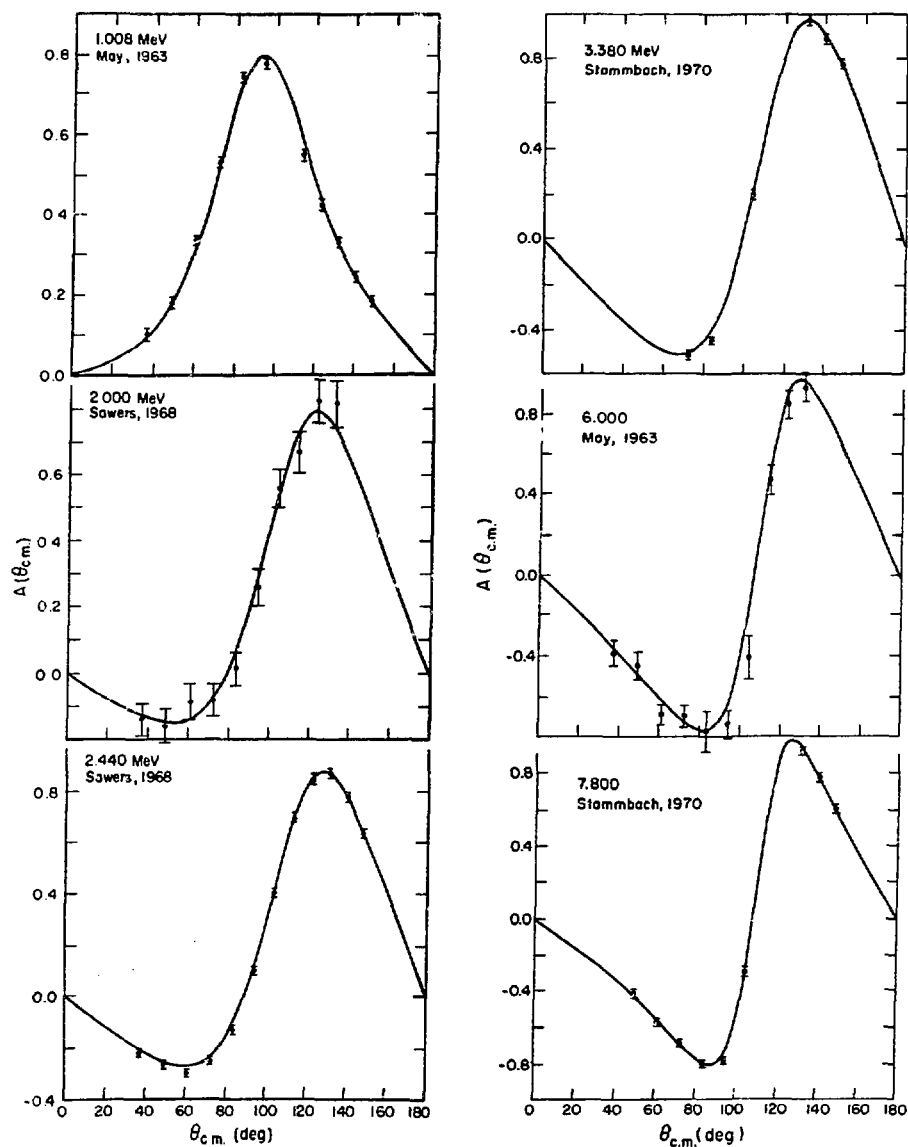


Fig. 12.

${}^4\text{He}(n,n){}^4\text{He}$ neutron polarizations for incident energies between 1.008 and 7.8 MeV.

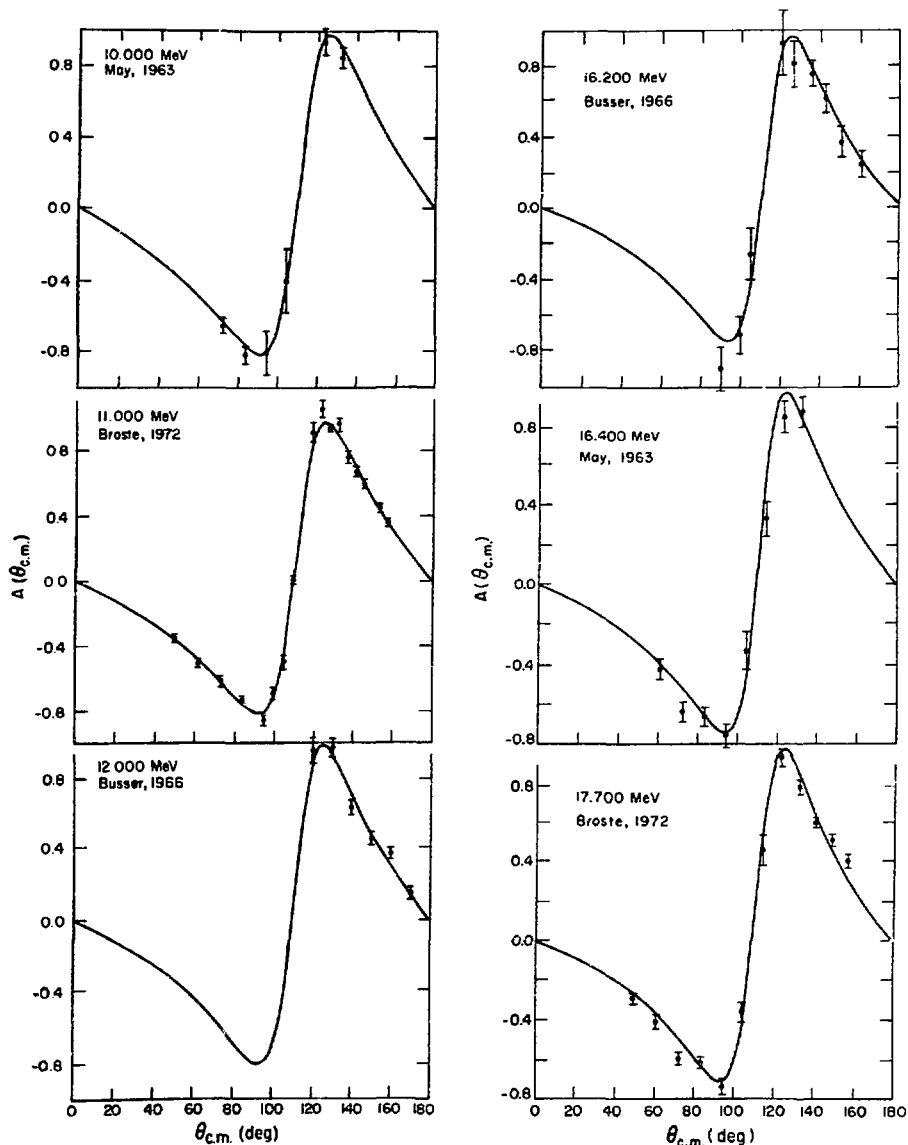


Fig. 13.

$^4\text{He}(n,n)^4\text{He}$ neutron polarizations for incident energies between 10.0 and 17.7 MeV.

SUMMARY DOCUMENTATION FOR ${}^6\text{Li}$

by

G. M. Hale, L. Stewart, and P. G. Young
Los Alamos Scientific Laboratory
Los Alamos, New Mexico

I. SUMMARY

The previous evaluation for ${}^6\text{Li}$ was extensively revised for Version V of ENDF/B (MAT 1303). All major cross-section files except radiative capture were updated. A new R-matrix analysis including recent experimental results was performed up to a neutron energy of 1 MeV, which includes the standards region for the ${}^6\text{Li}(n,t){}^4\text{He}$ reaction. Extensive revisions were made in the MeV region to include a more precise representation of the $(n,n'd)$ reaction. In the new representation, the $(n,n'd)$ cross section is grouped into ${}^6\text{Li}$ excitation energy bins, which preserves the kinematic energy-angle relationships in the emitted neutron spectra. Finally, correlated error data were added up to a neutron energy of 1 MeV, triton angular distributions from the ${}^6\text{Li}(n,t){}^4\text{He}$ reaction were included below 1 MeV, and radioactive decay data were added to Files 8 and 9. Except for the covariance and (n,t) angular distribution files, the evaluation covers the neutron energy range of 10^{-5} eV to 20 MeV.

II. STANDARDS DATA

The ${}^6\text{Li}(n,\alpha)$ cross section is regarded as a standard below $E_n=100$ keV. The Version V cross sections for ${}^6\text{Li}$ below 1 MeV were obtained from multi-channel, multilevel R-matrix analyses of reactions in the ${}^7\text{Li}$ system, similar to those from which the Version IV evaluation were taken. New data have become available since Version IV was released and most of this new experimental information has been incorporated into the Version V analysis.

For Version IV, the ${}^6\text{Li}(n,\alpha)$ cross section was determined mainly by fitting the Harwell total cross section (reference 3 below), since this was presumably the most accurately known data included in the analysis. However, in addition to the Harwell total, the data base for the analysis included the shapes of the $n-{}^6\text{Li}$ elastic angular distributions and polarizations, ${}^6\text{Li}(n,\alpha)T$ angular distributions and integrated cross sections (normalized), and $t-\alpha$ elastic angular distributions.

Since the time of the Version IV analysis, new data have become available whose precision equals or betters that of the Harwell total cross section. The present analysis includes the following new measurements while retaining most of the data from the previous analysis:

<u>Measurement</u>	<u>References</u>	<u>Approximate Precision</u>
$n-{}^6\text{Li } \sigma_T$	Harvey, ORNL ⁴	0.5-1%
${}^6\text{Li}(n,\alpha)$ integrated cross section	Lamaze, NBS ²¹	1-2% (relative)
${}^4\text{He}(t,t) {}^4\text{He}$ differential cross section	Jarmie, LASL ³⁵	0.4-1%
${}^4\text{He}(t,t) {}^4\text{He}$ analyzing power	Hardekopf, LASL ³⁶	1%

Fits to the (n,α) data included in the Version V analysis are shown in Figs. 1 and 2. In Fig. 1, the data are plotted as $\sigma \cdot E_n$; in both figures, the Version IV evaluation is represented by the dashed curves. The good agreement with Lamaze's new ${}^6\text{Li}(n,\alpha)$ integrated cross section measurement²¹ is particularly encouraging, since these are close to the values most consistent with the accurate new $t + \alpha$ measurements.^{35,36} On the other hand, a shape difference persists between the fit and measurements of the total cross section in the region of the precursor dip and at the peak of the 245-keV resonance. However, we feel that including these precise new data in the analysis has reduced the uncertainty of the new ${}^6\text{Li}(n,\alpha)$ cross section significantly (to the order of 3%) over that of previous evaluations in the region of the resonance.

III. ENDF/B-V FILES

File 1. General Information

MT=451. Descriptive data.

File 2. Resonance Parameters

MT=151. Effective scattering radius = 0.23778×10^{-12} cm.

Resonance parameters not given.

File 3. Neutron Cross Sections

The 2200 m/s cross sections are as follows:

MT=1	Sigma =	936.64	b
MT=2	Sigma =	0.71046	b
MT=102	Sigma =	0.03850	b
MT=105	Sigma =	935.89	b

MT=1. Total Cross Section

Below 1 MeV, the values are taken from an R-matrix analysis by Hale, Dodder, Witte (described in Ref. 2) which takes into account data from all reactions possible in ${}^7\text{Li}$ up to 3 MeV neutron energy. Total cross section data considered in this analysis were those of Refs. 3 and 4. Between 1 and 5 MeV, the total was taken to be the sum of MT=2, 4, 24, 102, 103, and 105, which generally follows the measurements of Refs. 5 and 6. Between 5 and 20 MeV, the total was determined by an average of the data of Refs. 6 and 7 which agrees with Ref. 8

except at the lowest energy. In this region, the total exceeds the sum of the measured partial cross sections by as much as 200-300 mb. This difference was distributed between the elastic and total $(n, n')d$ cross sections.

MT=2. Elastic Cross Section

Below 3 MeV, the values are taken from the R-matrix analysis cited for MT=1, which includes the elastic measurements of Refs. 9 and 10. These calculations were matched smoothly in the 3-5 MeV region to a curve which lies about 50 mb above Batchelor (Ref. 26) between 5 and 7.5 MeV, and about 13% above the data of Refs. 14, 27, 28, and 29 at 10 to 14 MeV.

MT=4. Inelastic Cross Section

Sum of MT=51 through MT=81.

MT=24. $(n, 2n)\alpha$ Cross Section

Passes through the point of Mather and Pain (Ref. 11) at 14 MeV, taking into account the measurements of Ref. 12.

MT=51, 52, 54-56, 58-81. $(n, n')d$ Continuum Cross Sections

Represented by continuum-level contributions in ${}^6\text{Li}$, binned in 0.5-MeV intervals. The energy-angle spectra are determined by a 3-body phase-space calculation, assuming isotropic center-of-mass distributions. At each energy, the sum of the continuum-level contributions is normalized to an assumed energy-angle integrated continuum cross section which approximates the difference of Hopkin's measurement (Ref. 13) and the contribution from the first and second levels in ${}^6\text{Li}$. The steep rise of the pseudo-level cross sections from their thresholds and the use of fixed bin widths over finite angles produces anomalous structure in the individual cross sections which is especially apparent near the thresholds. Some effort has been made to smooth out these effects, but they remain to some extent.

MT=53. $(n, n_1)d$ Discrete Level Cross Sections

Cross section has p-wave penetrability energy dependence from threshold to 3.2 MeV. Matched at higher energies to a curve which lies 15-20% above Hopkins (Ref. 13) and passes through the 10-MeV point of Cookson (Ref. 14).

MT=57. $(n, n_2)\gamma$ Cross Section

Rises rapidly from threshold, peaks at 5 mb and falls off gradually to 20 MeV. No data available except upper limits.

MT=102. (n, γ) Cross Sections

Unchanged from Version IV, which was based on the thermal measurement of Jurney (Ref. 15) and the Pendlebury evaluation (Ref. 16) at higher energies.

MT=103. (n, p) Cross Sections

Threshold to 9 MeV, based on the data of Ref. 17. Extended to 20 MeV through the 14-MeV data of Refs. 18 and 19.

MT=105. (n, t) Cross Sections

Below 3 MeV, values are taken from the R-matrix analysis of Ref. 2, which includes (n, t) measurements from Refs. 20-24. Between 3 and 5 MeV, the values are based on Bartle's measurements (Ref. 24). At higher energies, the cross sections are taken from the evaluation of Ref. 16, extended to 20 MeV considering the data of Kern (Ref. 25).

File 4. Neutron Secondary Angular Distributions

MT=2. Elastic Angular Distributions

Legendre coefficients determined as follows:

Below 2 MeV, coefficients up to $L=2$ were taken from the R-matrix analysis of Ref. 2, which takes into account elastic angular distribution measurements from Refs. 9 and 10 above 2 MeV. The coefficients represent fits to the measurements of Refs. 13 and 26 in the 3.5-7.5 MeV range, that of Ref. 14 at 1 MeV, and those of Refs. 27-29 at 14 MeV. Extrapolation of the coefficients to 20 MeV was aided by optical model calculations.

MT=24. $(n, 2n)$ Angular Distributions

Laboratory distributions obtained by integrating over energy the 4-body phase-space spectra that result from transforming isotropic center-of-mass distributions to the laboratory system.

MT=51 - 81. (n, n') Angular Distributions

Obtained by transforming distributions that are isotropic in the 3-body center-of-mass system to equivalent 2-body distributions in the laboratory system. MT=53 and 57 are treated as real levels and assumed to be isotropic in the two-body reference system. Data available indicate departure from isotropy for the first real level (MT=53) and this anisotropy will be included in a later update.

MT=105. (n,t) Angular Distributions

Legendre coefficients obtained from the R-matrix analysis of Ref. 2 are supplied at energies below 1 MeV. The analysis takes into account (n,t) angular distribution measurements from Refs. 23 and 30.

File 5. Neutron Secondary Energy Distributions

MT=24. (n,2n) Energy Distributions

Laboratory distributions obtained by integrating over angle the 4-body phase-space spectra that result from transforming isotropic center-of-mass distributions to the laboratory system.

File 8. Radioactive Nuclide Production

MT=103. (n,p) ${}^6\text{He}$

${}^6\text{He}$ beta decays, with a half-life of 808 ms, back to ${}^6\text{Li}$ with a probability of unity.

MT=105. (n,t) ${}^4\text{He}$

Tritium, which is the only radioactive product of this reaction, beta decays to ${}^3\text{He}$ with a probability of unity and with a lifetime of 12.33 years.

File 9. Radioactive Nuclide Multiplicities

MT=103. (n,p) Multiplicity

A multiplicity of one is given for the production of ${}^6\text{He}$.

MT=105. (n,t) Multiplicity

A multiplicity of one is given for the production of tritium.

File 12. Gamma-Ray Multiplicities

MT=57. (n,n₂) γ Multiplicity

Multiplicity of one assumed for the 3.562-MeV gamma ray. Energy taken from reference 31.

MT=102. (n, γ) Multiplicity

Energies and transition arrays for radiative capture taken from Ref. 15, as reported in Ref. 31. The LP flag was used to describe the MT=102 photons.

File 14. Gamma-Ray Angular Distributions

MT=57. (n,n₂) γ Angular Distributions.

The gamma is assumed isotropic.

MT=102. (n, γ) Angular Distributions

The two high-energy gammas are assumed isotropic. Data on the 477-keV gamma indicate isotropy.

File 33. Cross Section Covariances

The relative covariances for MT=1, 2, and 105 below 1 MeV are given in File 33. They are based on calculations using the covariances of the R-matrix parameters in first-order error propagation.

MT=1. Total

Relative covariances are entered as NC-type sub-subsections, implying that they are to be constructed from those for MT=2 and 105. They are not intended for use at energies above 1.05 MeV.

MT=2, 105. Elastic and (n,t)

Relative covariances among these two cross sections are entered explicitly as NI-type sub-subsections in the LB=5 (direct) representation. Although values for the 0.95-1.05 MeV bin are repeated in a 1.05-20 MeV bin, the covariances are not intended for use at energies above 1.05 MeV.

REFERENCES

1. G. M. Hale, L. Stewart, and P. G. Young, LA-6518-MS (1976).
2. G. M. Hale, Proc. Internat. Specialists Symposium on Neutron Standards and Applications, Gaithersburg (1977).
3. K. M. Diment and C. A. Uttley, AERF-PR/NP 15 and AERE-PR/NP 16 (1969). Also private communication to L. Stewart.
4. J. A. Harvey and N. W. Hill, Proc. Conf. on Nuclear Cross Sections and Technology, Vol. 1, 244 (1975).
5. H. H. Knitter, C. Budtz-Jorgensen, M. Mailly, and R. Vogt, CBNM-VG (1976).
6. C. A. Goulding and P. Stoler, EANDC(US)-176U, 161 (1972).
7. D. G. Foster and D. W. Glasgow, Phys. Rev. C3, 576 (1971).
8. A. Bratenahl, J. M. Peterson, and J. P. Stoering, Phys. Rev. 110, 927 (1958), J. M. Peterson, A. Bratenahl, and J. P. Stoering, Phys. Rev. 120, 521 (1960).
9. R. O. Lane, Ann. Phys. 12, 135 (1961).
10. H. H. Knitter and A. M. Coppola, FANDC(E)-57U (1967). Also Ref. 5 above.
11. D. S. Mather and L. F. Pain, AWRE-0-47/69 (1969).
12. V. J. Ashby et al., Phys. Rev. 129, 1771 (1963).
13. J. C. Hopkins, D. M. Drake, and H. Condé, Nucl. Phys. A107, 139 (1968), and J. C. Hopkins, D. M. Drake, and H. Condé, LA-3765 (1967).

14. J. A. Cookson and D. Dandy, Nucl. Phys. A91, 273 (1967).
15. E. T. Jurney, LASL, private communication (1973).
16. E. D. Pendlebury, AWRE-0-60/64 (1964).
17. R. Bass, C. Bindhardt, and K. Kruger, EANDC(E)-57U (1965).
18. G. M. Frye, Phys. Rev. 93, 1086 (1954).
19. M. E. Battat and F. L. Ribe, Phys. Rev. 89, 8 (1953).
20. M. G. Sowerby, B. H. Patrick, C. A. Uttley, and K. M. Diment, J. Nucl. Energy 24, 323 (1970). $^{6}\text{Li}/^{10}\text{B}$ Ratio Converted Using ENDF/B-IV $^{10}\text{B}(\text{n},\alpha)$ Cross Section.
21. G. P. Lamaze, O. A. Wasson, R. A. Schrack, and A. D. Carlson, Proc. Internat. Conf. on the Interactions of Neutrons with Nuclei, Vol. 2, 1341 (1976).
22. W. P. Poenitz, Z. Phys. 268, 359 (1974).
23. J. C. Overley, R. M. Sealock, and D. H. Ehlers, Nucl. Phys. A221, 573 (1974).
24. C. M. Bartle, Proc. Conf. on Nuclear Cross Sections and Technology, Vol. 2, 688 (1975), and private communication (1976).
25. R. D. Kern and W. E. Kreger, Phys. Rev. 112, 926 (1958).
26. R. Batchelor and J. H. Towle, Nucl. Phys. 47, 385 (1963).
27. A. H. Armstrong, J. Gammel, L. Rosen, and G. M. Frye, Nucl. Phys. 52, 505 (1964).
28. C. Wong, J. D. Anderson, and J. W. McClure, Nucl. Phys. 33, 680 (1962).
29. F. Merchez, N. V. Sen, V. Regis, and R. Bouchez, Compt. Rend. 260, 3922 (1965).
30. I. G. Schroder, E. D. McGarry, G. DeLeeuw-Giertz, and S. DeLeeuw, Proc. Conf. on Nuclear Cross Sections and Technology, Vol. 2, 240 (1975).
31. F. Ajzenberg-Selove, and T. Lauritsen, Nucl. Phys. A227, 55 (1974).
32. M. S. Coates et al., Neutron Standards Reference Data, IAEA, Vienna, p. 105 (1974).
33. S. J. Friesenhahn et al., INTEL-RT-7011-001 (1974).
34. W. Fort and J. P. Marquette, Proceedings of a Panel on Neutron Standard Reference Data, Nov. 20-24 (1972), IAEA, Vienna.
35. N. Jarmie et al., BAPS 20, 596 (1975).
36. R. A. Hardekopf et al., LA-6188 (1977).

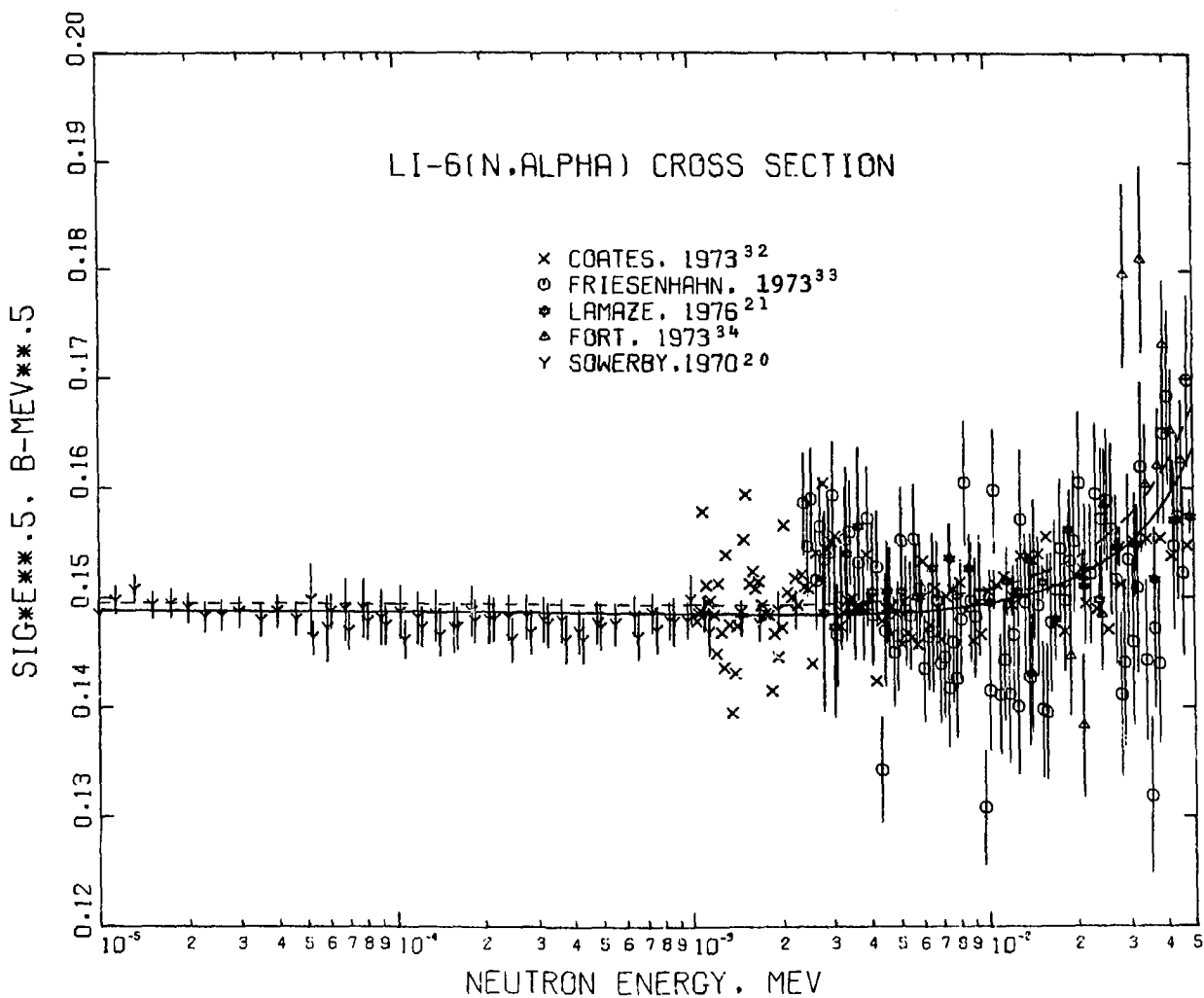


Fig. 1.

The Version V ${}^6\text{Li}(n,t){}^4\text{He}$ cross section times $\sqrt{E_n}$ plotted versus E_n for neutron energies between 10 eV and 50 keV. The dashed curve is ENDF/B-IV; the experimental data are from references 20, 21, 32-34.

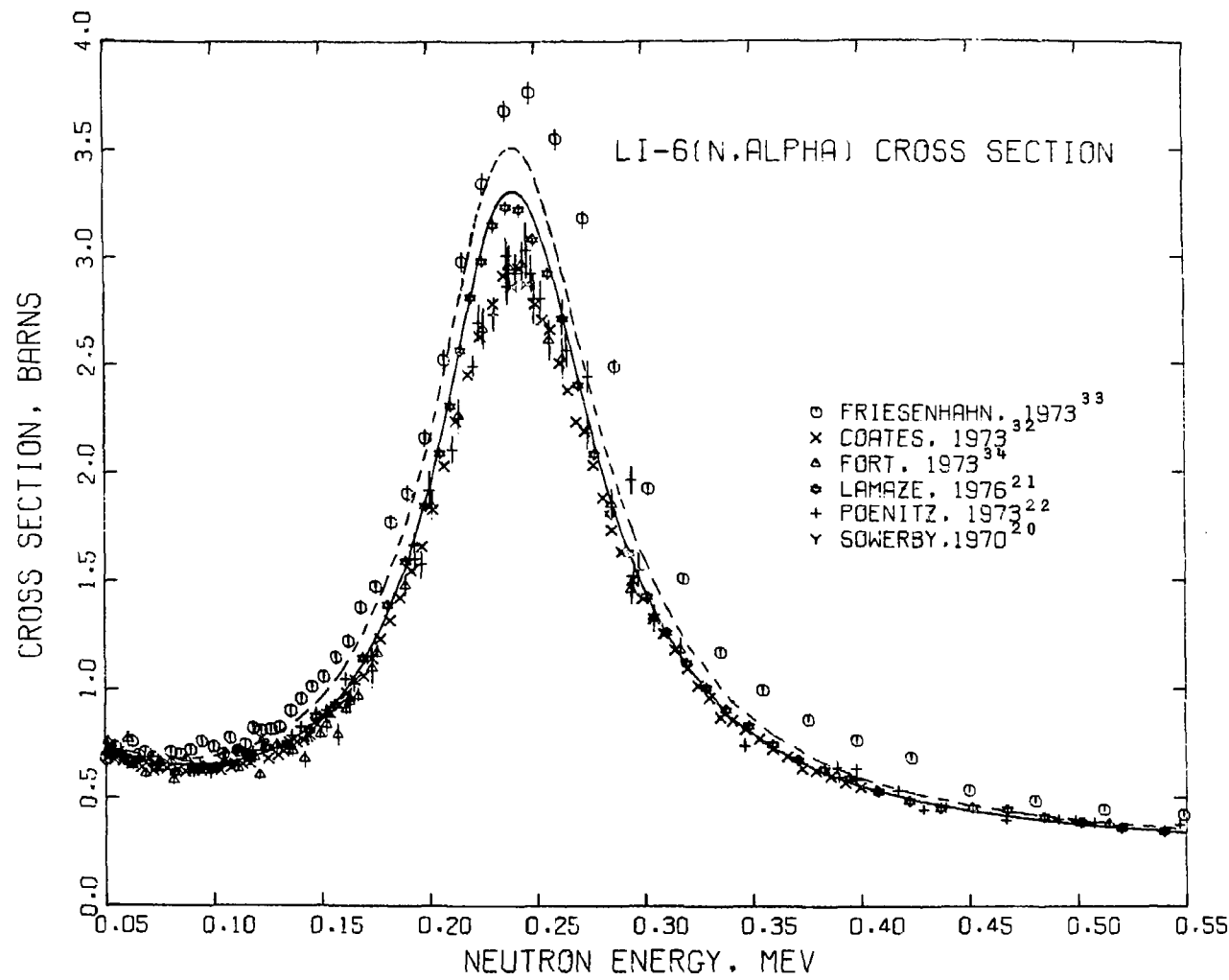


Fig. 2.

The Version V ${}^6\text{Li}(n,t){}^4\text{He}$ cross section from 50 to 550 keV. The dashed curve is ENDF/B-IV; the experimental data are from references 20-22, 32-34.

SUMMARY DOCUMENTATION FOR ^7Li

by

L. Stewart, D. G. Foster, Jr., M. E. Battat, and R. J. LaBauve
Los Alamos Scientific Laboratory
Los Alamos, New Mexico

I. SUMMARY

The ^7Li evaluation for ENDF/B-V (MAT 1272) was carried over from Version IV with only minor format modifications being included. The evaluation of all the neutron data except the total cross section is based upon a 1964 evaluation by Pendlebury (AWRE 0-61/64) as adapted by Battat and LaBauve for Version II of ENDF/B. The total cross section above 0.5 MeV was re-evaluated by Foster as described below and photon production data added by LaBauve and Stewart for Version IV of ENDF/B. The evaluation covers the energy range from 10^{-5} eV to 20 MeV. Covariance data are not included in the file but will be available in a new evaluation forthcoming from LASL.

II. ENDF/B-V FILES

File 1. General Information

MT=451. Descriptive data.

File 2. Resonance Parameters

MT=151. Effective scattering radius = 0.28906×10^{-12} cm.

Resonance parameters not given.

File 3. Neutron Cross Sections

MT=1. Total Cross Section

Below 100 keV, based on analysis of available total cross section and radiative capture measurements (Hu58, Hu60, Ho58, and Ho59) with an expression of the form $\sigma_T = \sigma_{n,n} + \sigma_{n,\gamma}$, where $\sigma_{n,n}$ = constant and $\sigma_{n,\gamma}$ has a $1/V$ energy dependence. The analysis resulted in $\sigma_{n,n} = 1.05$ b and $\sigma_{n,\gamma} = 0.036$ b at thermal.

100 - 500 keV, based on available experimental data (Hu58, Hy60, Ho58, and Ho59).

0.5 - 20 MeV, analysis by Foster (LASL) used. Evaluation from 0.5 to 1.3 MeV based on measurements of Me70. Above 1.3 MeV, based on Go71, slightly normalized to improve agreement with Fo71, Br58, Co52, and Pe60. Accuracy is approximately 2% at 0.5 MeV and 1% above 1 MeV. Polynomial smoothing was used throughout.

MT=2. Elastic Cross Section

0 - 100 keV, see MT=1 summary.

0.1 - 20 MeV, based on experimental data of Ar63, Ba63B, Bo59, Gr59, La61, To56, Wi56, and Wo62.

MT=3. Nonelastic Cross Section (not included in file).

In order to determine the individual reaction cross sections, a total nonelastic cross section was evaluated with the elastic cross section, with each adjusted such that their sum equaled the MT=1 cross section. Experimental nonelastic measurements that were considered include Co59, Go59, Mc63, and Ri53.

MT=4. Inelastic Cross Section

Sum of MT=51 and 91.

MT=16. (n,2n) Cross Section

Threshold - 20 MeV, smooth curve through experimental data of As63 at 10.2 and 14.1 MeV, smoothly extrapolated to 20 MeV, to obtain total (n,2n). Then divided into MT=16 and MT=24 components as described under MT=24.

MT=24. (n,2nd) α Cross Section

Threshold - 20 MeV, the total (n,2n) cross section is divided into (n,2n) ^6Li and (n,2nd) α components assuming that the latter reaction will dominate as the neutron energy increases above its threshold (9.98 MeV).

MT=51. (n,n' γ) Cross Section

Threshold - 20 MeV, the energy-dependent cross section to the 478-keV first-excited state of ^7Li , which is the only ^7Li level stable to particle decay, is based mainly on the experimental data of Ba63B, and Fr55 below 4 MeV and Be62 near 14 MeV, with a smooth interpolation between and extrapolation to 20 MeV.

MT=91. (n,n't) α Cross Section

Threshold - 20 MeV, the cross section to discrete and continuum states in ^7Li unstable to t- α breakup is based mainly on the experimental data of Ba63B, Ro62, and Th54, together with the results of Brown et al., and Osborne (see Hu58, Hu60).

MT=102. (n, γ) Cross Section

Below 150 keV, based on thermal value of 36 mb (Hu60) with $1/V$ energy dependence until the cross section falls to 10 μb .

0.15 - 20 MeV, held constant at 10 μb to 15 MeV, decreasing to 8.6 μb at 20 MeV.

MT=104. (n, d) Cross Section

Threshold - 20 MeV, smooth curve through the experimental data of Ba53, Ba63B, and Mi61.

MT=251. Average Cosine of Scattering Angle

Derived from evaluated files.

MT=252. Average-Logarithmic Energy Decrement

Derived from evaluated files.

MT=253. Gamma

Derived from evaluated files.

File 4. Neutron Angular Distributions

MT=2. Elastic Scattering Angular Distributions

Legendre coefficients given in center-of-mass system with transformation matrix (Al69). See Pe64 for evaluation details.

MT=16. ($n, 2n$) Angular Distributions

Tabular data (isotropic) in the laboratory system. See Pe64 for evaluation details.

MT=24. ($n, 2nd$) α Angular Distributions

Tabular data (isotropic) in the laboratory system. See Pe64 for evaluation details.

MT=51. ($n, n'\gamma$) Angular Distributions

Tabular data (isotropic) in the cm system. See Pe64 for evaluation details.

MT=91. ($n, n't$) α Angular Distributions

Tabular data (anisotropic) in the laboratory system. See Pe64 for evaluation details.

File 5. Neutron Energy Distributions

The tabulated spectra of Pendlebury (Pe64) were approximated by use of ENDF/B law 9, as described below.

MT=16. (n,2n) Energy Distribution

Energy range is 8.3 to 20 MeV. Distribution approximated by ENDF/B law 9, with theta (MeV) equal to $0.21\sqrt{E}$. This corresponds to an average theta of 0.7 MeV in the 8.3 to 15 MeV energy interval.

MT=24. (n,2nd) α Energy Distribution

Energy range is 10 to 20 MeV. Distribution approximated by ENDF/B law 9, with theta (MeV) equal to $0.1133\sqrt{E}$. This corresponds to an average theta of 0.4 MeV in the 10 to 15 MeV energy interval.

MT=91. (n,n't) α Energy Distribution

Distributions approximated using law 9. Theta values obtained by linear interpolation between following points:

E = 2.821	MeV.	Theta = 0.10	MeV
E = 5.8	MeV.	Theta = 0.70	MeV
E = 8.0	MeV.	Theta = 2.80	MeV
E = 15.0	MeV.	Theta = 5.35	MeV

Data include the cross section to the second level and do not always conserve energy.

File 12. Gamma-Ray Multiplicities

MT=51. (n,n' γ) Multiplicity

The first level in ^7Li is the only known gamma emitter. Multiplicity of 1.0 assumed at all energies.

MT=102. (n, γ) Multiplicity

Thermal capture spectrum measurements are inconclusive. Rough estimates of transition probabilities were made using level energies of Selove and Lauritsen (private communication). LP flag used to indicate primary transitions.

File 14. Gamma-Ray Angular Distributions

MT=51. (n,n' γ) Angular Distributions

Assumed isotropic at all energies.

MT=102. (n, γ) Angular Distributions

Assumed isotropic at all energies.

REFERENCES

Al69 H. Alter, Atomics International, private communication (1969).
Ar63 A. H. Armstrong and L. Rosen, WASH-1042, p. 23 (1963).
As63 V. J. Ashby, H. C. Catron, M. D. Goldberg, R. W. Hill, J. M. LeBlanc, L. L. Newkirk, J. P. Stoering, C. J. Taylor, and M. A. Williamson, Phys. Rev. 129, 1771 (1963).
Ba53 M. F. Battat and F. L. Ribe, Phys. Rev. 89, 80 (1953).
Ba63A J. F. Barry, J. Nuc. Eng. 17, 273 (1963).
Ba63B R. Batchelor and J. H. Towle, Nuc. Phys. 47, 385 (1963).
Be62 J. Benveniste, A. C. Mitchell, C. D. Schrader, and J. H. Zenger, Nucl. Phys. 38, 300 (1962).
Bo59 N. A. Bostrom, I. L. Morgan, J. T. Prud'homme, P. L. Okhuysen, and O. M. Hudson, WADC-TN-59-107 (1959).
Br58 A. Bratenahl et al., Phys. Rev. 110, 927 (1958).
Co52 J. H. Coon et al., Phys. Rev. 88, 562 (1952).
Co59 A. V. Cohen, Unpublished (1959).
Fo71 D. G. Foster, Jr., D. W. Glasgow, Phys. Rev. C3, 576 (1971).
Fr55 J. M. Freeman, A. M. Lane, and B. Rose, Phil. Mag. 46, 17 (1955).
Go59 V. M. Gorbachev and L. B. Poretskii, S. J. At. Eng. 4, 259 (1958), J. Nucl. Eng. 9, 159 (1959).
Go71 C. A. Goulding et al., (RPI), private communication (1971).
Gr59 B. C. Groseclose, Mis. 59-4223 (1959).
Ho58 R. J. Howerton, UCRL 5226 (1958).
Ho59 R. J. Howerton, UCRL 5226 (Revised) (1959).
Hu58 D. J. Hughes and R. B. Schwartz, BNL 325, Second Edition (1958).
Hu60 D. J. Hughes, B. A. Magurno and M. K. Brussel, Supplement No. 1 to BNL 325, Second Edition (1960).
La61 R. O. Lane, A. S. Langsdorf, Jr., J. E. Monahan, and A. J. Elwyn, Annals of Physics 12, 135 (1961).
Mc63 M. H. McGregor, R. Booth, and W. P. Ball, Phys. Rev. 130, 1471 (1963).
Me70 J. W. Meadows and J. F. Whalen, Nucl. Sci. Eng. 41, 351 (1970).
Mi61 K. M. Mikhailina, A. A. Nomofilov, T. A. Romanova, V. A. Sviridov, F. A. Tikhomirov, and K. D. Tolstov, Sov. Progress in Neutron Physics, Ed. P. A. Krupchitskii (1961).
Pe60 J. M. Peterson et al., Phys. Rev. 120, 521 (1960).
Pe64 E. D. Pendlebury, AWRE 0-61/64 (1964).
Ri53 F. L. Ribe, R. W. Davis, and J. M. Holt, LA-1589 (1953).
Ro62 L. Rosen and L. Stewart, Phys. Rev. 126, 1150 (1962).
Th54 R. G. Thomas, LA-1697 (1954).
To56 R. G. Thomas, M. Walt, R. B. Walton, and R. G. Allen, Phys. Rev. 101, 759 (1956).
Wi56 H. B. Willard, J. K. Bair, J. D. Kington, and H. O. Cohn, Phys. Rev. 101, 765 (1956).
Wo62 C. Wong, J. D. Anderson, and J. W. McClure, Nuc. Phys. 33, 680 (1962).

SUMMARY DOCUMENTATION FOR ^{10}B

by

G. M. Hale, L. Stewart, and P. G. Young
Los Alamos Scientific Laboratory
Los Alamos, New Mexico

I. SUMMARY

All cross sections below a neutron energy of 1.5 MeV except the (n,p) and (n,t) reactions were revised for the Version V evaluation of ^{10}B (MAT 1305). The data above 1.5 MeV were carried over from ENDF/B-IV. Other changes to the file include the addition of evaluated cross sections and secondary gamma-ray spectra from the $^{10}\text{B}(n,\gamma)^{11}\text{B}$ reaction, as well as covariance data for cross sections below 1.5 MeV. Except for the covariance file, the evaluated data cover the energy range from 10^{-5} eV to 20 MeV. Partial documentation is provided in LA-6472-PR (1976) and LA-6518-MS (1976).

II. STANDARDS DATA

The $^{10}\text{B}(n,\alpha)^7\text{Li}$ and $^{10}\text{B}(n,\alpha_1\gamma)^7\text{Li}$ reactions are neutron standards at energies below 100 keV. The major reactions below 1 MeV were obtained for the Version V evaluation from multichannel, multilevel R-matrix analyses of reactions in the ^{11}B system, similar to those from which the Version IV evaluation were taken. New data have become available since Version IV was released and most of this new experimental information has been incorporated into the present analyses.

We have added Spencer's measurements of σ_T (Sp73) and Sealock's $^{10}\text{B}(n,\alpha_1)$ angular distributions (Se76) to the data set that was analyzed for Version IV. In addition, we have replaced Friesenhahn's integrated (n,α_1) cross section with the recent measurements of Schrack et al. (both with GeLi and NaI detectors) at NBS (Sc76), and have deleted Friesenhahn's total (n,α) cross section from the data set. The resulting fit to the (n,α) and $(n,\alpha\gamma)$ data is shown in Figs. 1 and 2, respectively. The integrated $^{10}\text{B}(n,\alpha)$ cross section has changed negligibly from the Version IV results at energies below 200 keV. At higher energies, however, the (n,α) cross section has dropped significantly in response to the new NBS data. Unfortunately, the rest of the data in the analysis do not seem particularly sensitive to such changes in the (n,α) cross section, with the result that our calculated cross section must be considered quite uncertain at energies above ~ 300 keV.

III. ENDF/B-V FILES

File 1. General Information

MT=451. Descriptive data.

File 2. Resonance Parameters

MT=451. Effective scattering radius = 0.40238×10^{-12} cm.

Resonance parameters not included.

File 3. Neutron Cross Sections

The 2200 m/s cross sections are as follows:

MT=1	Sigma =	3839.1	b
MT=2	Sigma =	2.0344	b
MT=102	Sigma =	0.5	b
MT=103	Sigma =	0.000566	b
MT=107	Sigma =	3836.6	b
MT=113	Sigma =	0.000566	b
MT=700	Sigma =	0.000566	b
MT=780	Sigma =	244.25	b
MT=781	Sigma =	3592.3	b

MT=1. Total Cross Section

0 to 1 MeV, calculated from R-matrix parameters obtained by fitting simultaneously data from the reactions $^{10}\text{B}(n,n)$, $^{10}\text{B}(n,\alpha_0)$, and $^{10}\text{B}(n,\alpha_1)$. Total neutron cross-section measurements included in the fit are those of Bo52, Di67, and Sp73.

1 to 20 MeV, smooth curve through measurements of Di67, Bo52, Ts62, Fo61, Co52, and Co54, constrained to match R-matrix fit at 1 MeV.

MT=2. Elastic Scattering Cross Section

0 to 1 MeV, calculated from the R-matrix parameters described for MT=1. Experimental elastic scattering data included in the fit are those of As70 and La71.

1 to 7 MeV, smooth curve through measurements of La71, Po70, and Ho69, constrained to be consistent with total and reaction cross section measurements.

7 to 14 MeV, smooth curve through measurements of Ho69, Co69, Te62, Va70, and Va65.

14 to 20 MeV, optical model extrapolation from 14-MeV data.

MT=4. Inelastic Cross Section

Threshold to 20 MeV, sum of MT=51-85.

MT=51-61. Inelastic Cross Sections To Discrete States

MT=51	Q=-0.717 MeV	MT=55	Q=-4.774 MeV	MT=59	Q=-5.923 MeV
52	-1.740	56	-5.114	60	-6.029
53	-2.154	57	-5.166	61	-6.133
54	-3.585	58	-5.183		

Threshold to 20 MeV, based on (n, n') measurements of Po70, Co69, Ho69, and Va70, and the $(n, x\gamma)$ measurements of Da56, Da60, and Ne70 using a gamma-ray decay scheme deduced from La66, Al66, Se66A, and Se66B. Hauser-Feshbach calculations were used to estimate shapes and relative magnitudes where experimental data were lacking.

MT=62-85. Inelastic Cross Sections to Groups of Levels

These sections were used to group (n, n') cross sections into 0.5-MeV wide excitation energy bins between $E_x=6.5$ and 18.0 MeV. This representation was used in lieu of MF=5, MT=91 to more accurately represent kinematic effects.

Threshold to 20 MeV, integrated cross section obtained by subtracting the sum of MT=2, 51-61, 103, 104, 107, and 113 from MT=1. Cross section distributed among the bands with an evaporation model using a nuclear temperature given by $T = 0.9728 \sqrt{E_n}$ (units MeV), taken from Ir67.

MT=102. (n, γ) Cross Section

0 to 1 MeV, assumed $1/V$ dependence with thermal value of 0.5 barn.

1 to 20 MeV, assumed negligible, set equal to zero.

MT=103. (n, p) Cross Section

Threshold to 20 MeV, sum of MT=700-703.

MT=104. (n, d) Cross Section

Threshold to 20 MeV, based on $^9\text{Be}(d, n)^{10}\text{B}$ measurements of Si65 and Ba60, and the (n, d) measurement of Va65.

MT=107. (n, α) Cross Section

0 to 20 MeV, sum of MT=780 and 781.

MT=113. $(n, t2\alpha)$ Cross Section

0 to 2.3 MeV, based on a single-level fit to the resonance measured at 2 MeV by Da61, assuming L=0 incoming neutrons and L=2 outgoing tritons.

2.3 to 20 MeV, smooth curve through measurements of Fr56 and Wy58, following general shape of Da61 measurement from 4 to 9 MeV.

MT=700-703. (n,p) Cross Section to Discrete Levels

0 to 20 MeV, crudely estimated from the calculations of Po70 and the (n,x γ) measurements of Ne70. Cross section for MT=700 assumed identical to MT=113 below 1 MeV. Gamma-ray decay scheme for ^{10}B from La66.

MT=780. (n, α_0) Cross Section

0 to 1 MeV, calculated from the R-matrix parameters described for MT=1. Experimental (n, α_0) data input to the fit were those of Ma68 and Da61. In addition, the angular distributions of Va72 for the inverse reaction were included in the analysis.

1 to 20 MeV, based on Da61 measurements, with smooth extrapolation from 8 to 20 MeV. Da61 measurement above approximately 2 MeV was renormalized by factor of 1.4.

MT=781. (n, α_1) Cross Section

0 to 1 MeV, calculated from the R-matrix parameters described for MT=1. Experimental (n, α_1) data included in the fit are those of Sc76. In addition, the absolute differential cross-section measurements of Se76 were included in the analysis.

1 to 20 MeV, smooth curve through measurements of Da61 and Ne70, with smooth extrapolation from 15 to 20 MeV. The Da61 data above approximately 2 MeV were renormalized by a factor of 1.4.

File 4. Neutron Angular Distributions

MT=2. Elastic Angular Distributions

0 to 1 MeV, calculated from the R-matrix parameters described for MF=3, MT=1. Experimental angular distributions input to the fit for both the elastic scattering cross section and polarization were obtained from the measurements of La71. Assignments for resonances above the neutron threshold are based on La71.

1 to 14 MeV, smoothed representation of Legendre coefficients derived from the measurements of La71, Ha73, Po70, Ho69, Co69, Va69, and Va65, constrained to match the R-matrix calculations at $E_n=1$ MeV.

14 to 20 MeV, optical model extrapolation of 14-MeV data.

MT=51-85. Inelastic Angular Distributions

Threshold to 20 MeV, assumed isotropic in center-of-mass.

File 12. Gamma Ray Multiplicities

MT=102. Capture Gamma Rays

0 to 20 MeV, capture spectra and transition probabilities derived from the thermal data of Th67, after slight changes in the probabilities and renormalization to the energy levels of Aj75. The LP flag is used to conserve energy and to reduce significantly the amount of data required in the file. Except for the modification due to the LP flag, the thermal spectrum is used over the entire energy range.

MT=781. 0.4776-MeV Photon from the (n, α_1) Reaction

0 to 20 MeV, multiplicity of 1.0 at all energies.

File 13. Gamma-Ray Production Cross Sections

MT=4. $(n, n\gamma)$ Cross Sections

Threshold to 20 MeV, obtained from MT=51-61 using ^{10}B decay scheme deduced from La66, Al66, Se66A, and Se66B.

MT=103. $(n, p\gamma)$ Cross Sections

Threshold to 20 MeV, obtained from MT=701-703 using ^{10}B decay scheme deduced from La66.

File 14. Gamma Ray Angular Distributions

MT=4. $(n, n\gamma)$ Angular Distributions

Threshold to 20 MeV, assumed isotropic.

MT=102. (n, γ) Angular Distributions

0 to 20 MeV, assumed isotropic.

MT=103. $(n, p\gamma)$ Angular Distributions

Threshold to 20 MeV, assumed isotropic.

MT=781. $(n, \alpha_1\gamma)$ Angular Distribution

0 to 20 MeV, assumed isotropic.

File 33. Cross-Section Covariances

The relative covariances for the most important reactions open below 1 MeV are given in File 33. These are calculated directly from the covariances of the R-matrix parameters, using first-order error propagation.

MT=2, 780, 781. (n,n) (n, α_0), and (n, α_1) Covariances.

0 to 1 MeV, relative covariances among these three reactions are entered explicitly using NI-type sub-subsections in the LB=5 (direct) representation.

1 to 20 MeV, all covariances set equal to zero. Not intended for use in this energy range.

MT=1, 107. Total and (n, α) Covariances.

0 to 1 MeV, for compactness, these covariances are constructed from those described above, using NC-type sub-subsections. The constructed covariances for the total cross section therefore neglect contributions from the (n, γ), (n,p), (n,t), and (n,n₁) reactions which are all presumed to be small in magnitude below 1 MeV. Note that although the total cross-section covariances are entered in the NC-type (derived) format, total cross-section data were included in the fit, and they influenced all the calculated covariances.

1 to 20 MeV, set equal to zero. Not intended for use in this energy range.

REFERENCES

Aj75 F. Ajzenberg-Selove, Nucl. Phys. A248, 6 (1975).
Al66 D. E. Alburger et al., Phys. Rev. 143, 692 (1966).
As70 A. Asami and M. C. Moxon, J. Nucl. Energy 24, 85 (1970).
Ba60 R. Bardes and G. E. Owen, Phys. Rev. 120, 1369 (1960).
Be56 R. L. Becker and H. H. Barschall, Phys. Rev. 102, 1384 (1956).
Bo51 C. K. Bockelman et al., Phys. Rev. 84, 69 (1951).
Bo69 D. Bogart and L. L. Nichols, Nucl. Phys. A125, 463 (1969).
Co52 J. H. Coon et al., Phys. Rev. 88, 562 (1952).
Co54 C. F. Cook and T. W. Bonner, Phys. Rev. 94, 651 (1954).
Co67 S. A. Cox and F. R. Pontet, J. Nucl. Energy 21, 271 (1967).
Co69 J. A. Cookson and J. G. Locke, Nucl. Phys. A146, 417 (1970).
Co73 M. S. Coates et al., private communication to L. Stewart (1973).
Da56 R. B. Day, Phys. Rev. 102, 767 (1956).
Da60 R. B. Day and M. Walt, Phys. Rev. 117, 1330 (1960).
Da61 E. A. Davis et al., Nucl. Phys. 27, 448 (1961).
Di67 K. M. Diment, AERE-R-5224 (1967).
Fo61 D. M. Fossan et al., Phys. Rev. 123, 209 (1961).
Fr56 G. M. Frye and J. H. Gammel, Phys. Rev. 103, 328 (1956).
Ha73 S. L. Hausladen, Thesis, Ohio Univ. COO-1717-5 (1973).
Ho69 J. C. Hopkins, private communication to LASL (1969).
Ir67 D. C. Irving, ORNL-TM-1872 (1967).
La66 T. Lauritsen and F. Ajzenberg-Selove, Nucl. Phys. 78, 1 (1966).
La77 R. O. Lane et al., Phys. Rev. C4, 380 (1971).
Ma68 R. L. Macklin and J. H. Gibbons, Phys. Rev. 165, 1147 (1968).
Mo66 F. P. Mooring et al., Nucl. Phys. 82, 16 (1966).
Ne54 N. G. Nereson, LA-1655 (1954).

Ne70 D. O. Nellis et al., Phys. Rev. C1, 847 (1970).
Po70 D. Porter et al., AWRE 0, 45/70 (1970).
Sc76 R. A. Schrack et al., Proc. ICINN (ERDA-CONF-760715-P2), 1345 (1976).
Se76 R. M. Sealock and J. C. Overley, Phys. Rev. C13, 2149 (1976).
Se66A R. E. Segel and R. H. Siemssen, Phys. Lett. 20, 295 (1966).
Se66B R. E. Segel et al., Phys. Rev. 145, 736 (1966).
Si65 R. H. Siemssen et al., Nucl. Phys. 69, 209 (1965).
Sp73 R. R. Spencer et al., EANDC(E) 147, AL (1973).
Te62 K. Tesch, Nucl. Phys. 37, 412 (1962).
Th67 G. E. Thomas et al., Nucl. Instr. Meth. 56, 325 (1967).
Ts63 K. Tsukada and O. Tanaka, J. Phys. Soc. Japan 18, 610 (1963).
Va63 V. Valkovic et al., Phys. Rev. 139, 331 (1965).
Va70 B. Vaucher et al., Helv. Phys. Acta, 43, 237 (1970).
Va72 L. Van der Zwan and K. W. Geiger, Nucl. Phys. A180, 615 (1972).
Wi55 H. B. Willard et al., Phys. Rev. 98, 669 (1955).
Wy58 M. E. Wyman et al., Phys. Rev. 112, 1264 (1958).

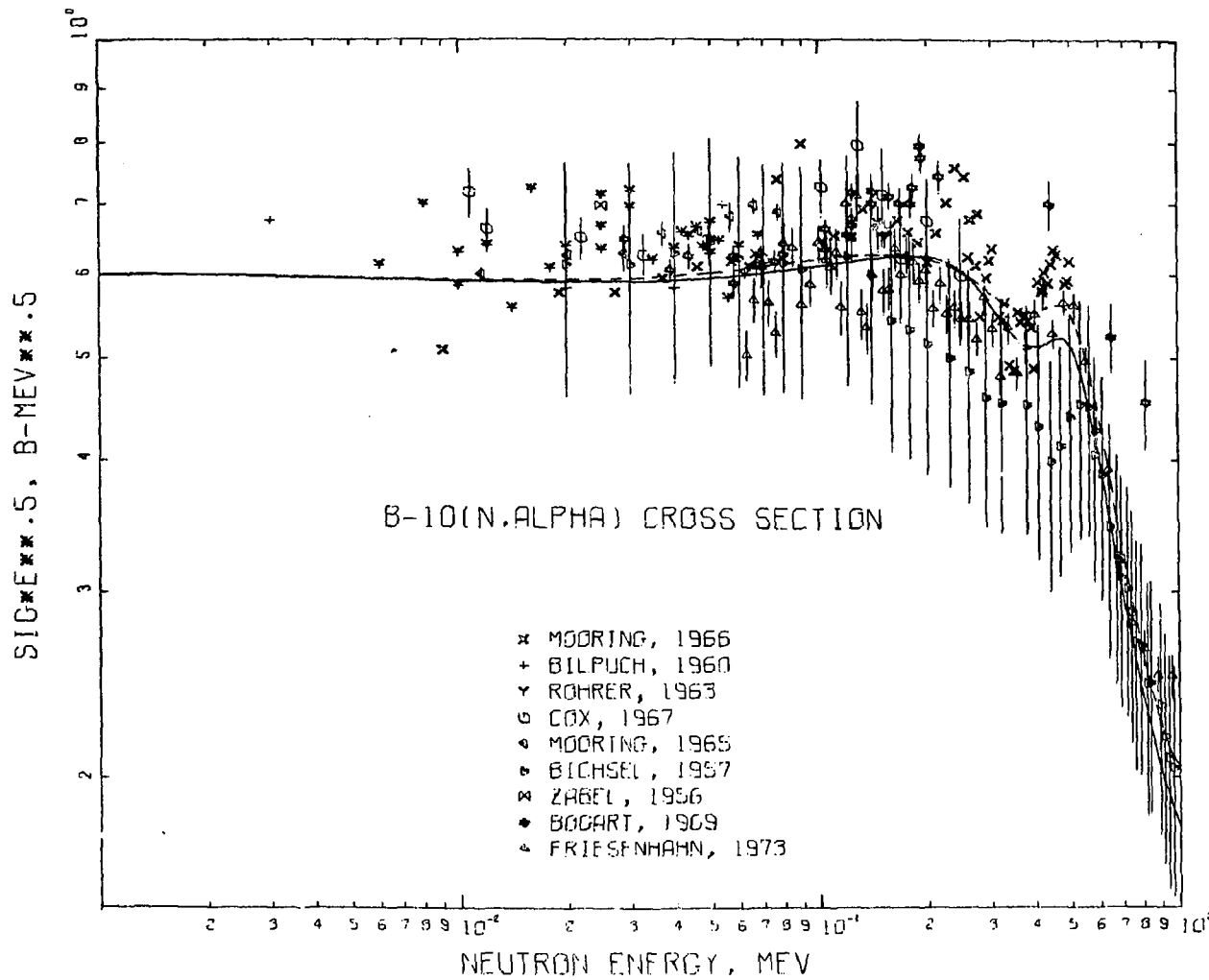


Fig. 1.
 Experimental and evaluated data for the $^{10}\text{B}(\text{n},\alpha)^7\text{Li}$ reaction from 1 keV to 1 MeV.
 The solid curve is ENDF/B-V and the dashed curve is ENDF/B-IV. References for
 experimental data are given in LA-6518-MS.

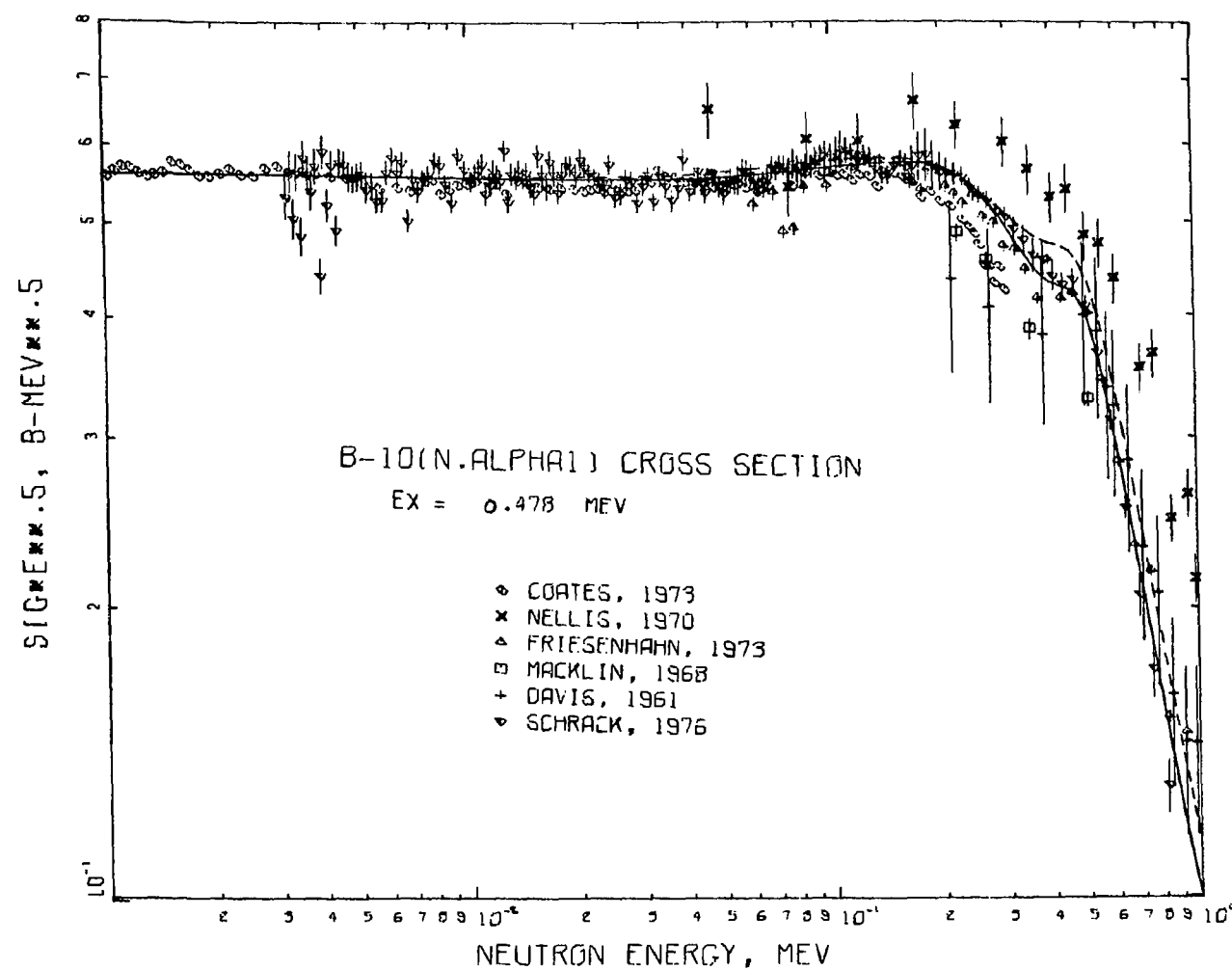


Fig. 2.

Experimental and evaluated data for the $^{10}\text{B}(n, \alpha_1\gamma)^7\text{Li}$ reaction from 1 keV to 1 MeV. The solid curve is ENDF/B-V and the dashed curve is ENDF/B-IV. References for experimental data are Co73, Da61, Ma68, Ne70, Sc76, and those included in LA-6518-MS.

SUMMARY DOCUMENTATION FOR ^{14}N

by

P. G. Young and D. G. Foster, Jr.
Los Alamos Scientific Laboratory
Los Alamos, New Mexico

I. SUMMARY

The ^{14}N evaluation for ENDF/B-V (MAT 1275) is the same as Version IV except for updating of the covariance data format. Basic documentation for the evaluation is given in LA-4725 (1972), and revisions are described in LA-5375-PR (1973). The evaluation covers the energy range 10^{-5} eV to 20 MeV.

II. ENDF/B-V FILES

File 1. General Information

MT=451. Descriptive Data

Thinning Note: Cross section data in MF=3 and 13 for MT=4, 16, 51-82, 102-108, 700-704, 720-723, 740-741, and 780-790 were thinned using a 2.5% thinning criterion. Similarly, in MF=4 the MT=2, 51-62 angular distributions were thinned using the requirement that the interpolated angular distribution have an RMS average deviation from a fine-grid set of less than 2.5% and that the maximum excursion at any angle be less than 5%.

File 2. Resonance Parameters

MT=151. Effective Scattering Radius = 0.89014×10^{-12} cm.

Resonance parameters not given.

File 3. Neutron Cross Sections

The 2200 m/s cross sections are as follows:

MT=1	Sigma = 11.851 barns
MT=2	Sigma = 9.957 barns
MT=3	Sigma = 1.894 barns
MT= 102	Sigma = 0.075 barns
MT= 103	Sigma = 1.819 barns

MT=1. Total Cross Section

Zero to 1 eV, $\sigma_T = 9.957 + 0.3013/\sqrt{E}$ (b), from absorption of 1.894 b at 2200 m/s and Me49 data above 1 eV.

1 eV to 10 keV, from data of Me49.

10 keV to 0.5 MeV, from Hi52, Bi59, Hu61, and Bi62 with energy scales adjusted to match, normalized separately to join time-of-flight data smoothly at 0.5 MeV.

0.5 MeV to 20 MeV, from Ca70, He70, and Fo71 using Ca70 alone at sharp resonances.

Smoothed by appropriate fits. Log-log interpolation is good to 1.3% to 0.4 MeV. Linear interpolation is good to 0.5% from 0.4 to 20 MeV. Absolute error less than 1% above 0.75 MeV, but may rise to 5% in eV region.

MT=2. Elastic Scattering Cross Section

Zero to 10 MeV, subtracted evaluated non-elastic cross section from the evaluated total, although direct elastic measurements of Fo55, Fo66, Bo57, Ch61, Ba67, Ph61, and Ne70 were considered.

10 to 12 MeV, Tr⁺ ion region.

12 to 20 MeV, Based upon data of Ch61, Ba67, Ne70, Ba63, and Bo68.

MT=4. Total Inelastic Cross Section

Sum of MT=51-82 cross sections

MT=16. (n,2n) Cross Section

Based upon data of Fe60, Br61, Bo65, and Pr60, estimated ± 30 per cent error.

MT=51-62. Inelastic Cross Section to Discrete States

MT=51	Q=-2.313 MeV	MT=55	Q=-5.691 MeV	MT=59	Q=-7.028 MeV
52	-3.945	56	-5.834	60	-7.966
53	-4.913	57	-6.198	61	-8.061
54	-5.106	58	-6.444	62	-8.489

Threshold to 15 MeV, from (n,ny) data of Di69, Or69, Cl69, Bu69, Ny69, Co68, and extensive measurements of Di73.

Above 15 MeV, smooth extrapolations.

MT=63-82 Inelastic Cross Section to Groups of Discrete States

Cross section is grouped into excitation energy bins of 0.5 MeV width centered above Q-values between -9.25 MeV and -18.75 MeV.

The integrated cross section over these bands was adjusted such that the difference between the total and non-elastic cross sections agreed with elastic data (see MT=2). The division of the cross section among the bands is based on Hauser-Feshbach and nuclear temperature calculations. Note that (n,np) and (n,n α) reactions are included with the discrete and binned inelastic data through use of LR flags (LR=28 and 22, respectively).

MT=102. Radiative Capture

Zero to 0.25 MeV, 1/V from 75 mb (\pm 10%) at thermal (Ju63).

0.25 to 1 MeV. Transition region.

1 to 20 MeV. Deduced from $^{14}\text{N}(p,\gamma)^{15}\text{O}$ data of Ku70, assuming charge independence. Energy scale adjusted to match foot hills of (p, γ) giant resonance to resonance clusters observed in ^{15}N compound nucleus.

MT=103. (n,p) Cross Section

Sum of MT=700-704.

MT=104. (n,d) Cross Section

Sum of MT=720-723.

MT=105. (n,t) Cross Section

Sum of MT=740-741.

MT=107. (n, α) Cross Section

Sum of MT=780-790.

MT=108. (n,2 α) Cross Section

Based on Li52, Mo67, and Hauser-Feshbach calculation.

MT=700. (n,p) Cross Section to ^{14}C Ground State

Zero to 4 MeV, from data of Jo50 and Ga59.

4 to 13 MeV, from inverse reaction data of Wo67.

13 to 20 MeV, smooth extrapolation.

MT=701-704, (n,p) Cross Sections to ^{14}C Excited States

MT=701 Q=-5.468 MeV Ex=6.095 MeV (6.58, 6.89-MeV level excitation cross sections are also included)

MT=702 Q=-6.102 MeV Ex=6.728 MeV

MT=703 Q=-6.385 Ex=7.012 MeV
704 -6.711 7.337

Threshold to 15 MeV, from (n,p γ) data of Or69, Di69, Cl69, Bu69, and Ny69.

15 to 20 MeV, smooth extrapolations.

MT=720. (n,d) Cross Section to ^{13}C Ground State.

Threshold to 15 MeV, from inverse cross section data of Ch61, Be63 near threshold and direct data of Mi68, Fe67, Ca57, and Za63 at 14 MeV.

15 to 20 MeV, smooth extrapolations.

MT=721-723 (n,d) Cross Section to Excited ^{13}C Levels

MT=721 Q=-8.411 MeV Ex=3.086 MeV
722 -9.009 3.684
723 -9.179 3.854

Threshold to 15 MeV, direct data of Fe67, Za63, Ca57 and (n,d γ) data of Or69 and Di69 below 13 MeV.

15 to 20 MeV, smooth extrapolations.

MT=740-741. (n,t) Cross Sections to ^{12}C Ground and 4.439 MeV-Excited State.

Threshold to 15 MeV, direct data of Ca59, Sc66, Re67, and Fe67.

15 to 20 MeV, smooth extrapolations.

MT=780-790. (n, α) Cross Section to Discrete ^{11}B States

MT=780 Q=-0.157 MeV Ex=0.000 MeV
781 -2.282 2.124
782 -4.602 4.444
783 -5.176 5.019
784 -6.900 6.743
785 -6.950 6.793
786 -7.453 7.296
787 -8.153 7.996
788 -8.723 8.566
789 -9.082 8.925
790 -9.342 9.185

Threshold to 6 MeV, from direct data of Jo50, Ge59, and Sc66.

6 to 15 MeV, used above direct data, together with (n, $\alpha\gamma$) data of Ha59, Di69, Or69, Ny69, and Bu69. Near 14 MeV, direct (n, α) data of Li52, Ba68, Le68, and Ma68 were also used.

15 to 20 MeV, smooth extrapolations.

File 4. Secondary Neutron Angular Distributions

MT=2. Elastic Angular Distributions

Zero to 8 MeV, based upon resonance theory analysis of data of Fo55, Fo66, Bo57, Ch61, and Ba67, using parameters from total and partial cross section analyses and Aj70.

8 to 15 MeV, based upon data of Ch61, Ba67, Ne70, and Ba63.

15 to 20 MeV, based upon optical model calculation.

MT=16. Angular Distribution for (n,2n) Reaction

In the absence of data, isotropy in the cm system is assumed, and the corresponding 3-body phase-space transformed to the laboratory system is given. For any reasonable cm distribution, the strong forward peaking of the transformation will dominate. Normalized for trapezoidal integration.

MT=51 to 62. Angular Distributions for Inelastic Scattering

Above 7 MeV taken from proton data of Do64, Ha70, and Od60 assuming charge symmetry, and neutron data of Ba63. Threshold shapes modeled after Hauser-Feshbach calculations.

MT=63-82. Angular Distributions for Inelastic Scattering

Assumed isotropic in cm at all energies.

File 5. Energy Distribution of Secondary Neutrons

MT=16. Spectrum of (n,2n) Secondary Neutrons

In the absence of data, only the 3-body phase-space distribution is given. Normalized for trapezoidal integration.

File 12. Photon Multiplicities

MT=102. (n, γ) Multiplicities

Zero to 0.25 MeV, thermal spectrum based primarily upon measurements of Th67, Jo69, Gr68, and Mo62. LP flags were used to designate primary gamma rays.

0.25 to 1 MeV. Transition region where thermal spectrum is phased into single ground-state transition.

1 to 20 MeV, deduced from $^{14}\text{N}(p,\gamma)^{15}\text{O}$ data of Ku70, who observed no significant transitions except to ground state.

File 13. Photon-Production Cross Sections

All (n,γ) cross sections agree with the excitation cross sections in MF=3 via the relevant decay scheme (Aj68, Aj70). However, MT=104, 105 include contributions from $(n,np\gamma)$ and $(n,nd\gamma)$.

MT=4. $(n,n\gamma)$ Cross Section

From data of Ha59, Di69, Or69, Cl69, Bu69, Ny69, Co68, and Di73.

MT=103. $(n,p\gamma)$ Cross Section

From data of Di69, Or69, Bu69, Ny69, and Cl69.

MT=104. $(n,nd\gamma) + (n,np\gamma)$ Cross Section

From data of Di69, Or69, Bu69, Ny69, and Cl69.

MT=105. $(n,t\gamma) + (n,nd\gamma)$ Cross Section

$(n,t\gamma)$ estimated from (n,t) as discussed under MF=3 MT=741.
 $(n,nd\gamma)$ estimated from MT=63-82.

MT=107. $(n,\alpha\gamma)$ Cross Section

From (n,α) data of Ga59, Sc66 and $(n,\alpha\gamma)$ data of Ha59, Di69, Ny69, Or69, and Bu69.

File 14. Photon Angular Distributions

Data on 9 strongest lines from inelastic scattering and particle reactions taken from Mo64.

MT=4. Inelastic Scattering to ^{14}N

The 1.63- and 4.91-MeV gamma are given as anisotropic. All remaining gamma rays are isotropic.

MT=102. (n,γ) Angular Distributions

Zero to 0.4 MeV, all photons are isotropic.

0.4 to 20 MeV, anisotropic distribution for the single ground state transition is based upon $^{14}\text{N}(p,\gamma)^{15}\text{O}$ data by Ku70.

MT=103. $(n,p\gamma)$ Angular Distributions

All isotropic.

MT=104. $(n,np\gamma)$ and $(n,nd\gamma)$ Angular Distributions

All isotropic except 3.85-MeV gamma ray.

MT=105. (n,nd γ) and (n,t γ) Angular Distributions

All isotropic.

MT=107. (n, $\alpha\gamma$) Angular Distributions

All isotropic.

File 33. Neutron Cross Section Corvariances

MT=1,2,4,102, 103, and 107. Smooth Cross Section Covariances

Covariances are based upon estimates of the uncertainty in the experimental measurements and theoretical calculations used in the evaluation. Format updated for Version V. Derived covariances are included explicitly.

REFERENCES

Aj68 F. Ajzenberg-Selove, and T. Lauritsen, (HAV), Nucl. Phys. A114, 1 (1968).
Aj70 F. Ajzenberg-Selove (PEN), Nucl. Phys. A152, 1 (1970).
Ba63 R. W. Bauer et al., (LRL), Nucl. Phys. 47, 241 (1963).
Ba67 R. W. Bauer et al., (LRL), Nucl. Phys. A93, 673 (1967).
Ba68 R. Bachinger and M. Uhl, (IRK), Nucl. Phys. A116 673 (1968).
Be63 R. E. Benenson and R. Yaramis, (COL), Phys. Rev. 129, 720 (1963).
Bi59 E. G. Bilpuch et al., (DKE), Private communication to BNL (1959),
Bi62 E. G. Bilpuch et al., (DKE), Private communication to R. J. Howerton (1962).
Bo57 N. A. Bostrom et al., (TNC), WADC-TR-57-446 (1957).
Bo65 M. Bormann et al., (HAM), Nucl. Phys. 63, 438 (1965).
Bo68 F. Boreli et al., (TEX), Phys. Rev. 174, 1221 (1968).
Br61 O. D. Brill et al., (RUS), Sov. Phys. Dokl. 6, 24 (1961).
Bu69 P. S. Buchanan (TNC). Private communication (1969).
Ca57 R. R. Carlson (LAS), Phys. Rev. 107, 1094 (1957).
Ca70 A. D. Carlson and R. J. Cerbone, (GGA), Nucl. Sci. Eng. 42, 28 (1970).
Ch61 L. F. Chase et al., (LOK), AFSWC-TR-61-15 (1961).
Cl69 G. Clayeux and G. Grenier (FR), CEA-R-3807 (1969).
Co68 H. Condé et al., (SWD), Neut. Cross Sect. and Tech. Conf., Washington, D.C., p. 763 (1968).
Di69 J. K. Dickens and F. G. Perey, (ORL), Nuc. Sci. Eng. 36, 280 (1969).
Di70 J. K. Dickens et al., ORNL-4864 (1973).
Do64 D. F. Donovan et al., (BNL), Phys. Rev. 133, B113 (1964).
Fe60 J. M. Ferguson and W. E. Thompson, (NRD), Phys. Rev. 118, 228 (1960).
Fe67 P. Fessenden and D. R. Maxson, (BRN), Phys. Rev. 158, 948 (1967).
Fo55 J. L. Fowler and C. H. Johnson, (ORL), Phys. Rev. 98, 728 (1955).
Fo66 J. L. Fowler et al., (ORL), Neut. Cross Sect. and Tech. Conf., Wash. D.C., p. 653 (1968).
Fo71 D. G. Foster, Jr. and W. Glasgow, (PNL), Phys. Rev. C3, 576 (1971).
Ga59 F. Gabbard et al., (RIC), Nucl. Phys. 14, 277 (1959).
Gr68 R. C. Greenwood, (MTR), Phys. Lett. 27B, 274 (1968).
Ha59 H. E. Hall and T. W. Bonner, (RIC), Nucl. Phys. 14, 295 (1959).
Ha70 L. Hansen, (LRL), Private communication (1970).
He70 H. T. Heaton et al., (NBS), Bull. Am. Phys. Soc. 15, 568 (1970).

Hi52 J. J. Hinckey et al., (MIT), Phys. Rev. 86, 483 (1952).
Hu61 C. M. Huddleston and F. P. Mooring, (ANL), ANL-6376, p. 13 (1961).
Jo50 C. H. Johnson and H. H. Barschall, (WIS), Phys. Rev. 80, 818 (1950).
Jo69 L. Jonsson and R. Hardell, (SWD), Symposium on Neutron Capture Gamma Rays, Studsvik (1969).
Ju63 E. T. Jurney and H. T. Motz, (LAS), ANL-9797, p. 241 (1963).
Ku70 H. M Kuan et al., (STF), Nucl. Phys. A151, 129 (1970).
Le68 B. Leroux et al., (FR), Nucl. Phys. A116, 196 (1968).
Li52 A. B. Lillie, (RIC), Phys. Rev. 87, 716 (1952).
Ma68 D. P. Maxson et al., (BRN), Nucl. Phys. A110, 609 (1968).
Me49 E. Melkonian, (COL), Phys. Rev. 76, 1750 (1949).
Mi68 D. Miljanio et al., (YUG), Nucl. Phys. A106, 401 (1968).
Mo62 H. T. Motz et al., (LAS), Pile Neutron Research in Physics (IAEA, Vienna 1962), p. 225
Mo64 I. L. Morgan et al., (TNC), TNC Nucl. Phys. Div. Ann. Rpt. (Aug. 1964).
Mo67 J. Mosner et al., (GER), Nucl. Phys. A103, 238 (1967).
Ne70 D. O. Nellis, (TNC), Private communication (1970).
Ny69 K. Nyberg, (SWD), Private communication to L. Stewart (1969).
Od60 Y. Oda et al., (TOK), J. Phys. Soc. Japan 15, 760 (1960).
Or69 V. J. Orphan et al., (GGA), GA-8006 (1969).
Ph61 D. D. Phillips (LAS), Private communication to R. J. Howerton (1961).
Pr60 J. T. Prudhomme et al., (TNC), AFSWC-TR-60-30 (1960).
Re67 D. Rendic (YUG), Nucl. Phys. A91, 604 (1967).
Sc66 W. Scobel et al., (HAM), Z. Physik 197, 124 (1966).
Th67 G. F. Thomas et al., (ANL), Nucl. Instr. Meth. 56, 325 (1967).
Wo67 C. Wong et al., (LRL), Phys. Rev. 160, 769 (1967).
Za63 M. R. Zatzick and D. R. Maxson, (BRN), Phys. Rev. 129, 1728 (1963).

SUMMARY DOCUMENTATION FOR ^{15}N

by

E. D. Arthur, P. G. Young, and G. M. Hale
Los Alamos Scientific Laboratory
Los Alamos, New Mexico

I. SUMMARY

The ^{15}N for ENDF/B-V (MAT 1307) is a new evaluation performed originally in 1975 and updated in 1978 for Version V. The data set covers the energy range 10^{-5} eV to 20 MeV and is partially documented in LA-6123-PR (1975) and LA-6164-PR (1975).

II. ENDF/B-V FILES

File 1. General Information

MT=451. Descriptive Data

General approach: The lack of experimental data, with the exception of total cross section measurements, led us to obtain cross sections with a variety of nuclear model codes. We used an energy dependent R-matrix analysis to fit the total cross section data of Ze71 for neutron energies from 0.8 to 5.4 MeV. As a starting point we used the level scheme reported in Ze71. Also used in the R-matrix analysis were the elastic angular distributions of Si62 and Ze71 in the energy range from 1.9 to 3.64 MeV. The parameters of the R-matrix analysis were then used to generate cross sections and to determine Legendre coefficients in the range from 1.0E-05 to 5.4 MeV. In the energy region from 6 to 20 MeV we used two statistical model codes to generate cross sections. With the first, COMNUC, we computed the angular distributions of elastically scattered neutrons. The Legendre coefficients obtained were then joined smoothly with those from the R-matrix analysis. We also obtained angular distributions of neutrons leading to the first seven excited states of ^{15}N . To generate neutron transmission coefficients for this part of the analysis, we used the global optical model parameters of Wilmore and Hodgson as reported by Pe74, and adjusted them to give good agreement with the measured total cross section. The generation of capture, inelastic, and non-elastic cross sections as well as neutron, gamma-ray, and charged-particle spectra was done with the statistical model code, GNASH. This newly developed code (Yo77) is based largely on the statistical model formalism of Uh71. Again, neutron

transmission coefficients were based on the optical model parameters of Wilmore and Hodgson. Transmission coefficients were generated for protons, deuterons, and ^4He , with the appropriate global forms reported in Pe74. For tritons we used the global parameters for ^3He reported in Pe74 since these were consistent with triton optical model parameters for individual light nuclei as compiled by Pe74. The Gilbert-Cameron level density model was used with standard values for level density parameters (Gi64). To account for direct and semi-direct processes we used the pre-equilibrium model of Blann and Cline (Cl71) and assumed a 10% preequilibrium fraction.

File 2. Resonance Parameters

MT=151. Effective scattering radius = 0.592916×10^{-12} cm

Resonance parameters not given.

File 3. Neutron Cross Sections

The 2200 m/s Cross Sections are:

MT= 1 Sigma = 4.4185 b
MT= 2 Sigma = 4.418 b
MT= 102 Sigma = 24.0E-06 b

MT=1. Total Cross Section

From 1.0E-05 eV to 5.4 MeV total cross section values are based on the R-matrix analysis described above. From 5.5 to 20 MeV, the evaluated cross section is based on the smoothed results of Ze71.

MT=2. Elastic Scattering Cross Section

Zero to 20 MeV, subtracted evaluated non-elastic from total to give elastic cross section.

MT=4. Inelastic Cross Section

Sum of MT=22, 28, 51-57, and 91 cross sections.

MT=16. (n,2n) Cross Section

Based on smooth curve drawn through results of the statistical model calculations described before.

MT=22. (n,n α) Cross Section

Based on smoothed results of statistical model calculation.

MT=28. (n,np) Cross Section

Based on smoothed results of statistical model calculation.

MT=51-57. Inelastic Cross Section to Discrete States

MT=51	Q=-5.27 MeV	MT=55	Q=-7.301 MeV
52	-5.299	56	-7.566
53	-6.324	57	-8.313
54	-7.155		

MT=91. (n,n) To Continuum

Continuum defined to begin at 0.1 MeV above last ^{15}N discrete level included in calculation, i.e., continuum begins at 8.413 MeV.

MT=102. (n, γ) Cross Section

Zero to 0.010 MeV, 1/V from 24.0E-06 b at thermal

6 to 20 MeV calculated from statistical model with Axel (Ax62) giant dipole resonance approximation for gamma-ray transmission coefficients.

0.010 to 6 MeV, cross section based on smoothed curve from region where 1/V dependence ends to region where calculated values begin.

MT=103. (n,p) Cross Section

Sum of MT=700, 701, and 718 cross sections.

MT=104. (n,d) Cross Section

Sum of MT=720, 721, 722, and 738 cross sections.

MT=105. (n,t) Cross Section

Sum of MT=740, 741, and 758 cross sections.

MT=107. (n, α) Cross Section

Sum of MT=780-785 and 798 cross sections.

MT=700, 701. (n,p) Cross Section to ^{15}C Ground and First Excited States

MT=700	Q=-8.990 MeV	EX=0. MeV
701	-9.737	0.747

MT=738. (n,p) To Continuum States of ^{15}C

Continuum defined to begin at 0.85 MeV, just above first excited state.

MT=720-722. (n,d) Cross Section to ^{14}C Ground, First, and Second Excited States

MT=720	Q=-7.984	MeV	EX=0.	MeV
721	-14.079		6.095	
722	-14.567		=6.583	

MT=738. (n,d) To Continuum States of ^{14}C

Continuum defined to begin at 6.681 MeV, just above second excited level in ^{14}C .

MT=740-742. (n,t) Cross Section to ^{13}C Ground, First and Second Excited States

MT=740	Q=-9.902	MeV	EX=0.	MeV
741	-12.992		3.09	
742	-13.586		3.684	

MT=758. (n,t) To Continuum States of ^{13}C

Continuum begins at 3.784 MeV, above second excited level in ^{13}C .

MT=780-785. (n, α) Cross Sections to ^{12}B Ground and First Five Excited States

MT=780	Q=-7.623	MeV	EX=0.	MeV
781	-8.576		0.953	
782	-9.297		1.674	
783	-10.244		2.621	
784	-10.343		2.72	
785	-11.013		3.39	

MT=798. (n, α) To Continuum States of ^{12}B

Continuum begins at 3.49 MeV, just above fifth excited state in ^{12}B .

File 4. Secondary Neutron and Charged Particle Angular Distributions

MT=2. Elastic Angular Distributions

Zero to 5.4 MeV, based on results obtained from R-matrix theory analysis.

6 to 20 MeV, based on optical model calculation

MT=16. Angular Distribution for (n,2n) Reaction

In the absence of data, isotropy in the laboratory system is assumed.

MT=22. Angular Distribution of Neutrons from (n,n α)

Reaction assumed isotropic in the laboratory system.

MT=28. Angular Distribution of Neutrons from (n,np) Reaction

Assumed isotropic in the laboratory system.

MT=51-57. Angular Distribution Calculated Using Hauser-Feshbach Theory.

MT=718. Angular Distribution of Protons from (n,p) Reaction

Assumed isotropic in the laboratory system.

MT=719. Angular Distribution of Protons from (n,np) Reaction

Assumed isotropic in the laboratory system.

MT=738. Angular Distribution of Deutrons from (n,d) Reaction

Assumed isotropic in the laboratory system.

MT=758. Angular Distribution of Tritons from (n,t) Reaction

Assumed isotropic in the laboratory system.

MT=798. Angular Distribution of Alphas from (n, α) Reaction

Assumed isotropic in the laboratory system.

MT=799. Angular Distribution of Alphas from (n,n α)

Assumed isotropic in the laboratory system.

File 5. Energy Distribution of Secondary Neutrons and Charged Particles

MT=16, 22, 28, 91, 718, 758, and 798. Calculated with Statistical Model Code, GNASH (Yo77).

MT=719. Used for Proton Spectra from (n,np) Reaction

MT=799. Used for Alpha Spectra from (n,n α) Reaction

File 13. Photon Production Cross Sections

MT=4, 16, 103, 104, 105 and 107, (n,n' γ), (n,2n γ), (n,p γ), (n,d γ), (n,t γ), (n, α γ) Cross Sections

Include both discrete and continuum contributions and were generated in the statistical model calculation with the GNASH code (Yo77).

File 14. Photon Angular Distributions

MT=4. (n,n' γ) to ^{15}N , all isotropic

MT=103. (n,p γ) to ^{15}C , all isotropic

MT=104. $(n, d\gamma)$ to ^{14}C , all isotropic
MT=105. $(n, t\gamma)$ to ^{13}C , all isotropic
MT=107. $(n, \alpha\gamma)$ to ^{12}B , all isotropic
MT=16. $(n, 2n\gamma)$ to ^{14}N , all isotropic

File 15. Energy Distribution of Secondary Photons

MT=4, 16, 103, 104, 105, 107. Generated using statistical model code
GNASH (Yo77).

REFERENCES

Aj70 F. Ajzenberg-Selove, Nucl. Phys. A152, 1 (1973).
Aj71 F. Ajzenberg-Selove, Nucl. Phys. A166, 1 (1971).
Ax62 L. P. Axel, Phys. Rev. 126, 671 (1972).
Cl71 C. K. Cline and M. Blann, Nucl. Phys. A172, 225 (1971).
Fe67 P. Fessenden and D. R. Maxson, Phys. Rev. 158, 948 (1967).
G165 A. Gilbert and A. G. L. Cameron, Can. J. of Phys. 43, 1446 (1965).
Pe74 C. M. Perey and F. G. Perey, Atomic and Nucl. Data Tables 13, 293 (1974).
Si62 C. P. Sikkema, Nucl. Phys. 32, 470 (1962).
U71 M. Uhl, Acta Physica Austria 31, 245 (1971).
Yo77 P. G. Young and E. D. Arthur, LA-6947 (1977).
Ze71 B. Zeitnitz et al., Nucl. Phys. A166, 443 (1971).

SUMMARY DOCUMENTATION FOR ^{16}O

by

P. G. Young, D. G. Foster, Jr., and G. M. Hale
Los Alamos Scientific Laboratory
Los Alamos, New Mexico

I. SUMMARY

The ENDF/B-V evaluation for ^{16}O (MAT 1276) is based upon the Version IV evaluation. The only change made from the Version IV data was to update the formats for the correlated error information in File 33. The evaluation covers the energy range 10^{-5} eV to 20 MeV and is partially documented in LA-5759-PR (1974). See also LA-5375-PR (1973) and LA-4780 (1972).

II. ENDF/B-V FILES

File 1. General Information

MT=451. Descriptive Data.

Thinning Note: Cross section data in MF=3 and 13 for MT=4, 51-89, 103, 104, 107, 780-783 were thinned above $E_n=6$ MeV using the requirement that interpolated values between any two points lie within 2% of the fine-grid value, providing that a certain basic grid (200 keV intervals below $E_n=10$ MeV and 500 keV above $E_n=10$ MeV) be maintained. Below $E_n=6$ MeV, a more stringent requirement of 1% was imposed on MT=780 and 107.

In a similar manner, the MT=2 Legendre coefficients in MF=4 were thinned with the requirement that the interpolated angular distribution have an rms deviation from the fine-grid set of less than 2.5% and that the maximum excursion at any angle be less than 5%.

File 2. Resonance Parameters

MT=151. Effective scattering radius = 0.54614×10^{-12} cm.

Resonance parameters not included.

File 3. Neutron Cross Sections

The 2200 m/s cross sections are as follows:

MT=1 Sigma = 3.7483 b

MT=2 Sigma = 3.7481 b
MT=102 Sigma = 0.1780 mb

MT=1. Total Cross Section

0.0 to 5.7 MeV, essentially calculated from R-Matrix parameters obtained by fitting simultaneously almost all available data for reactions $^{16}\text{O}(\text{n},\text{n})^{16}\text{O}$, $^{16}\text{O}(\text{n},\alpha_0)^{13}\text{C}$, $^{13}\text{C}(\alpha_0,\alpha_0)^{13}\text{C}$ at energies below $E_n=5.7$ MeV. Data for total are smoothed composite of Sc71 and normalized Ci68, with inserts of Ci68, normalized composite Fo73, and normalized Fo61 for narrow structure. Fo73 and Fo61 energy scales adjusted to match Ci68. Resolution corrections applied simultaneously to total and (n,α_0) to give same width and consistent heights to peaks. Level scheme is based on Jo73. 0.44-MeV resonance from normalized data of Ok55. Inserts from the smoothed composite are used over some narrow resonances, and over regions where it appears to better represent the experimental cross section. $^{16}\text{O}(\text{n},\gamma)$ capture cross section has been added at low energies, and the $\text{n}-^{16}\text{O}$ total cross section added in the vicinity of the $\text{n}-^{16}\text{O}$ minimum at $E_n=2.35$ MeV.

5.7 to 20.0 MeV, based on a smoothed, empirical fit to the composite of experimental data described above.

MT=2. Elastic Scattering Cross Section

0.0 to 5.7 MeV, R-matrix calculations.

6 to 11 MeV, obtained by subtracting the sum of MT=4, 102, 103, 104, and 107 from MT=1. However, adjustments were made to certain reaction channels, particularly MT=51, to enhance agreement with the elastic measurements of Ph61, Ch61, and especially Ne72, Ki72, and Bu73.

11 to 14 MeV, smooth curve drawn so as to agree with 14-MeV measurements of Ba63, Mc66, and Be67.

14 to 20 MeV, optical model extrapolation using parameters from fit of 14-MeV data of Ba63, adjusted to give correct total cross sections up to 20 MeV.

MT=4. Inelastic Cross Section

Threshold to 20 MeV, sum of MT=51-89.

MT=51-70. Inelastic Cross Section to Discrete States

MT=51 Q=-6.052 MeV	MT=58 Q=-10.354 MeV	MT=65 Q=-11.63 MeV
52 -6.131	59 -10.952	66 -12.053
53 -6.917	60 -11.080	67 -12.442
54 -7.119	61 -11.096	68 -12.528
55 -8.872	62 -11.26	69 -12.795
56 -9.597	63 -11.44	70 -12.967
57 -9.847	64 -11.521	

Threshold to 20 MeV, MT=52-55, 59, and 60 are based mainly on $(n, n\gamma)$ data of Di70, Or70, Dr70, Bu71, Ny69, Cl69, and En64 below 15 MeV and were extrapolated to 20 MeV with compound nucleus reaction theory calculations. The remaining MT numbers are based on compound nucleus calculations normalized to give an MT=3 in agreement with elastic data of Ba62, Be67, and Mc66 at 14 MeV. At lower energies, adjustments made, especially to MT=51, to enhance agreement with (n, n') measurements of Ne72, Ki72 and with elastic measurements of Ne72, Ki72, and Bu73. Integral data from sphere transmission measurements (Wo72) were also factored into deriving some of the 14-MeV data.

MT=71-89. Inelastic Cross Section to Groups of Discrete States

Data combined into 0.3-MeV wide excitation energy bins centered about Q-values between -13.15 MeV (MT=71) and -18.55 MeV (MT=89). This representation was used in lieu of MF=5, MT=91, which does not preserve kinematic relationships.

Threshold to 20 MeV, integrated cross section adjusted to give a nonelastic cross section in agreement with the evaluated total and elastic. The cross section was divided among bands according to a nuclear temperature calculation using T=2 MeV. Please note that much of the cross section to levels above 9 MeV subsequently results in charged particle emission. MT=56-58, 61-66, 68-70, 72-73, 75, 77-78, 80, 82-83, 85, 87, and 89, are flagged as decaying by alpha emission. This choice leads to a total alpha emission cross section similar to data of Li52, Da68, and Bo66 below 17 MeV. The remaining MT numbers above MT=66 are flagged as being proton emitters.

MT=102. (n, γ) Cross Section

1/V variation from 178 μb at 2200 m/s, from Ju64.

MT=103. (n, p) Cross Section

Threshold to 15 MeV, used evaluation of S165, raised 5 per cent above 12 MeV.

15 to 20 MeV, based on experimental data of Bo66, Se62, De62, and Ma54.

MT=104. (n, d) Cross Section

Threshold to 20 MeV, compound nucleus reaction theory calculation normalized to single datum point of Li52 at 14 MeV.

MT=107. (n, α) Cross Section

Threshold to 20 MeV, sum of MT=780-783.

MT=780. (n, α) Integrated Cross Section to ^{13}C Ground State

0.0 to 5.7 MeV, essentially calculated from R-matrix fit described under MT=1. Energy scale of Ba72 adjusted to match Ci68 total cross section and resolution corrections applied to give width and height of peaks consistent with total. Normalization of 0.85 for Ba72 determined from R-matrix fit and applied. Level scheme based on Jo73.

5.7 to 20 MeV, based on data of Da63, Da68, Si68, Ba73, and composite of Mc66A, Ma68, and Le68 at 14 MeV.

MT=781-783. (n, α) Cross Section to Excited Levels of ^{13}C

Threshold to 15 MeV, used (n, α) data of Da63 and (n, $\alpha\gamma$) data of Di70, Or70, Cl69, Ny69, En64, and Bu71.

15 to 20 MeV, based on data of Si68.

File 4. Neutron Angular Distributions

MT=2. Elastic Angular Distributions

0.0 to 5.7 MeV, calculated from R-matrix fit (see MF=3, MT=1). Measured angular distributions input to the fit were those of Ch61, Fo58, Fo70, Hi58, Hu62, Jo67, Ki72, La60, Li66, Ma62, and Ph61.

5.7 to 14 MeV, smooth curve through coefficients derived from fits to elastic data of Ph61, Ne72, Ch61, Ba63, Be67, Mc66, Ki72, and Bu73.

14.0 to 20 MeV, from optical model calculation using parameters from fit to 14 MeV data of Ba63, adjusted to give correct total cross sections up to 20 MeV.

MT=51-89. Inelastic Angular Distributions

Threshold to 20 MeV, assumed isotropic in center-of-mass system except for MT=51-55 above 10 MeV which are based on fits of the 14-MeV measurements of Ba63 and Mc66. Note that the sum MT=51 and 52 is consistent with isotropy at 8.56 MeV (Ki72).

File 7. Thermal Scattering Low Data

Provided by D. Finch (SRL). Constrained to match MF=3, MT=2 data.

File 12. Photon Multiplicities

MT=102. Radiative Capture

Based on experimental data from Ju64 and private communication.

File 13. Gamma Ray Cross Sections

MT=4. ($n, n\gamma$) Cross Sections

Threshold to 15 MeV, based mainly on data of Di70, Or70, Dr70, Lu70, Bu69, Ny69, Cl69, and En64. Data generated from MF=3 MT=51-60 using an ^{16}O decay scheme from Aj70.

15 to 20 MeV, based on extrapolation of MT=51-60 using compound nucleus reaction theory calculations.

Note that the first excited level of ^{16}O at 6.052 MeV is assumed to decay with emission of two 0.51-MeV gamma rays.

MT=22. ($n, n\alpha\gamma$) Cross Sections

Threshold to 20 MeV, smooth curve based crudely on ($n, n\alpha$) cross section and known levels in ^{12}C , adjusted to agree with composite of 14-MeV data of Cl69, and Or70.

MT=103. ($n, p\gamma$) Cross Sections

Threshold to 20 MeV, based on crude division of MF=3, MT=103 cross section among available levels according to $(2*J+1)$.

MT=107. ($n, \alpha\gamma$) Cross Sections

Threshold to 15 MeV, based mainly on ($n, \alpha\gamma$) data of Di70, Or70, Cl69, Ny69, En64, Bu71, and (n, α) data of Da63.

15 to 20 MeV, based on data of Si68.

File 14. Gamma Ray Angular Distributions

MT=4. ($n, n\gamma$) Angular Distributions

Assumed isotropic except for the 6.131-MeV gamma, which is based on the angular distribution measurement of Dr70, Lu70, Bu71, and Di70, and the 6.917-MeV gamma, which is based on the two-angle measurements of Di70.

MT=22. ($n, n\alpha\gamma$) Angular Distributions

Assumed isotropic.

MT=103. ($n, p\gamma$) Angular Distributions

Assumed isotropic.

MT=107. ($n, \alpha\gamma$) Angular Distributions

Assumed isotropic.

File 33. Neutron Cross Section Covariances

MT=1, 2, 4, 103, 107. Smooth Cross Section

Covariances are based upon estimates of the uncertainty in the experimental measurements and theoretical calculations used in the evaluation. Format updated for Version-V. For more details, see separate summary documentation for covariances.

REFERENCES

Ad49 R. K. Adair et al., Phys. Rev. 75, 1124 (1949).
Aj70 F. Ajzenberg-Selove, Nucl. Phys. A52, 1 (1970).
Ba63 R. W. Bauer et al., Nucl. Phys. 47, 241 (1963).
Ba73 J. K. Bair and F. X. Haas, Phys. Rev. C7, 1356 (1973).
(n, α_0) cross sections obtained by detail balance from this reference.
Be67 P. L. Beach et al., Phys. Rev. 156, 1201 (1967).
Bo66 M. Bormann et al., Proc. IAEA Conf. Nucl. Data, Paris (1966), p.225.
Bu71 P. S. Buchanan et al., ORO-2791-32 (1971).
Bu73 W. P. Bucher et al., BRL-R-1652 (1973).
Ch61 L. F. Chase et al., AFSWC-TR-61-15 (1961).
Ci68 S. Cierjacks et al., KFK-1000 (1960).
Cl69 G. Clayeux and G. Grenier, CEA-R-3807 (1969).
Da63 E. A. Davis et al., Nucl. Phys. 48 169 (1963).
Da68 D. Dandy et al., AWRE 060/68 (1968).
De62 J. A. DeJuren et al., Phys. Rev. 127, 1229 (1962).
Di70 J. K. Dickens and F. G. Perey, Nucl. Sci. Eng. 40, 283 (1970).
Dr70 D. M. Drake et al., Nucl. Sci. Eng. 40, 294 (1970).
En64 F. C. Engesser and W. E. Thompson, J. Nucl. Eng. 21, 487 (1967).
Fo58 J. L. Fowler and H. O. Cohn, Phys. Rev. 109, 89 (1958).
Fo61 D. B. Fossan et al., Phys. Rev. 123, 209 (1961).
Fo70 J. L. Fowler and C. H. Johnson, Phys. Rev. C2, 124 (1970).
Fo73 J. L. Fowler et al., Phys. Rev. C8, 545 (1973).
Hi58 R. W. Hill, Phys. Rev. 109, 2105 (1959).
Hu62 W. Hunzinger and P. Huber, Helv. Phys. Acta 35, 351 (1962).
Jo48 W. B. Jones, Jr., Phys. Rev. 74, 364 (1948).
Jo67 C. H. Johnson and J. L. Fowler, Phys. Rev. 162, 890 (1967).
Jo73 C. H. Johnson, Phys. Rev. C7, 561 (1973).
Ju64 E. T. Jurney and H. T. Motz, Bull. Am. Phys. Soc. 9, 176 (1964).
Ki72 W. E. Kinney and F. G. Perey, ORNL-4760 (1972).
La60 R. O. Lane et al., ANL-6172 (1960).
Le68 B. Leroux et al., Nucl. Phys. A116, 196 (1968).
Li52 A. B. Lillie, Phys. Rev. 87, 716 (1952).
Li66 D. Lister and A. Sayres, Phys. Rev. 143, 745 (1966).
Lu70 B. Lundberg et al., Physica Scripta 2, 273 (1970).
Ma54 H. C. Martin, Phys. Rev. 93, 498 (1954).
Ma62 J. P. Martin and M. S. Zucker, Bull. Am. Phys. Soc. 7, 72 (1962).
Ma68 D. R. Maxson and R. D. Murphy, Nucl. Phys. A110, 555 (1968).
Mc66 W. J. McDonald et al., Nucl. Phys. 75, 353 (1966).
Mc66A W. N. McDonald and W. Jack, Nucl. Phys. 88, 457 (1966).
Me49 E. Melkonian, Phys. Rev. 76, 1750 (1949).
Ne71 D. O. Nellis and P. S. Buchanan, private communication (1971).

Ne72 D. O. Nellis and P. S. Buchanan, DNA-2716 (1972).
Ny69 K. Nyberg, private communication to L. Stewart (1969).
Ok55 A. Okazaki, Phys. Rev. 99, 55 (1955).
Or70 V. J. Orphan et al., Nucl. Sci. Eng. 42, 352 (1970).
Ph61 D. D. Phillips, private communication to BNL (1961).
Sc71 R. B. Schwartz, private communication (1971).
Se62 K. W. Seemann and W. E. Moore, KAPL-2214 (1962).
Si68 Von I. Sick et al., Helv. Phys. Acta 41, 573 (1968).
Sl65 E. L. Slaggie and J. T. Reynolds, KAPL-M-6452 (1965).
Wo72 C. Wong et al., UCRL-51144, Rev. 1 (1972).

SUMMARY DOCUMENTATION FOR ^{27}Al

by

P. G. Young and D. G. Foster, Jr.
Los Alamos Scientific Laboratory
Los Alamos, New Mexico

I. SUMMARY

The ENDF/B-IV evaluation for ^{27}Al was carried over for Version V as MAT 1313. Besides minor format changes, the only new data included are correlated errors in File 33. The evaluation covers the energy range 10^{-5} eV to 20 MeV. Documentation for the evaluation is LA-4726 (1972), as updated by LA-5759-PR (1974).

II. ENDF/B-V FILES

File 1. General Information

MT=451. Descriptive data.

File 2. Resonance Parameters

MT=151. Effective scattering radius = 0.32752×10^{-12} cm.

Resonance parameters not given.

File 3. Neutron Cross Sections

The 2200 m/s cross sections are:

MT=1 σ = 1.580 b
MT=2 σ = 1.348 b
MT=102 σ = 0.232 b

MT=1. Total Cross Section

Below 4.6 keV: 1/V fit to Me52 and Hi50 (normalized to Me52), using thermal capture σ of 232 mb (Go71) and resulting in a total of 1.580 b.

4.6 - 189 keV: From Ga65 normalized to Me52 via Hi59 at low energies and to Pe72 at high energies.

209 - 475 keV: From Pe72 with energy scale corrected to match Ci68 at higher energies.

.475 - 11.5 MeV: Composite of Pe72 and Sc69, normalized to their weighted average, with inserts of normalized Ci68 where needed to preserve resolution.

11.5 - 20 MeV: Composite of Pe72, Fo71, Al66, and Pe60 normalized to their weighted average. Slope at 20 MeV includes guidance from Ta55.

Smoothing between 4.6 keV and 2 MeV by approximate Breit-Wigner fits where possible, connected by polynomial fits. 2 - 12 MeV smoothed by running cubic polynomial fits. Above 12 MeV fitted secondary polynomial to middles of running polynomial fits.

MT=2. Elastic Scattering Cross Section

Below 5 MeV: Subtracted nonelastic from total.

5 to 16 MeV: Mainly based on elastic data of Ho69, St59, Ki70, St65, Co58, Co59, Be58, Mi68, Be56, and Ka72 together with the evaluated total and the nonelastic measurements listed below.

16 to 20 MeV: Smooth extrapolation to 1/2 the total at 20 MeV.

MT=3. Nonelastic Cross Section (implicit - not in file)

Below 9 MeV: Based on the nonelastic measurements of Ba58, Be56, Ta55, De65, on the sum of MT=4, 102, 103, 107, and on the difference between the evaluated total and the elastic measurements of Ho69, Ki70, Be56, and Mi68.

9 to 16 MeV: Based on nonelastic measurements of Ba58, Ta55, Gr55, Ph52, Ma57, De61, Fl56, Ch67, and on the difference between MT=1 and MT=2 data of St59, St65, Co58, Co59, and Be58.

16 to 20 MeV: Difference between MT=1 and MT=2.

MT=4. Inelastic Cross Section

Threshold to 5 MeV: Sum of MT=51-63.

5 to 9 MeV: Based on (n,n') data of Th63, To67, the evaluated (n,n') data of Di71 which includes consideration of several other measurements, and the (n,n γ) data of Di71, Or71, and Di73.

9 to 20 MeV: The difference between MT=1 and the sum of MT=2, 16, 102, 103, 104, 105, and 107.

MT=16. (n,2n) Cross Section

Threshold to 20 MeV: Estimated using a nuclear temperature calculation assuming that highly excited states in ^{27}Al decay 50 per cent by neutron emission.

MT=51 - 63. Inelastic Cross Section to Discrete States

MT=51	Q=-0.843 MeV	MT=56	Q=-3.001 MeV	MT=60	Q=-4.409 MeV
52	-1.013	57	-3.678	61	-4.508
53	-2.210	58	-3.956	62	-4.580
54	-2.732	59	-4.055	63	-4.811
55	-2.980				

Threshold to 5 MeV: Based on the (n,n') data of To62, Wi63, Ts61, and the (n,ny) data of Ch68, Ma65, Di71, Or71, and Di73.

5 to 9 MeV: Based on an evaluation of several measurements given in Di71 (Table B1).

9 to 20 MeV: Smooth extrapolation passing through 14 MeV data of St65, and Bo65A.

MT=64 - 90. Inelastic Cross Section To Groups Of Discrete States
in Energy Bins Centered About Q-values Between
-5.25 MeV and -18.875 MeV.

Threshold to 20 MeV: Integrated cross section over bands obtained by subtracting MT=51-63 from MT=4. Cross section divided among bands according to a nuclear temperature calculation using temperatures based on (n,n') data of Th63, and Gr53. The cross section to the bands with MT=64-71 was adjusted extensively to produce agreement with the 14-MeV measurements of secondary neutron spectra by Ka72.

(Please note that much of the cross section to bands above $E_x=9$ MeV subsequently results in charged particle emission. Since these data are not included explicitly as (n,nx) reactions, it is important that users involved in certain calculations (e.g., local heating) be aware of this information.)

MT=102. (n, γ) Cross Section

Below 1 keV: 1/V from thermal value of 232 mb (Go71).

1 to 140 keV: From B168, 6-keV resonance has width deduced from total cross section. Small resonances nearby also from total.

Above 140 keV: Mainly from He50, He53, and Ca62.

MT=103. (n,p) Cross Section (see Yo72 for more details)

Threshold to 4 MeV: Based on the measurements of He54 and Gr67, extrapolated from 3 MeV to threshold with an L=0 penetrability function for the outgoing p + ^{27}Mg channel.

4 to 20 MeV: Smooth curve through the measurements of He54, Gr67, Ca62, Ba66, and Ma60.

MT=104. (n,d) Cross Section

Threshold to 20 MeV: Smooth curve through single datum of Gl61.

MT=105. (n,t) Cross Section

Threshold to 20 MeV: Smooth curve with same shape as MT=104.
Reaching maximum of 15 mb at 20 MeV.

MT=107. (n, α) Cross Section (see Yo72 for more details)

Threshold to 20 MeV: Based on a smooth curve through experimental data, mainly those of Bu63, Pa65, and Li66, with results from Gr67, Sc61, Gr58, Ba61, Ma65, Ga62, Im64, Ke59 and several 14-MeV points also being considered. The curve was extrapolated from 6 MeV to threshold with an L=0 penetrability function for the outgoing $\alpha + {}^{24}\text{Na}$ channel.

File 4. Neutron Angular Distributions

MT=2. Elastic Angular Distributions

From smooth curves through plots of coefficients from fits to all available data above .25 MeV, without evaluation of measurements. Mainly from Ta57, Ch66, To62, Ts61, Ki70, and Be58, with optical-model bridge to Si62. Some of data augmented before fitting by zero-degree point slightly above Wick limit, and coefficients adjusted empirically afterwards to obey Wick limit. But only barely at higher energies.

MT=16. (n,2n) Angular Distributions

Assumed isotropic in CM, using 2-body kinematics to estimate transformation to laboratory system.

MT=51 - 63. Inelastic Neutron Angular Distributions

Anisotropic distributions based on measurements by Ts61, To62, Wi63, Mi68, Ta70, Gl72, St65, Bo65A, and Ka72 were incorporated over varying energy ranges from threshold to 20 MeV. In several regions where data were lacking, isotropy was assumed.

MT=64 - 90. Inelastic Neutron Angular Distributions

Assumed isotropic in the center-of-mass system.

File 5. Neutron Energy Distributions

MT=16. (n,2n) Energy Distributions

Based on statistical theory.

File 12. Gamma Ray Multiplicities

MT=102. (n,γ) Capture Multiplicities

The ^{28}Al decay scheme for excitation by radiative capture with thermal neutrons from Ha69 was adopted after some modification to enhance agreement with experiment. The results have been compared with the less detailed data of Ba67, Ju71, and Ma69, and are reasonably consistent. Some of the lines in Ra70 below 1 MeV appear to be spurious and have been dropped. Spectrum for thermal neutrons is assumed to apply at all energies.

File 13. Gamma Ray Smooth Cross Sections

MT=4. $(n,n\gamma)$ Cross Sections

Threshold to 5 MeV, based on the (n,n') data of To62, Wi63, Ts61, and the $(n,n\gamma)$ data of Ch68, Ma65, Di71, Or71, and Di73.

5 to 20 MeV. Mainly from $(n,n\gamma)$ data of Di73, Or71, and Di71, Dr73, Pe64, Be66, Cl69, En67, Bo65, Ma68, Ca60 and Pr60, supplemented by statistical theory calculations.

MT=28. $(n,np\gamma)$ Cross Sections

Threshold to 20 MeV, based on the measurements of Di73, Or71, En67, Pr60, Cl69, Be66, Bo65, and on statistical theory.

MT=103. $(n,p\gamma)$ Cross Sections

Threshold to 9 MeV, used data of Di71.

9 to 20 MeV. Smooth Extrapolation.

File 14. Gamma Ray Angular Distributions

MT=4. $(n,n\gamma)$ Angular Distributions Assumed Isotropic.

MT=28. $(n,np\gamma)$ Angular Distributions Assumed Isotropic.

MT=103. $(n,p\gamma)$ Angular Distributions Assumed Isotropic.

File 15. Gamma Ray Energy Distributions

MT=4. $(n,n\gamma)$ Energy Distributions

Statistical theory calculation adjusted to fit measurement of Di73.

MT=28. $(n,np\gamma)$ Energy Distributions

Statistical theory calculation adjusted to fit measurement of Di73.

File 33. Neutron Cross Section Covariances

Based on revised version of Table 6 in LA-4726. Errors are given only for MT=1, 2, 4, 16, 102, 103, and 107. MT=2 is taken from experiment between 9 and 17 MeV, and derived everywhere else. MT=4 is derived above 9 MeV. The derivation formulas are given by NC-type sub-subsections with LTY=0 in MT=2 and MT=4.

REFERENCES

Ba58 W. P. Ball et al., (LRL), Phys. Rev. 110, 1392 (1958).
 Ba61 B. P. Bayhurst and R. J. Prestwood, (LAS), Phys. Rev. 121, 1438 (1961).
 Ba66 R. Base, EANDC(E)-66U, p. 64, and Private communication (1966).
 Ba67 G. A. Bartholomew et al., Nucl. Data A3, 367 (1967).
 Be55 J. R. Beyster et al., (LAS), Phys. Rev. 98, 1216 (1955).
 Be56 J. R. Beyster et al., (LAS), Phys. Rev. 104, 1319 (1956).
 Be58 S. Berko et al., Nucl. Phys. 6, 210 (1958).
 Be66 V. M. Bezotosnyi et al., (RUS), Sov. J. Nucl. Phys. 3, 632 (1966).
 B168 R. C. Block, Private communication to R. J. Howerton (1968).
 Bo59 N. A. Bostrom et al., (TNC), WADC-TN-59-107 (1959).
 Bo65 V. N. Bockharev and V. V. Nedorov (LEB), Sov. J. Nucl. Phys. 1, 574 (1965).
 Bo65A G. C. Bonazzola et al., (TUR), Phys. Rev. 140, 835 (1965).
 Bu63 J. P. Butler and D. C. Santry, Can. J. Phys. 41, 372 (1963).
 Ca60 R. L. Caldwell et al., (SOC), Nucl. Sci. Eng. 8, 173 (1960).
 Ca62 G. Calvi et al., Nucl. Phys. 39, 621 (1962).
 Ca67 A. D. Carlson and H. H. Barschall, Phys. Rev. 158, 1142 (1967).
 Ch66 J. P. Chien and A. B. Smith, Nucl. Sci. Eng. 26, 500 (1966).
 Ch67 A. Chatterjee and A. M. Ghose (BOS), Phys. Rev. 161, 1181 (1967).
 Ch68 K. C. Chung et al., (KTY), Nucl. Phys. 68, 476 (1968).
 Ci68 S. Cierjacks et al., KFK-1000 (1968).
 Cl69 G. Clayeux and G. Grenier (FR), CEA-R-3807, (1969).
 Co58 J. H. Coon et al., (LAS), Phys. Rev. 111, 250 (1958).
 Co59 J. H. Coon (LAS), Private communications to R. J. Howerton (1959).
 De61 Yu. G. Degtyarev and V. G. Nadochii, Sov. J. At. Energy 11, 1043 (1961).
 De65 Yu. G. Degtyarev (RUS), J. Nucl. Energy 20, 818 (1965).
 Di71 J. K. Dickens (ORNL), ORNL-TM-3284, 1971.
 Di73 J. K. Dickens et al., ORNL-TM-4232 (1973).
 Dr70 D. M. Drake et al., (LAS), Nucl. Sci. Eng. 40, 294 (1970).
 En67 F. C. Engesser and W. E. Thompson (NRD), J. Nucl. Energy 21, 487 (1967).
 Fe67 J. M. Ferguson and J. C. Albergotti (NRD), Nucl. Phys. 98, 65 (1967).
 Fl56 N. N. Flerov and V. M. Talyzin (RUS), Atomnaya Energiya 1, 155 (1956).
 Fo71 D. G. Foster, Jr. and D. W. Glasgow, Phys. Rev. C3, 576 (1971).
 Ga62 F. Gabbard and B. D. Kern (KTY), Phys. Rev. 128, 1276 (1962).
 Ga65 J. B. Garg et al., Private communication to R. J. Howerton (1965).
 Gl61 R. N. Glover and E. Wilgold (CBR), Nucl. Phys. 24, 630 (1961).
 Gl72 D. W. Glasgow, Private communication (1972).
 Go71 D. T. Goldman, Unpublished evaluation (1971).
 Gr53 E. R. Graves and L. Rosen (LAS), Phys. Rev. 89, 343 (1953).
 Gr55 E. R. Graves and R. W. Davis (LAS), Phys. Rev. 97, 1205 (1955).
 Gr58 J. A. Grundl et al., (LAS), Phys. Rev. 109, 425 (1958).
 Gr67 J. A. Grundl (LAS), Nucl. Sci. Eng. 30, 69 (1967).
 Ha69 R. Hardell et al., Nucl. Phys. A126, 392 (1969).

He50 R. L. Henkel and H. H. Barschall, Phys. Rev. 80, 145 (1950).
He53 R. L. Henkel, Private communication to Sigma Center (1953).
Hi59 C. T. Hibdon, Phys. Rev. 114, 179 (1959).
Ho69 B. Holmqvist and T. Wiedling (AE), AE-366 (1969).
Im64 W. L. Imhog (LOK), private communication to NNCSC (1964).
Jo64 G. D. Joanou and C. A. Stevens (GA), GA-5884 (1964).
Ju71 E. T. Jurney, Private communication (1971).
Ka72 J. L. Kammerdiener, Thesis, University of California at Davis (1972).
Ke59 B. D. Kern et al., (NRD), Nucl. Phys. 10, 226 (1959).
Ki70 W. E. Kinney and F. G. Perey (ORL), ORNL-4516 (1970).
La57 A. Langsdorf et al., Phys. Rev. 107, 1077 (1957).
Li66 H. Liskien and A. Paulsen, Nucleonics 8, 315 (1966).
Ma57 M. H. MacGregor et al., (LRL), Phys. Rev. 108, 726 (1957).
Ma60 G. S. Mani et al., (HAR), Nucl. Phys. 19, 535 (1960).
Ma65 S. C. Mathur et al., (TNC), Nucl. Phys. 73, 561 (1965).
Ma68 G. N. Maslov et al., (RUS), Sov. J. At. Energy 24, 704 (1968).
Ma69 R. E. Maerker and F. J. Muckenthaler, ORNL-4382 (1969).
Me52 A. W. Merrison and E. R. Wiblin, Proc. Roy. Soc. (L) 215, 278 (1952).
Mi68 A. Mittler et al., (KTY), Bull. Am. Phys. Soc. 13, 1420 (1968).
Or71 V. J. Orphan and C. G. Hoot, Gulf-RT-A10743 (1971).
Pa65 A. Paulsen and H. Liskien (GEL), J. Nucl. Energy 19, 907 (1965).
Pe64 J. L. Perkin (ALD), Nucl. Phys. 60, 561 (1964).
Pe72 F. G. Perey et al., ORNL-4823 (1972).
Ph52 D. D. Phillips et al., (LAS), Phys. Rev. 88, 600 (1952).
Pr60 J. T. Prudhomme et al., (TNC), AFSWC-TR-60-30 (1960).
Ra70 N. C. Rasmussen et al., GA-10248 (1970).
Sc61 H. W. Schmitt and J. Halperin (ORL), Phys. Rev. 121, 827 (1961).
Sc70 R. B. Schwartz, private communication (1970).
St59 C. St. Pierre et al., (MON), Phys. Rev. 115, 999 (1959).
St62 T. P. Stuart et al., Phys. Rev. 125, 276 (1962).
St65 P. H. Stelson and R. L. Robinson (ORL), Nucl. Phys. 68, 97 (1965).
Ta55 H. I. Taylor et al., (RIC), Phys. Rev. 100, 174 (1955).
Ta70 S. Tanaka et al., Nucl. Data for Reactors, IAEA p. 317 (1970).
Th63 D. B. Thompson (LAS), Phys. Rev. 129, 1649 (1963).
To62 J. H. Towle and W. B. Gilboy, Nucl. Phys. 39, 300 (1962).
To67 J. H. Towle and R. O. Owens (ALD), Nucl. Phys. A100, 257 (1967).
Ts61 K. Tsukada et al., Physics of Fast and Intermediate Reactors, Vienna (1961).
Wi63 D. Winterhalter (ZAG), Nucl. Phys. 43, 339 (1963).
Yo72 P. G. Young, LASL Memo T-2-99 to the Norm. and Standards Subcommittee of CSEWG (1972).

SUMMARY DOCUMENTATION FOR ^{182}W

by

P. G. Young, J. Otter,[†] E. Ottewitte,[†] and P. Rose[†]
Los Alamos Scientific Laboratory
Los Alamos, New Mexico

I. SUMMARY

The ^{182}W evaluation for ENDF/B-V (MAT 1128) was carried over intact from Version IV with only minor format changes being made. The evaluation of the neutron files was performed at Atomics International and is documented in TI-707-130-026 (1973). The gamma-ray production data were evaluated at Los Alamos Scientific Laboratory and are documented in LA-5793 (1975). The ENDF/B-V data span the energy range 10^{-5} eV to 20 MeV.

II. ENDF/B-V FILES

File 1. General Information

MT=451. Descriptive Data

Atomic mass and Q-values taken from Ref. 1.

File 2. Resonance Parameters

MT=151. (A) Resolved Resonances Evaluation

Potential scattering cross section = 8.0 ± 1.0 b at E=0.

2200 m/s Cross Sections (barns)		
	<u>CALC</u>	<u>MEAS (Ref. 2)</u>
CAP	20.5	20.7 ± 0.5
SCAT	11.6	

Resolved Resonance Parameters

- 100 eV	from	fit to capture
4.16 eV	frcm	Ref. 2
5 - 250 eV	from	evaluation, Refs. 2, 3, and 4
250 -1250 eV	from	evaluation, Refs. 3 and 4
1250 -4500 eV	from	Ref. 4
1920 -2198 eV	from	Ref. 3

[†]Atomics International

MT=151. (B) Unresolved Resonances Evaluation

Potential scattering cross section = 8.5 ± 1.0 b at $E_n=0$.
Total cross section = 8.85 b at $E_n=100$ keV (calculated).

Unresolved resonance parameters from automated optimized fit to
the evaluated measured capture cross section.

AV L=0 level spacing ($E_n=0$) = 57.45 eV, energy dep. from Ref. 5.
AV Capture level width = 0.0901 eV, energy independent
L=0 Strength function = $1.8E-4$, energy independent
L=1 Strength function = $0.272E-4$, energy independent
L=2 Strength function = 0.0

Average capture cross section uncertainty at energy E

<u>E (keV)</u>	<u>Uncertainty (%)</u>
100	15
90	10
10	10
4.5	17

Resonance integral (capture) 596 b calculation, 590 ± 10 b measure-
ment (Ref. 6).

File 3. Neutron Cross Sections

MT=1. Total Cross Section

The total cross section was evaluated using a least squares spline
fit to experimental data for this isotope. Spline fits of exper-
imental data for natural tungsten were also factored into the
evaluation (see MAT 1129 for Refs.). The total cross section
curve was smoothly joined to the evaluated total cross section
in the unresolved resonance range below 100 keV. Isotopic data
references are Whalen⁷ (100-650 keV), Martin⁸ (0.65-20 MeV), and
Foster and Glasgow⁹ (2.5-15 MeV). General references for the
total cross section are Goldberg et al.² and Devaney and Foster.¹⁰
The uncertainty in the total cross section is probably less than
7% over the energy range from 600 keV to 20 MeV. Between 300 keV
and 600 keV the uncertainty increases to 10% and from 100 to 200
keV the uncertainty is estimated to be 15%.

MT=2. Elastic Cross Section

The elastic cross section was obtained by subtracting the nonelastic
cross sections from the evaluated total cross section. The elastic
cross section is in good agreement with the data of Lister¹¹
between 300 keV and 1.5 MeV. Between 1 MeV and 9 MeV the eval-
uated curve lies above 2PLUS-COMNUC results. At 4.3 MeV the
cross section is some 15% lower than the experimental data point
of Kinney and Perey¹² for natural tungsten. Our evaluation is,
however, in agreement with their data above 5 MeV.

MT=4. Total Inelastic Cross Section

Equal to the sum of the level excitation and continuum cross sections. The total inelastic cross section for this isotope is in general agreement with the data of Owens et al.¹³ for natural tungsten between 5 and 7 MeV.

MT=16. (n,2n) Cross Section

The semi-empirical techniques of Pearlstein¹⁴ and W. D. Lu et al.¹⁵ were used to deduce the n,2n cross section. The evaluated curve at 14.8 MeV is in agreement with Dilg et al.¹⁶ and Druzhinin et al.¹⁷

MT=17. (n,3n) Cross Section

The n,3n cross sections were deduced using the semi-empirical techniques of S. Pearlstein¹⁴ and W. D. Lu.¹⁵ An effective threshold for the n,3n reaction was set 1.25 MeV above the theoretical threshold.

MT=28. (n,pn) Cross Section

The shape of the n,pn excitation curve is based upon the experimental data of J. F. Barry et al.¹⁸ for ¹⁸⁶W (see MAT 1131). The curve has been shifted in energy by the difference in the reaction Q for this isotope and ¹⁸⁶W. The cross section contains contributions from the n,np and n,d reactions.

MT=51. Inelastic Excitation (Direct and Compound Nucleus) to the 2⁺ Level

The cross sections were calculated using 2PLUS-COMNUC. They have been renormalized via a least squares fit to data of D. Lister et al.¹⁹ with a 10% uncertainty in the adjusted curve.

MT=52-58, 91. Inelastic Excitation (Compound Nucleus Only).

Calculation by the COMNUC code for the 329, 680, 1220, 1258, 1289, 1331, and 1374 keV levels plus the continuum. The 329-keV level excitation curve was renormalized to the data of D. Lister.¹⁹ The uncertainty in the adjusted cross sections is about 10%.

MT=102. Radiative Capture Cross Section

The radiative capture cross section was evaluated between 10 keV and 150 keV using a least squares fit to experimental data (see MF=2, MT=151). This fit was combined and joined to the theoretical cross sections computed between 100 keV and 4 MeV using the COMNUC code. Above 4 MeV the COMNUC results were joined to the collective and direct interaction capture cross sections calculated using the theory of V. Benzi and G. Reffo.²⁰ The uncertainty in the radiative capture cross section is probably less than 15% for energies between 100 keV and 200 keV. Above 200 keV the cross

section is reliable only to the extent of the validity of the theoretical models.

MT=103. (n,p) Cross Section

The shape of the n,p excitation curve is based upon the experimental data of J. F. Barry et al.¹⁸ for ¹⁸⁶W (see MAT 1131). The curve has been shifted in energy to pass through the data point reported by M. Lindner et al.²¹ (3.5 ± 0.35 mb at 14.1 MeV).

MT=107. (n,α) Cross Section

The n,α cross section evaluation is based upon data of A. Rubino and D. Zubke²² for ¹⁸¹Ta. The few experimental data points for isotopes of tungsten between 14 and 15 MeV qualitatively substantiate the use of this curve. The evaluation has not been extended below 11 MeV.

File 4. Neutron Angular Distributions

MT=2. Elastic Angular Distributions

The angular distributions for elastic scattering are given as Legendre polynomial coefficients in the cm system. These data were calculated by 2PLUS-COMNUC codes for each isotope. As little isotopic experimental data existed, the calculated data were averaged according to abundance and compared to natural tungsten data. The comparison indicated that the experimental data contained direct inelastic reactions to the first level. With the calculated first-level direct inelastic included, agreement within experimental error was generally indicated over all energies. This agreement also supports the validity of the inelastic angular file below. The natural tungsten experimental data were taken from Refs. 23-30. Error estimates for this section are difficult because it appears that pure elastic scatter has not been measured except at low energies. Because of the good agreement overall with the combined data, this file is estimated to be accurate to 15% at energies below 1 MeV, and within a factor of two at energies above 1 MeV for all scattering angles.

MT=51-58, 91. Angular Distribution of Inelastic Scattered Neutrons

Angular distributions are given as Legendre polynomial coefficients in the laboratory frame of reference. These data are based upon 2PLUS-COMNUC calculations. They include anisotropic contributions from direct inelastic excitation of the 2⁺ level. Compound level and continuum excitations are isotropic in the laboratory system. Errors are small simply due to the predominance of isotropy.

File 5. Neutron Energy Distributions

MT=16, 17. Nuclear Temperatures for the (n,2n) and (n,3n) Reactions

Temperature of first emitted neutron same as for MT=91. Temperatures of second and third emitted neutrons deduced by conservation of energy assuming the kinetic energy of an emitted neutron is 2^*KT .

MT=91. Nuclear Temperature for Inelastic Continuum

References 31-34 were used in deriving temperatures. Least squares Weisskopf level spacing was fit to natural tungsten data. Isotopic data adjusted using deformed nucleus level density formula of Gilbert and Cameron.³⁴

File 12. Gamma Ray Multiplicities

MT=102. Multiplicities for Gamma Ray Production from Radiative Capture

Multiplicities at neutron energies below 1 eV are based on a preliminary thermal measurement for natural W by Jurney³⁵ and from 1 eV to 1000 eV on calculations by Yost et al.³⁶ At higher energies the multiplicities are based on an analysis of natural W measurements (Dickens,³⁸ $E_n=1-20$ MeV) using statistical calculations similar to those described by Troubetzkoy,³⁷ with the multiplicities chosen to give rough agreement with the measurements. The theory was used at all energies to divide the natural W data into isotopic components.

File 13. Gamma Ray Production Cross Sections

MT=4. Gamma Ray Production Cross Sections from Inelastic, (n,2n), and (n,3n) Reactions

The cross sections for discrete photons are based on the level excitation cross sections in MF=3, MT=51-58, mainly using the level decay scheme of Way.³⁹ The cross sections for continuum gamma rays are based on a statistical theory analysis of the Dickens³⁸ measurements on natural W. The theory was used for interpolation, smoothing, and separation of the data into isotopic components.

File 14. Gamma Ray Angular Distributions

MT=4, 102. Angular Distributions of Gamma Rays from Radiative Capture, Inelastic, (n,2n), and (n,3n) Reactions

Gamma rays from all reactions are assumed isotropic in the laboratory system.

File 15. Gamma Ray Energy Distributions

MT=4. Energy Distributions of Gamma Rays from Inelastic, (n,2n), and (n,3n) Reactions

The spectra at all energies are based on a statistical theory analysis of the Dickens³⁸ measurements with natural W. The theory was used as described above (MF=13, MT=4). Arbitrary adjustments were made to the theoretical fits in regions where agreement with experiment was poor (mainly below $E_n=5$ MeV).

MT=102. Energy Distributions of Gamma Rays From Radiative Capture

Spectra at neutron energies below 1 eV are based on a preliminary thermal measurement by Jurney³⁵ and from 1 eV to 1000 eV on calculations by Yost et al.³⁶ At higher energies the spectra are based on statistical calculations using parameters obtained by analyzing the Dickens³⁸ measurement for $E_n=1-3$ MeV. The theory was used at all energies to divide the natural W data into separate isotopic components.

(Note: No information is provided in this evaluation on electron production from internal conversion. Such information might be important for local heating and radiation damage problems.)

REFERENCES

1. A. H. Wapstra and N. B. Gove, Nucl. Data Tables 9, 267 (1971).
2. M. D. Goldberg et al., BNL-325, 2nd Edition, Supplement 2, (1966).
3. Z. M. Bartolome et al., Nucl. Sci. Eng. 37, p. 137 (1969).
4. F. J. Rahn and H. Camarda, personal communication, Columbia (1970).
5. J. L. Cook et al., AAEC/TM-392 (1967).
6. M. Drake, (1968) for American Institute of Phys. Handbook (1972).
7. J. F. Whalen, ANL-7210, 16 (1966).
8. R. C. Martin, PhD Thesis, RPT (1967).
9. D. G. Foster and D. W. Glasgow, Phys. Rev. 3C, 576 (1971).
10. J. J. Devaney and D. G. Foster, Jr., Los Alamos report LA-4928 (1972).
11. D. Lister et al., ANL-7288 (1967).
12. W. E. Kinney and F. G. Perey, ORNL-4803 (1973).
13. R. O. Owens et al., Nucl. Phys. A112, 337 (1968).
14. S. Pearlstein, Nucl. Sci. Eng. 23, 238 (1965).
15. W. B. Lu et al., Phys. Rev. C1, 350 (1970).
16. Dilg et al., Nucl. Phys. A118, 9 (1968).
17. Druzhinin et al., Sov. J. Nucl. Phys. 4, 515 (1966).
18. J. F. Barry et al., Proc. Phys. Soc. 74, 632 (1959).
19. D. Lister et al., Phys. Rev. 162, 1077 (1967).
20. V. Benzi and G. Reffo, CCDN-NW10, ENEA Neutron Compilation Center (1969).
21. M. Lindner et al., Lawrence Livermore Laboratory, private communication (1972).
22. A. Rubino and D. Zubke, Nucl. Phys. 85, 606 (1966).
23. A. B. Smith and P. A. Moldauer, BAPS 5, 409 (1960).
24. F. T. Kuchnir et al., Phys. Rev. 176, 1405 (1968).

25. W. Walt and H. Barschall, Phys. Rev. 93, 1062 (1954).
26. K. Tsukada et al., Nucl. Phys. A125, 641 (1966).
27. R. W. Hill, Phys. Rev. 109, 2105 (1958).
28. W. Kinney, private communication (1972).
29. D. B. Thomson, Phys. Rev. 129, 1649 (1963).
30. H. Nauta, Nucl. Phys. 2, 124 (1956).
31. S. G. Buccino et al., Nucl. Phys. 60, 17 (1964).
32. R. O. Owens and J. H. Towle, Nucl. Phys. A112, 337 (1968).
33. W. E. Kinney, ORNL, private communication (1972).
34. A. Gilbert and A. G. W. Cameron, Can. J. Phys. 43, 1446 (1965).
35. E. T. Jurney, private communication (1973).
36. K. J. Yost, J. E. White, C. Y. Fu, and W. E. Ford, Nucl. Sci. Eng. 47, 209 (1972).
37. E. S. Troubetzkoy, Phys. Rev. 122, 212 (1961).
38. J. K. Dickens, private communication (1972).
39. K. Way, Nuclear Data Bl-1, 1 (1966).

SUMMARY DOCUMENTATION FOR ^{183}W

by

P. G. Young, J. Otter,[†] E. Ottewitte,[†] and P. Rose[†]
Los Alamos Scientific Laboratory
Los Alamos, New Mexico

I. SUMMARY

The ^{183}W evaluation for ENDF/B-V (MAT 1129) was carried over intact from Version IV with only minor format changes being made. The evaluation of the neutron files was performed at Atomics International and is documented in TI-707-130-026 (1973). The gamma-ray production data were evaluated at Los Alamos Scientific Laboratory and are documented in LA-5793 (1975). The ENDF/B-V data span the energy range 10^{-5} eV to 20 MeV.

II. ENDF/B-V FILES

File 1. General Information

MT=451. Descriptive Data

Atomic mass and Q-values taken from Ref. 1.

File 2. Resonance Parameters

MT=151. (A) Resolved Resonances Evaluation

Potential scattering cross section = 8.0 ± 1.0 b at $E_n=0$.

2200 m/s Cross Sections (barns)

	<u>CALC</u>	<u>MEAS (Ref. 2)</u>
CAP	10.0	10.2 ± 3.0
SCAT	3.4	

Resolved Resonance Parameters

-1.5 eV	from	fit to capture
0 - 150 eV	from	Ref. 2
150 - 175 eV	from	evaluation, Refs. 2 and 3
175 - 760 eV	from	Ref. 3

[†] Atomics International

MT=151. (B) Unresolved Resonances Evaluation

Potential scattering cross section = 8.5 ± 1.0 b at $E_n=0$.
 Total cross section = 11.3 b at $E_n=45$ keV (calculated).

Unresolved resonance parameters from automated optimized fit to the evaluated measured capture cross section. The competitive reaction width for $L=2$, $J=1$ is for the L to $L-2$ elastic scattering process.

AV $L=0$ level spacing ($E_n=0$) = 12.53 eV, energy dep. from Ref. 4.
 AV Capture level width = 0.0801 eV, energy independent
 $L=0$ Strength function = $2.125E-4$ eV, energy independent
 $L=1$ Strength function = $0.227E-4$ eV, energy independent
 $L=2$ Strength function = $2.56E-4$ eV, energy independent

Average capture cross section uncertainty at energy E

<u>E (keV)</u>	<u>Uncertainty (%)</u>
45	11
10	12
5	20
2.5	40

Resonance integral (capture) 355 b calculation, 380 ± 15 b measurement (Ref. 5).

File 3. Neutron Cross Sections

MT=1. Total Cross Section

There are no experimental data for ^{183}W . The total cross section was evaluated using a least squares spline fit to experimental data for natural tungsten.⁶⁻¹⁰ The total cross section curve was smoothly joined to the evaluated total cross section in the energy range below 100 keV. The lack of direct experimental data introduces a large uncertainty in the total cross section between 100 keV and 700 keV (see Ref. 10).

MT=2. Elastic Cross Section

The elastic cross section was obtained by subtracting the nonelastic cross sections from the evaluated total cross section. Between 1 MeV and 9 MeV, the evaluated curve lies above 2PLUS-COMNUC results. At 4.3 MeV the cross section is some 15% lower than the experimental data point of Kinney and Perey¹¹ for natural tungsten. Our evaluation is, however, in agreement with their data above 5 MeV.

MT=4. Total Inelastic Cross Section

Equal to the sum of the level excitation and continuum cross sections. The total inelastic cross section for this isotope is in general agreement with the data of Owens et al.¹² for natural tungsten between 5 and 7 MeV.

MT=16. (n,2n) Cross Section

The semi-empirical techniques of Pearlstein¹³ and W. D. Lu et al.¹⁴ were used to deduce the n,2n cross section.

MT=17. (n,3n) Cross Section

The n,3n cross sections were deduced using the semi-empirical techniques of S. Pearlstein¹³ and W. D. Lu.¹⁴ An effective threshold for the n,3n reaction was set 1.25 MeV above the theoretical threshold.

MT=28. (n,pn) Cross Section

The shape of the n,pn excitation curve is based upon the experimental data of J. F. Barry et al.¹⁵ for ¹⁸⁶W (see MAT 1131). The curve has been shifted in energy by the difference in the reaction Q for this isotope and ¹⁸⁰W. The cross section contains contributions from the n,np and n,d reactions.

MT=51, 52. Inelastic Excitation (Direct and Compound Nucleus) to the 46.5 and 99 keV Levels.

The cross sections were calculated using the 2PLUS-COMNUC codes. No experimental data has been reported.

MT=53-59, 91. Inelastic Excitation (Compound Nucleus Only).

Calculation by the COMNUC code for the 207, 209, 292, 309, 412, 453, and 595-keV levels plus the continuum. The theoretical cross sections were used without modification.

MT=102. Radiative Capture Cross Section

The radiative capture cross section was evaluated between 10 keV and 100 keV using a least squares fit to experimental data (see MF=2, MT=151). This fit was combined and joined to the theoretical cross sections computed between 100 keV and 4 MeV using the COMNUC code. Above 4 MeV the COMNUC results were joined to the collective and direct interaction capture cross sections calculated using the theory of V. Benzi and G. Reffo.¹⁶ The uncertainty in the radiative capture cross section is 11% between 45 keV and 90 keV. Between 90 keV and 200 keV the uncertainty is probably less than 25%. Above 200 keV the cross section is reliable only to the extent of the validity of the theoretical models.

MT=103. (n,p) Cross Section

The shape of the n,p excitation curve is based upon the experimental data of J. F. Barry et al.¹⁵ for ¹⁸⁶W (see MAT 1131). The curve has been shifted in energy to pass through the data point reported by M. Lindner et al.¹⁷ (4.2 ± 0.42 mb at 14.1 MeV).

MT=107. (n,α) Cross Section

The n,α cross section evaluation is based upon data of A. Rubino and D. Zubke¹⁸ for ^{181}Ta . The few experimental data points for isotopes of tungsten between 14 and 15 MeV qualitatively substantiate the use of this curve. The evaluation has not been extended below 11 MeV.

File 4. Neutron Angular Distributions

MT=2. Elastic Angular Distributions

The angular distributions for elastic scattering are given as Legendre polynomial coefficients in the cm system. These data were calculated by 2PLUS-COMNUC codes for each isotope. As little isotopic experimental data existed, the calculated data were averaged according to abundance and compared to natural tungsten data. The comparison indicated that the experimental data contained direct inelastic reactions to the first 2 levels. With the calculated first-and second-level direct inelastic included, agreement within experimental error was generally indicated over all energies. This agreement also supports the validity of the inelastic angular file below. The natural tungsten experimental data were taken from Refs. 19-26. Error estimates for this section are difficult because it appears that pure elastic scatter has not been measured except at low energies. Because of the good agreement overall with the combined data, this file is estimated to be accurate to 15% at energies below 1 MeV, and within a factor of two at energies above 1 MeV for all scattering angles.

MT=51-59, 91. Angular Distribution of Inelastic Scattered Neutrons

Angular distributions are given as Legendre polynomial coefficients in the laboratory frame of reference. These data are based upon 2PLUS-COMNUC calculations. They include anisotropic contributions from direct inelastic excitation of the $^{3/2}+$ and $^{5/2}+$ levels. Compound level and continuum excitations are isotropic in the laboratory system. Errors are small simply due to the predominance of isotropy.

File 5. Neutron Energy Distributions

MT=16, 17. Nuclear Temperatures for the $(n,2n)$ and $(n,3n)$ Reactions

Temperature of first emitted neutron same as for MT=91. Temperatures of second and third emitted neutrons deduced by conservation of energy assuming the kinetic energy of an emitted neutron is $2*KT$.

MT=91. Nuclear Temperatures For Inelastic Continuum

References 27-30 were used in deriving temperatures. Least squares Weisskopf level spacing was fit to natural tungsten data.

Isotopic data adjusted using deformed nucleus level density formula of Gilbert and Cameron.³⁰

File 12. Gamma Ray Multiplicities

MT=102. Multiplicities for Gamma Ray Production from Radiative Capture

Multiplicities at neutron energies below 1 eV are based on a preliminary thermal measurement for natural W by Jurney³¹ and from 1 eV to 1000 eV on calculations by Yost et al.³² At higher energies the multiplicities are based on an analysis of natural W measurements (Dickens,³⁴ $E_n=1-20$ MeV) using statistical calculations similar to those described by Troubetzkoy,³³ with the multiplicities chosen to give rough agreement with the measurements. The theory was used at all energies to divide the natural W data into isotopic components.

File 13. Gamma Ray Production Cross Sections

MT=4. Gamma Ray Production Cross Sections from Inelastic, (n,2n), and (n,3n) Reactions

The cross sections for discrete photons are based on the level excitation cross sections in MF=3, MT=51-59, mainly using the level decay scheme of Artna.³⁵ The cross sections for continuum gamma rays are based on a statistical theory analysis of the Dickens³⁴ measurements on natural W. The theory was used for interpolation, smoothing, and separation of the data into isotopic components.

File 14. Gamma Ray Angular Distributions

MT=4, 102. Angular Distributions of Gamma Rays from Radiative Capture, Inelastic, (n,2n), and (n,3n) Reactions

Gamma rays from all reactions are assumed isotropic in the laboratory system.

File 15. Gamma Ray Energy Distributions

MT=4. Energy Distributions of Gamma Rays from Inelastic, (n,2n), and (n,3n) Reactions

The spectra at all energies are based on a statistical theory analysis of the Dickens³⁴ measurements with natural W. The theory was used as described above (MF=13, MT=4). Arbitrary adjustments were made to the theoretical fits in regions where agreement with experiment was poor (mainly below $E_n=5$ MeV).

MT=102. Energy Distributions of Gamma Rays from Radiative Capture

Spectra at neutron energies below 1 eV are based on a preliminary thermal measurement by Jurney³¹ and from 1 eV to 1000 eV on

calculations by Yost et al.³² At higher energies the spectra are based on statistical calculations using parameters obtained by analyzing the Dickens³⁴ measurement for $E_n=1-3$ MeV. The theory was used at all energies to divide the natural W data into separate isotopic components.

(Note: No information is provided in this evaluation on electron production from internal conversion. Such information might be important for local heating and radiation damage problems.)

REFERENCES

1. A. H. Wapstra and N. B. Gove, Nucl. Data Tables 9, 267 (1971).
2. M. D. Goldberg et al., BNL-325, 2nd Edition, Supplement 2 (1966).
3. Z. M. Bartolome et al., Nucl. Sci. Eng. 37, p. 137 (1969).
4. J. L. Cook et al., AAEC/TM-392 (1967).
5. M. Drake, (1968) for American Institute of Phys. Handbook (1972).
6. J. F. Whalen, ANL-7210, 16 (1966).
7. M. Davadeenam, PhD Thesis Duke University (1967).
8. W. H. Kao et al., Chinese J. Phys. 5, 43 (1967).
9. J. M. Peterson et al., Phys. Rev. 120, 521 (1960).
10. J. J. Devaney and D. G. Foster, Jr., Los Alamos report LA-4928 (1972).
11. W. E. Kinney and F. G. Perey, ORNL-4803 (1973).
12. R. O. Owens et al., Nucl. Phys. A112, 337 (1968).
13. S. Pearlstein, Nucl. Sci. Eng. 23, 238 (1965).
14. W. D. Lu et al., Phys. Rev. C1, 350 (1970).
15. J. F. Barry et al., Proc. Phys. Soc. 74, 632 (1959).
16. V. Benzi and G. Reffo, CCDN-NW10, ENEA Neutron Compilation Center (1969).
17. M. Lindner et al., Lawrence Livermore Laboratory, private communication (1972).
18. A. Rubino and D. Dubke, Nucl. Phys. 85, 606 (1966).
19. A. B. Smith and P. A. Moldauer, BAPS 5, 409 (1960).
20. F. T. Kuchnir et al., Phys. Rev. 176, 1405 (1968).
21. W. Walt and H. Barschall, Phys. Rev. 93, 1062 (1954).
22. K. Tsukada et al., Nucl. Phys. A125, 641 (1966).
23. R. W. Hill, Phys. Rev. 109, 2105 (1958).
24. W. Kinney, private communication (1972).
25. D. B. Thomson, Phys. Rev. 129, 1649 (1963).
26. H. Nauta, Nucl. Phys. 2, 124 (1956).
27. S. G. Buccino et al., Nucl. Phys. 60, 17 (1964).
28. R. O. Owens and J. H. Towle, Nucl. Phys. A112, 337 (1968).
29. W. E. Kinney, ORNL, private communication (1972).
30. A. Gilbert and A. G. W. Cameron, Can. J. Phys. 43, 1446 (1965).
31. E. T. Jurney, private communication (1973).
32. K. J. Yost, J. E. White, C. Y. Fu, and W. E. Ford, Nucl. Sci. Eng. 47, 209 (1972).
33. E. S. Troubetzkoy, Phys. Rev. 122, 212 (1961).
34. J. K. Dickens, private communication (1972).
35. A. Artna, Nuclear Data B1-1, 37 (1966).

SUMMARY DOCUMENTATION FOR ^{184}W

by

P. G. Young, J. Otter,[†] E. Ottewitte,[†] and P. Rose[†]
Los Alamos Scientific Laboratory
Los Alamos, New Mexico

I. SUMMARY

The ^{184}W evaluation for ENDF/B-V (MAT 1130) was carried over intact from Version IV with only minor format changes being made. The evaluation of the neutron files was performed at Atomics International and is documented in TI-707-130-026 (1973). The gamma-ray production data were evaluated at Los Alamos Scientific Laboratory and are documented in LA-5793 (1975). The ENDF/B-V data span the energy range 10^{-5} eV to 20 MeV.

II. ENDF/B-V FILES

File 1. General Information

MT=451. Descriptive Data

Atomic mass and Q-values taken from Ref. 1.

File 2. Resonance Parameters

MT=151. (A) Resolved Resonances Evaluation

Potential scattering cross section = 8.0 ± 1.0 b at $E_n=0$.

2200 m/s Cross Sections (barns).

	<u>CALC</u>	<u>MEAS (Ref. 2)</u>
CAP	1.8	1.8 ± 0.2
SCAT	3.9	

Resolved Resonance Parameters

-11.76	eV	from	fit to capture
102	eV	from	evaluation, Refs. 2 and 3
150 -	2060	eV	from evaluation, Refs. 2, 3, and 4
2080 -	2110	eV	from Ref. 3
2200 -	2650	eV	from Ref. 4

[†] Atomics International

MT=151. (B) Unresolved Resonances Evaluation

Potential scattering cross section = 8.5 ± 1.0 b at $E_n=0$.
Total cross section = 1.1 b at $E_n=100$ keV (calculated).

Unresolved resonance parameters from automated optimized fit to
the evaluated measured capture cross section.

AV L=0 level spacing ($E_n=0$) = 80.3 eV, energy dep. from Ref. 5.
AV Capture level width = 0.0731 eV, energy independent
L=0 Strength function = 2.3E-4 , energy independent
L=1 Strength function = 0.18E-4 , energy independent
L=2 Strength function = 1.45E-4 , energy independent

Average capture cross section uncertainty at energy E

<u>E (keV)</u>	<u>Uncertainty (%)</u>
100	15
90	10
10	10
4.5	20

Resonance integral (capture) 16.2 b calculation, 13 ± 2 b measure-
ment (Ref. 6).

File 3. Neutron Cross Sections

MT=1. Total Cross Section

The total cross section was evaluated using a least squares spline
fit to experimental data for this isotope. Spline fits of exper-
imental data for natural tungsten were also factored into the
evaluation (see MAT 1129 for references). The total cross section
curve was smoothly joined to the evaluated total cross section
in the unresolved resonance range below 100 keV. Isotopic data
references are Whalen⁷ (100-650 keV), Martin⁸ (0.65-20 MeV), and
Foster and Glasgow⁹ (2.5-15 MeV). General references for the
total cross section are Goldberg et al.² and Devaney and Foster.¹⁰
The uncertainty in the total cross section is probably less than
7% over the energy range from 600 keV to 20 MeV. Between 300 keV
and 600 keV the uncertainty increases to 10% and from 100 to 200
keV the uncertainty is estimated to be 15%.

MT=2. Elastic Cross Section

The elastic cross section was obtained by subtracting the nonelastic
cross sections from the evaluated total cross section. The elastic
cross section is in good agreement with the data of Lister¹¹
between 300 keV and 0.8 MeV. Between 0.8 MeV and 1.5 MeV, the
elastic cross section is somewhat higher than the experimental
data. Between 1 MeV and 9 MeV the evaluation curve lies above
2PLUS-COMNUC results. At 4.3 MeV the cross section is some 15%
lower than the experimental data point of Kinney and Perey¹² for
natural tungsten. Our evaluation is, however, in agreement with
their data above 5 MeV.

MT=4. Total Inelastic Cross Section

Equal to the sum of the level excitation and continuum cross sections. The total inelastic cross section for this isotope is in general agreement with the data of Owens et al.¹³ for natural tungsten between 5 and 7 MeV.

MT=16. (n,2n) Cross Section

The semi-empirical techniques of Pearlstein¹⁴ and W. D. Lu et al.¹⁵ were used to deduce the n,2n cross section.

MT=17. (n,3n) Cross Section

The n,3n cross sections were deduced using the semi-empirical techniques of S. Pearlstein¹⁴ and W. D. Lu.¹⁵ An effective threshold for the n,3n reaction was set 1.25 MeV above the theoretical threshold.

MT=28. (n,pn) Cross Section

The shape of the n,pn excitation curve is based upon the experimental data of J. F. Barry et al.¹⁶ for ¹⁸⁶W (see MAT 1131). The curve has been shifted in energy by the difference in the reaction Q for this isotope and ¹⁸⁶W. The cross section contains contributions from the n,np and n,d reactions.

MT=51. Inelastic Excitation (Direct and Compound Nucleus) to the 2⁺ Level

The cross sections were calculated using 2PLUS-COMNUC. They have been renormalized via a least squares fit to data of D. Lister et al.¹⁷ with a 10% uncertainty in the adjusted curve.

MT=52-59, 91. Inelastic Excitation (Compound Nucleus Only).

Calculation by the COMNUC code for the 365, 748, 904, 1007, 1135, 1223, 1270, and 1287 keV-levels plus the continuum. The 365-, 904-, and 1007-keV level excitation curves were renormalized to the data of D. Lister.¹⁷ The uncertainty is about 10% in the 365-keV level data and 15% in the 904- and 1007-keV level data.

MT=102. Radiative Capture Cross Section

The radiative capture cross section was evaluated between 10 keV and 150 keV using a least squares fit to experimental data (see MF=2, MT=151). This fit was combined and joined to the theoretical cross sections computed between 100 keV and 4 MeV using the COMNUC code. Above 4 MeV the COMNUC results were joined to the collective and direct interaction capture cross sections calculated using the theory of V. Benzi and G. Reffo.¹⁸ The uncertainty in the radiative capture cross section is probably less than 15% for energies between 100 keV and 200 keV. Above 200 keV the cross

section is reliable only to the extent of the validity of the theoretical models.

MT=103. (n,p) Cross Section

The shape of the n,p excitation curve is based upon the experimental data of J. F. Barry et al.¹⁶ for ¹⁸⁶W (see MAT 1131). The curve has been shifted in energy to agree with the ratio of (n,p) measurements reported by Coleman¹⁹ for ¹⁸⁴W and ¹⁸⁶W at 14.5 MeV.

MT=107. (n,α) Cross Section

The n,α cross section evaluation is based upon data of A. Rubino and D. Zubke²⁰ for ¹⁸¹Ta. The few experimental data points for isotopes of tungsten between 14 and 15 MeV qualitatively substantiate the use of this curve. The evaluation has not been extended below 11 MeV.

File 4. Neutron Angular Distributions

MT=2. Elastic Angular Distributions

The angular distributions for elastic scattering are given as Legendre polynomial coefficients in the cm system. These data were calculated by 2PLUS-COMNUC codes for each isotope. As little isotopic experimental data existed, the calculated data were averaged according to abundance and compared to natural tungsten data. The comparison indicated that the experimental data contained direct inelastic reactions to the first level. With the calculated first-level direct inelastic included, agreement within experimental error was generally indicated over all energies. This agreement also supports the validity of the inelastic angular file below. The natural tungsten experimental data were taken from Refs. 21-28. Error estimates for this section are difficult because it appears that pure elastic scatter has not been measured except at low energies. Because of the good agreement overall with the combined data, this file is estimated to be accurate to 15% at energies below 1 MeV, and within a factor of two at energies above 1 MeV for all scattering angles.

MT=51-59, 91. Angular Distribution of Inelastic Scattered Neutrons

Angular distributions are given as Legendre polynomial coefficients in the laboratory frame of reference. These data are based upon 2PLUS-COMNUC calculations. They include anisotropic contributions from direct inelastic excitation of the 2⁺ level. Compound level and continuum excitations are isotropic in the laboratory system. Errors are small simply due to the predominance of isotropy.

File 5. Neutron Energy Distributions

MT=16, 17. Nuclear Temperatures for the (n,2n) and (n,3n) Reactions

Temperature of first emitted neutron same as for MT=91. Temperatures of second and third emitted neutrons deduced by conservation of energy assuming the kinetic energy of an emitted neutron is $2*KT$.

MT=91. Nuclear Temperature for Inelastic Continuum

References 29-32 were used in deriving temperatures. Least squares Weisskopf level spacing was fit to natural tungsten data. Isotopic data adjusted using deformed nucleus level density formula of Gilbert and Cameron.³²

File 12. Gamma Ray Multiplicities

MT=102. Multiplicities for Gamma Ray Production from Radiative Capture

Multiplicities at neutron energies below 1 eV are based on a preliminary thermal measurement for natural W by Journey³³ and from 1 eV to 1000 eV on calculations by Yost et al.³⁴ At higher energies the multiplicities are based on an analysis of natural W measurements (Dickens,³⁶ $E_n=1-20$ MeV) using statistical calculations similar to those described by Troubetzkoy,³⁵ with the multiplicities chosen to give rough agreement with the measurements. The theory was used at all energies to divide the natural W data into isotopic components.

File 13. Gamma Ray Production Cross Sections

MT=4. Gamma Ray Production Cross Sections from Inelastic, (n,2n), and (n,3n) Reactions

The cross sections for discrete photons are based on the level excitation cross sections in MF=3, MT=51-59, mainly using the level decay scheme of Martin.³⁷ The cross sections for continuum gamma rays are based on a statistical theory analysis of the Dickens³⁶ measurements on natural W. The theory was used for interpolation, smoothing, and separation of the data into isotopic components.

File 14. Gamma Ray Angular Distributions

MT=4, 102. Angular Distributions of Gamma Rays from Radiative Capture, Inelastic, (n,2n), and (n,3n) Reactions

Gamma rays from all reactions are assumed isotropic in the laboratory system.

File 15. Gamma Ray Energy Distributions

MT=4. Energy Distributions of Gamma Rays from Inelastic, (n,2n), and (n,3n) Reactions

The spectra at all energies are based on a statistical theory analysis of the Dickens³⁶ measurements with natural W. The theory was used as described above (MF=13, MT=4). Arbitrary adjustments were made to the theoretical fits in regions where agreement with experiment was poor (mainly below $E_n=5$ MeV).

MT=102. Energy Distributions of Gamma Rays from Radiative Capture

Spectra at neutron energies below 1 eV are based on a preliminary thermal measurement by Jurney³³ and from 1 eV to 1000 eV on calculations by Yost et al.³⁴ At higher energies the spectra are based on statistical calculations using parameters obtained by analyzing the Dickens³⁶ measurement for $E_n=1-3$ MeV. The theory was used at all energies to divide the natural W data into separate isotopic components.

(Note: No information is provided in this evaluation on electron production from internal conversion. Such information might be important for local heating and radiation damage problems).

REFERENCES

1. A. H. Wapstra and N. B. Gove, Nucl. Data Tables 9, 267 (1971).
2. M. D. Goldberg et al., BNL-325, 2nd Edition, Supplement 2, (1966).
3. Z. M. Bartolome et al., Nucl. Sci. Eng. 37, p. 137 (1969).
4. F. J. Rahn and H. Camarda, personal communication, Columbia (1970).
5. J. L. Cook et al., AAEC/TM-392 (1967).
6. M. Drake, (1968) for American Institute of Phys. Handbook (1972).
7. J. F. Whalen, ANL-7210, 16 (1966).
8. R. C. Martin, PhD Thesis, RPT (1967).
9. D. G. Foster, and D. W. Glasgow, Phys. Rev. 3C, 576 (1971).
10. J. J. Devaney and D. G. Foster, Jr., Los Alamos report LA-4928 (1972).
11. D. Lister et al., ANL-7288 (1967).
12. W. E. Kinney and F. G. Perey, ORNL-4803 (1973).
13. R. O. Owens et al., Nucl. Phys. A112, 337 (1968).
14. S. Pearlstein, Nucl. Sci. Eng. 23, 238 (1965).
15. W. D. Lu et al., Phys. Rev. C1, 350 (1970).
16. J. F. Barry et al., Proc. Phys. Soc. 74, 632 (1959).
17. D. Lister et al., Phys. Rev. 162, 1077 (1967).
18. V. Benzi and G. Reffo, CCDN-NW10, ENEA Neutron Compilation Center (1969).
19. R. F. Coleman, Proc. Phys. Soc. 73, 215 (1959).
20. A. Rubino and D. Zubke, Nucl. Phys. 85, 606 (1966).
21. A. B. Smith and P. A. Moldauer, BAPS 5, 409 (1960).
22. F. T. Kuchnir et al., Phys. Rev. 176, 1405 (1968).
23. W. Walt and H. Barschall, Phys. Rev. 93, 1062 (1954).
24. K. Tsukada et al., Nucl. Phys. A125, 641 (1966).
25. R. W. Hill, Phys. Rev. 109, 2105 (1958).

26. W. Kinney, private communication (1972).
27. D. B. Thomson, Phys. Rev. 129, 1649 (1963).
28. H. Nauta, Nucl. Phys. 2, 124 (1956).
29. S. G. Buccino et al., Nucl. Phys. 60, 17 (1964).
30. R. O. Owens and J. H. Towle, Nucl. Phys. A112, 337 (1968).
31. W. E. Kinney, ORNL, private communication (1972).
32. A. Gilbert and A. G. W. Cameron, Can. J. Phys. 43, 1446 (1965).
33. E. T. Jurney, private communication (1973).
34. K. J. Yost, J. E. White, C. Y. Fu, and W. E. Ford, Nucl. Sci. Eng. 47, 209 (1972).
35. E. S. Troubetzkoy, Phys. Rev. 122, 212 (1961).
36. J. K. Dickens, private communication (1972).
37. M. J. Martin, Nuclear Data B1-1, 63 (1966).

SUMMARY DOCUMENTATION FOR ^{186}W

by

P. G. Young, J. Otter,[†] E. Ottewitte,[†] and P. Rose[†]
Los Alamos Scientific Laboratory
Los Alamos, New Mexico

I. SUMMARY

The ^{186}W evaluation for ENDF/B-V (MAT 1131) was carried over intact from Version IV with only minor format changes being made. The evaluation of the neutron files was performed at Atomics International and is documented in TI-707-130-026 (1973). The gamma-ray production data were evaluated at Los Alamos Scientific Laboratory and are documented in LA-5793 (1975). The ENDF/B-V data span the energy range 10^{-5} eV to 20 MeV.

II. ENDF/B-V FILES

File 1. General Information

MT=451. Descriptive Data

Atomic mass and Q-values taken from Ref. 1.

File 2. Resonance Parameters

MT=151. (A) Resolved Resonances Evaluation

Potential scattering cross section = 8.0 ± 1.0 b at $E_n=0$.

2200 m/s Cross Sections (barns).

	<u>CALC</u>	<u>MEAS (Ref. 2)</u>
CAP	37.5	38 ± 2
SCAT	0.39	

Resolved Resonance Parameters

18.81	eV	from	evaluation of Refs. 2 and 4 plus adjustment from fit to capture cross section
100	-	250 eV	from evaluation of Refs. 2-4
250	-	3200 eV	from evaluation of Refs. 3-4

[†]Atomics International

MT=51. (B) Unresolved Resonances Evaluation

Potential scattering cross section = 8.5 ± 1.0 b at $E_n=0$.
 Total cross section = 9.1 b at $E_n=100$ keV (calculated).

Unresolved resonance parameters from automated optimized fit to the evaluated measured capture cross section.

AV L=0 level spacing (E=0) = 99.1 eV, energy dep. from Ref. 5
 AV Capture level width = 0.0530 eV, energy independent
 L=0 Strength function = 2.2E-4, energy independent
 L=1 Strength function = 0.252E-4, energy independent
 L=2 Strength function = 1.45E-4, energy independent

Average capture cross section uncertainty at energy E

<u>E (keV)</u>	<u>Uncertainty (%)</u>
100	11
90	8
45	8
22.5	14
10	11
4.5	17

Resonance integral (capture) 522 b calculation, 490 ± 50 b measurement (Ref. 6).

File 3. Neutron Cross Sections

MT=1. Total Cross Section

The total cross section was evaluated using a least squares spline fit to experimental data for this isotope. Spline fits of experimental data for natural tungsten were also factored into the evaluation (see MAT 1129 for Refs). The total cross section curve was smoothly joined to the evaluated total cross section in the unresolved resonance range below 100 keV. Isotopic data references are Whalen⁷ (100-650 keV), Martin⁸ (0.65-20 MeV), and Foster and Glasgow⁹ (2.5-15 MeV). General references for the total cross section are Goldberg et al.² and Devaney and Foster.¹⁰ The uncertainty in the total cross section is probably less than 7% over the energy range from 600 keV to 20 MeV. Between 300 keV and 600 keV the uncertainty increases to 10% and from 100 to 200 keV the uncertainty is estimated to be 15%.

MT=2. Elastic Cross Section

The elastic cross section was obtained by subtracting the nonelastic cross sections from the evaluated total cross section. The elastic cross section is in good agreement with the data of Lister¹¹ between 300 keV and 0.7 MeV. Between 0.7 MeV and 1.5 MeV, the elastic cross section is some 10% higher than the experimental data. Between 1 MeV and 9 MeV the evaluated curve lies above 2PLUS-COMNUC results. At 4.3 MeV the cross section is some 15% lower than the experimental data point of Kinney and Perey¹² for natural tungsten. Our evaluation is, however, in agreement with their data above 5 MeV.

MT=4. Total Inelastic Cross Section

Equal to the sum of the level excitation and continuum cross section. The total inelastic cross section for this isotope is in general agreement with the data of Owens et al.¹³ for natural tungsten between 5 and 7 MeV.

MT=16. (n,2n) Cross Section

The semi-empirical techniques of Pearlstein¹⁴ and W. D. Lu et al.¹⁵ were used to deduce the n,2n cross section. The evaluated curve at 14.8 MeV is in agreement with Druzhinin et al.¹⁶

MT=17. (n,3n) Cross Section

The n,3n cross sections were deduced using the semi-empirical techniques of S. Pearlstein¹⁴ and W. D. Lu.¹⁵ An effective threshold for the n,3n reaction was set 1.25 MeV above the theoretical threshold.

MT=28. (n,pn) Cross Section

The shape of the n,pn excitation curve is based upon the experimental data of J. F. Barry et al.¹⁷ The uncertainty in the cross section is 25% at energies well above the observed threshold. The cross section contains contributions from the n,np and n,d reactions.

MT=51. Inelastic Excitation (Direct and Compound Nucleus) to the 2⁺ Level

The cross sections were calculated using 2PLUS-COMNUC. They have been renormalized via a least squares fit to data of D. Lister et al.¹⁸ with a 10% uncertainty in the adjusted curve.

MT=52-59, 91. Inelastic Excitation (Compound Nucleus Only).

Calculation by the COMNUC code for the 401, 730, 840, 850, 960, 1040, 1110, and 1250 keV levels plus the continuum. The 401, 730, and 942-keV level excitation curves were renormalized to the data of D. Lister.¹⁸ The uncertainty in the adjusted cross sections is about 10%. The sum of the 840 and 850 keV level COMNUC results were renormalized to the 863 ± 10 keV excitation data of D. Lister. Likewise, the sum of the 1040 and 1110 keV levels were renormalized to the 1035 ± 10 keV experimental data. The summed levels have a 15% cross section uncertainty.

MT=102. Radiative Capture Cross Section

The radiative capture cross section was evaluated between 10 keV and 4 MeV using a least squares spline fit to experimental data (see MF=2, MT=151). Comparisons with COMNUC theoretical results were excellent. Adjustments were made, however, to the data fit

in the neighborhood of the 2^+ threshold to better fit the theoretical calculations. These adjustments improved the reconstructed elemental file comparison with experiment. Above 4 MeV the data fit was joined to theoretical capture cross sections calculated between 4 and 20 MeV. The theory of Benzi and Reffo¹⁹ was used to determine the collective and direct interaction cross section.

MT=103. (n,p) Cross Section

The n,p cross section evaluation is based upon experimental data of J. F. Barry et al.¹⁷ Uncertainty is 25% at energies well above the observed threshold.

MT=107. (n, α) Cross Section

The n, α cross section evaluation is based upon data of A. Rubino and D. Zubke²⁰ for ^{181}Ta . The few experimental data points for isotopes of tungsten between 14 and 15 MeV qualitatively substantiate the use of this curve. The evaluation has not been extended below 11 MeV.

File 4. Neutron Angular Distributions

MT=2. Elastic Angular Distributions

The angular distributions for elastic scattering are given as Legendre polynomial coefficients in the cm system. These data were calculated by 2PLUS-COMNUC codes for each isotope. As little isotopic experimental data existed, the calculated data were averaged according to abundance and compared to natural tungsten data. The comparison indicated that the experimental data contained direct inelastic reactions to the first level. With the calculated first-level direct inelastic included, agreement within experimental error was generally indicated over all energies. This agreement also supports the validity of the inelastic angular file below. The natural tungsten experimental data were taken from Refs. 21-28. Error estimates for this section are difficult because it appears that pure elastic scatter has not been measured except at low energies. Because of the good agreement overall with the combined data, this file is estimated to be accurate to 15% at energies below 1 MeV, and within a factor of two at energies above 1 MeV for all scattering angles.

MT=51-59, 91. Angular Distribution of Inelastic Scattered Neutrons

Angular distributions are given as Legendre polynomial coefficients in the laboratory frame of reference. These data are based upon 2PLUS-COMNUC calculations. They include anisotropic contributions from direct inelastic excitation of the 2^+ level. Compound level and continuum excitations are isotropic in the laboratory system. Errors are small simply due to the predominance of isotropy.

File 5. Neutron Energy Distributions

MT=16, 17. Nuclear Temperatures for the (n,2n) and (n,3n) Reactions

Temperature of first emitted neutron same as for MT=91. Temperatures of second and third emitted neutrons deduced by conservation of energy assuming the kinetic energy of an emitted neutron is $2 \cdot K_T$.

MT=91. Nuclear Temperature for Inelastic Continuum

References 29-32 were used in deriving temperatures. Least squares Weisskopf level spacing was fit to natural tungsten data. Isotopic data adjusted using deformed nucleus level density formula of Gilbert and Cameron.³²

File 12. Gamma Ray Multiplicities

MT=102. Multiplicities for Gamma Ray Production from Radiative Capture

Multiplicities at neutron energies below 1 eV are based on a preliminary thermal measurement for natural W by Journey³³ and from 1 eV to 1000 eV on calculations by Yost et al.³⁴ At higher energies the multiplicities are based on an analysis of natural W measurements (Dickens,³⁶ $E_n=1-20$ MeV) using statistical calculations similar to those described by Troubetzkoy,³⁵ with the multiplicities chosen to give rough agreement with the measurements. The theory was used at all energies to divide the natural W data into isotopic components.

File 13. Gamma Ray Production Cross Sections

MT=4. Gamma Ray Production Cross Sections from Inelastic, (n,2n), and (n,3n) Reactions

The cross sections for discrete photons are based on the level excitation cross sections in MT=3, MT=51-59, mainly using the level decay scheme of Gove.³⁷ The cross sections for continuum gamma rays are based on a statistical theory analysis of the Dickens³⁶ measurements on natural W. The theory was used for interpolation, smoothing, and separation of the data into isotopic components.

File 14. Gamma Ray Angular Distributions

MT=4, 102. Angular Distributions of Gamma Rays from Radiative Capture, Inelastic, (n,2n), and (n,3n) Reactions

Gamma rays from all reactions are assumed isotropic in the laboratory system.

File 15. Gamma Ray Energy Distributions

MT=4. Energy Distributions of Gamma Rays from Inelastic, (n,2n), and (n,3n) Reactions

The spectra at all energies are based on a statistical theory analysis of the Dickens³⁶ measurements with natural W. The theory was used as described above (MF=13, MT=4). Arbitrary adjustments were made to the theoretical fits in regions where agreement with experiment was poor (mainly below $E_n=5$ MeV).

MT=102. Energy Distributions of Gamma Rays from Radiative Capture

Spectra at neutron energies below 1 eV are based on a preliminary thermal measurement by Jurney³³ and from 1 eV to 1000 eV on calculations by Yost et al.³⁴ At higher energies the spectra are based on statistical calculations using parameters obtained by analyzing the Dickens³⁶ measurement for $E_n=1-3$ MeV. The theory was used at all energies to divide the natural W data into separate isotopic components.

(Note: No information is provided in this evaluation on electron production from internal conversion. Such information might be important for local heating and radiation damage problems.)

REFERENCES

1. A. H. Wapstra and N. B. Gove, Nucl. Data Tables 9, 267 (1971).
2. M. D. Goldberg et al., BNL-325, 2nd Edition, Supplement 2, (1966).
3. Z. M. Bartolome et al., Nucl. Sci. Eng. 37, p. 137 (1969).
4. F. J. Rahn and H. Camarda, personal communication, Columbia (1970).
5. J. L. Cook et al., AAEC/TM-392 (1967).
6. M. Drake, (1968) for American Institute of Phys. Handbook (1972).
7. J. F. Whalen, ANL-7210, 16 (1966).
8. R. C. Martin, PhD Thesis, RPT (1967).
9. D. G. Foster and D. W. Glasgow, Phys. Rev. 3C, 576 (1971).
10. J. J. Devaney and D. G. Foster, Jr., Los Alamos report LA-4928 (1972).
11. D. Lister et al., ANL-7288 (1967).
12. W. E. Kinney and F. G. Perey, ORNL-4803 (1973).
13. R. O. Owens et al., Nucl. Phys. A112, 337 (1968).
14. S. Pearlstein, Nucl. Sci. Eng. 23, 238 (1965).
15. W. D. Lu et al., Phys. Rev. C1, 350 (1970).
16. Druzhinin et al., Sov. J. Nucl. Phys. 4, 515 (1966).
17. J. F. Barry et al., Proc. Phys. Soc. 74, 632 (1959).
18. D. Lister et al., Phys. Rev. 162, 1077 (1967).
19. V. Benzi and G. Reffo, CCDN-NW10, ENEA Neutron Compilation Center (1969).
20. A. Rubino and D. Zubke, Nucl. Phys. 85, 606 (1966).
21. A. B. Smith and P. A. Moldauer, BAPS 5, 409 (1960).
22. F. T. Kuchnir et al., Phys. Rev. 176, 1405 (1968).
23. W. Walt and H. Barschall, Phys. Rev. 93, 1062 (1954).
24. K. Tsukada et al., Nucl. Phys. A125, 641 (1966).
25. R. W. Hill, Phys. Rev. 109, 2105 (1958).

26. W. Kinney, private communication (1972).
27. D. B. Thomson, Phys. Rev. 129, 1649 (1963).
28. H. Nauta, Nucl. Phys. 2, 124 (1956).
29. S. G. Buccino et al., Nucl. Phys. 60, 17 (1964).
30. R. O. Owens and J. H. Towle, Nucl. Phys. A112, 337 (1968).
31. W. E. Kinney, ORNL, private communication (1972).
32. A. Gilbert and A. G. W. Cameron, Can. J. Phys. 43, 1446 (1965).
33. E. T. Jurney, private communication (1973).
34. K. J. Yost, J. E. White, C. Y. Fu, and W. E. Ford, Nucl. Sci. Eng. 47, 209 (1972).
35. E. S. Troubetzkoy, Phys. Rev. 122, 212 (1961).
36. J. K. Dickens, private communication (1972).
37. N. B. Gove, Nuclear Data B1-2, 1 (1966).

SUMMARY DOCUMENTATION FOR ^{233}U

by

L. Stewart, D. G. Madland, and P. G. Young
Los Alamos Scientific Laboratory
Los Alamos, New Mexico

and

L. Weston and G. de Saussure
Oak Ridge National Laboratory
Oak Ridge, Tennessee

and

F. Mann
Hanford Engineering and Development Laboratory
Richland, Washington

and

N. Steen
Bettis Atomic Power Laboratory
West Mifflin, Pennsylvania

I. SUMMARY

A new evaluation of neutron-induced reactions on ^{233}U was carried out for Version V of ENDF/B (MAT 1393). The analysis was divided among several laboratories. The thermal data evaluation was performed at BAPL and LASL, the resolved and unresolved resonance regions were evaluated at ORNL and HEDL, and evaluation of the data from 10 keV to 20 MeV and assembly of the composite file was carried out at LASL. In addition, fission product yield data were provided by the CSEWG Yield Subcommittee (T. England, chairman), and radioactive decay data by C. Reich (INEL). Partial documentation of the evaluation is provided in LA-7200-PR³ and in reference 16. The evaluation covers the energy range 10^{-5} eV to 20 MeV. Gamma-ray production and covariance data will be added to the file in a later MOD 1 update.

II. ENDF/B-V FILES

File 1. General Information

MT=451. Descriptive data.

MT=452. $\bar{\nu}$ Total

Sum of prompt plus delayed $\bar{\nu}$. Used thermal value recommended by CSEWG Standards Subcommittee of 2.4947 on 5-27-78. This value is 1% larger than recommended by Lemmel¹ and 0.13% smaller than Version IV.

MT=455. $\bar{\nu}$ Delayed

The delayed yields and spectra were evaluated by Kaiser and Carpenter at ANL-Idaho (see Ref. 2 for technical details). The same six-group yields appear in Version IV but the spectra have been changed for Version V.

MT=456. $\bar{\nu}$ Prompt

The energy dependence of prompt $\bar{\nu}$ is changed significantly from Version IV. Although the thermal value is slightly lower, the value around 1.5 MeV is significantly higher and has a different shape with three slightly different slopes. This evaluation relies heavily on the measurements with respect to ^{235}U and ^{252}Cf using the CSEWG recommended standards. In particular, the data of Boldeman, Sergachev, Nurpeisov, and Block⁵⁻⁷ were weighted at all energies while the Mather⁸ measurements were relied upon only at high energies. Smirenkin, Flerov, and Protopopov⁹⁻¹¹ also contributed in the high-energy range. This evaluation decouples the thermal value based on η measurements from the fast range. Otherwise, the $\bar{\nu}$ - η discrepancy would be perpetuated to 20 MeV.

MT=458. Energy Release in Fission

These values were taken directly from an evaluation by R. Sher¹² (Stanford).

File 2. Resonance Parameters

MT=151. (a) Resolved Resonance Region

Resolved range extends to 60 eV. Multi-level parameters provided by de Saussure (ORNL) in Adler-Adler formalism from analysis by Reynolds (KAPL). Version IV used single-level Breit-Wigner representation but had large fluctuations in fission in File 3 background.

(b) Unresolved Resonance Region

Unresolved range extends to 10 keV. Version IV was pointwise over this range. A reevaluation of the point-wise cross sections begun by Mann (HEDL) were used as the starting point by Weston (ORNL), who obtained new average cross sections for fission and capture which require no File 3 backgrounds. Cross sections based on Carlson and Behrens,⁴ Weston,¹⁷ Cao,¹⁸ and Nizamuddin¹⁹ for fission. Weston's data²⁰ were used for capture using a potential

scattering radius of 0.9893. Reasonable agreement with Patten-den's total cross section²¹ was obtained, especially below 1 keV. New measurements are needed in this range.

File 3. Neutron Cross Sections

Thermal Range

The 2200 m/s ($E_n=0.0253$ eV) data are as follows:

Eta	2.2959	Capture	45.76 b
Alpha	0.0866	Fission	528.45 b
ν Prompt	2.4873	Absorption	574.21 b
ν Total	2.4947	Elastic	12.6 b
		Total	586.81 b

The capture and fission cross sections were renormalized by N. Steen (BAPL). The elastic scattering in the thermal range changed significantly from Version IV to conform to Leonard's thermal and Weston's evaluation in unresolved range. The total was adjusted accordingly. Elastic and total changes made by LASL.

10 keV - 20 MeV

Much of the File 3 data above 50 keV relied heavily on model calculations performed by Madland (LASL). Calculations were particularly important for this isotope since experimental information was often insufficient if not completely missing. A detailed description of the methods used can be found in reference 3. Note that for convenience, many of the specific references found in BNL-325 are not repeated here.

MT=1. Total Cross Section

No measurements exist from 10 to 40 keV; therefore, an extrapolation was made to give reasonable agreement with recent ANL data¹³ above 40 keV and cross sections predicted by Madland. The present evaluation is based on recent ANL measurements¹³ and earlier work of Green (Bettis) and Foster (Hanford). See BNL-325 (Ref. 5). No measurements exist above 15 MeV. This reevaluation resulted in an increased total cross section up to 7 MeV, the increase near 1.6 MeV being as large as 8%. Use of the Foster data resulted in a decrease of 4.8% near 14 MeV.

MT=2. Elastic Cross Section

(Obtained from total minus reaction). The increased total cross section required a significant increase in the elastic cross section over the energy range to 7 MeV. At 14 MeV the elastic was decreased due to the decrease in the total.

MF=4. Inelastic Cross Section

Sum of MT=51-54 and MT=91. These data were taken from model calculations of discrete and continuum compound inelastic scattering and coupled-channel direct inelastic scattering.

MT=16, 17. (n,2n) and (n,3n) Cross Sections

Taken from Hauser-Feshbach statistical model calculations performed by Madland.

MT=18. (n,f) Cross Sections

Data from 10 keV to 100 keV sparse and reasonably discrepant.

Above 100 keV, we relied heavily on the ratio measurements of Carlson and Behrens⁴ and those of Meadows,¹⁴ normalized to Version V ²³⁵U fission. The absolute data of Poenitz¹⁵ were also employed, although good agreement among the sets was lacking. The evaluated curve was drawn as smoothly as possible due to the magnitude of the discrepancy among the sets.

MT=51-54. Discrete Inelastic Cross Sections

Taken from compound and direct inelastic scattering model.

MT=102. Radiative Capture Cross Section

No data exist above 10 keV except for the α measurements of Diven and Hopkins (see Ref. 5) which extend to 1 MeV. Extrapolated to 20 MeV assuming a rise due to direct capture.

MT=251, 252, 253. μ_L , ξ , γ

Calculated from MF=3 and 4 data and input by Kinsey at BNL.

File 4. Neutron Angular Distributions

All neutron angular distributions isotropic in laboratory system except for the elastic (MT=2) which was taken from Version IV. The elastic and direct inelastic should be modified in the next update.

File 5. Neutron Energy Distributions

MT=16, 17. (n,2n), (n,3n) Energy Distributions

Represented by an evaporation spectrum with LF=9.

MT=18. (n,f) Neutron Energy Distributions

Represented by an energy-dependent Watt spectrum with an average energy at thermal of 2.073 MeV. This spectrum based on Grundl ratio data to ²³⁵U and ²³⁹Pu.

MT=91. Inelastic Continuum Energy Distributions

Represented by an evaporation spectrum with LF=9.

MT=455. Delayed Neutron Spectra

Evaluated in six time groups by Kaiser and Carpenter² at ANL-
Idaho.

File 8. Fission Product Yields and Decay Data

MT=454. Individual Fission Product Yields

Direct yields before neutron emission.

MT=459. Cumulative Yields

Cumulative yields along each isobaric chain after neutron emission taken from set 5D.3/78. Values recommended by CSEWG Yields Subcommittee (England, chairman).

Note: Both direct and cumulative yields are normalized by the same factors based on B. F. Rider evaluation. The isomeric state model, LA-6595-MS (ENDF-241), and delayed neutron emission branchings (Pn values) for 102 emitters, and pairing effects, LA-6430-MS (ENDF-240), have been incorporated.

Uncertainties are based on the total yield to each ZA. When there is an isomeric state, the independent nuclide yield to each state has a larger uncertainty than the total yield in state distributions. (Uncertainties average 50% but can be larger). Any yield with an uncertainty of 45-64% may be model estimate or a value assigned in the wings of the mass distribution. These small yields may be accurate only within a factor of two.

Data prepared for ENDF/B-V by T. R. England (Ref. LA-UR-78-687).

MT=457. Radioactive Decay Data

Evaluated by C. Reich (INEL).

Q (ALPHA) - 1974 Version of Wapstra-Bos-Gove mass tables.

Half-life - Average of values by Vaninbroukx²² and Jaffy et al.²³

Alpha Energies and Intensities - Are based mainly on the results of Ellis²⁴ with a few deletions based on level-scheme considerations. Energies and intensities of the two most prominent alpha groups are those recommended by Rytz.²⁵

Gamma-Ray Energies and Intensities - Based on results of Kroger and Reich.²⁶

Gamma-Ray Multipolarities - Taken from level scheme considerations
(see reference 26).

General Note. The decay data (MT=457) were translated into the ENDF/B-V format by Mann and Schenter at HEDL. Also, much of the above data provided by other laboratories were first input in the file by Bob Kinsey at BNL and then sent to LASL. His help was significant and is gratefully acknowledged in assembling this file.

REFERENCES

1. H. D. Lemmel, Proc. of a symposium on Neutron Standards and Applications held at NBS on March 28-31, 1977. See p. 170.
2. Kaiser and Carpenter, private communication to BNL (1978).
3. D. G. Madland and P. G. Young, LA-7200-PR (1978) p. 11 and p. 13.
4. G. W. Carlson and J. W. Behrens, Nucl. Sci. Eng. 66, 205 (1978).
5. D. I. Garber and R. R. Kinsey, BNL-325, Vol. 11 (1976).
6. J. W. Boldeman, J. Nucl. Ener. 25, 321 (1971), and Boldeman, Bertram, and Walsh, Nucl. Phys. A265, 337 (1976).
7. L. Reed, R. W. Hockenbury, and R. C. Block, report COO-3058-39, p. 9 (Sept. 1973).
8. D. S. Mather, Nuc. Phys. 66, 149 (1965).
9. G. N. Smirenkin, At. Ener. 4, 88 (1958).
10. N. N. Flerov, At. Ener. 10, 86 (1961).
11. A. N. Protopopov, At. Ener. 5, 71 (1958).
12. R. Sher, S. Fiarman, and C. Beck, private communication to BNL (1976).
13. W. P. Poenitz, J. F. Whalen, P. Guenther, and A. B. Smith, Nucl. Sci. Eng. 68, 358 (1978).
14. J. W. Meadows, Nucl. Sci. Eng. 54, 317 (1974).
15. W. P. Poenitz, ANL-NDM-36 (1978).
16. L. Stewart, D. Madland, and P. Young, Trans. Am. Nuc. Soc. 28, 721 (1978).
17. L. Weston et al, Nucl. Sci. Eng. 42, 143 (1970).
18. M. Cao et al., J. Nucl. Ener. 24, 111 (1970).
19. S. Nizamuddin and J. Blons, Nucl. Sci. Eng. 54, 116 (1974).

20. L. Weston et al., Nucl. Sci. Eng. 34, 1 (1968).
21. N. Pattenden et al, Nucl. Sci. Eng. 17, 404 (1963).
22. R. Vaninbroukx et al., Phys. Rev. C13, 315 (1976).
23. A. H. Jaffy et al., Phys. Rev. C9, 1991 (1974).
24. Y. A. Ellis, Nucl. Data Sheets B6, #3, 257 (1971).
25. A. Rytz, At. Data and Nucl. Data Tables 12, #5, 479 (1973).
26. L. A. Kroger and C. W. Reich, Nucl. Phys. A259, 29 (1976).

SUMMARY DOCUMENTATION FOR ^{242}Pu

by

F. Mann and R. Schenier
Hanford Engineering and Development Laboratory
Richland, Washington

and

D. G. Madland and P. G. Young
Los Alamos Scientific Laboratory
Los Alamos, New Mexico

I. SUMMARY

A new evaluation of neutron-induced reactions on ^{242}Pu was performed for Version V of ENDF/B (MAT 1342). The analysis was divided between HEDL, where the resolved and unresolved resonance regions were evaluated, and LASL, where the data above a neutron energy of 10 keV were evaluated. These evaluations are documented in HEDL-TME-77-54 (Ma77B) and LASL-7533-MS (Ma78). Additionally, decay data were provided by C. Reich (INEL), thermal data by R. Benjamin (SRL), and gamma-ray production data by R. Howerton (LLL). The evaluation covers the energy range 10^{-5} eV to 20 MeV and includes covariance data at all energies.

II. ENDF/B-V FILES

File 1. General Information

MT=451. Descriptive data

MT=452. $\bar{\nu}$ Total

Sum of MT=456 and a delayed $\bar{\nu}$ of 0.015 from the measurement of Kr70 as compiled by Ma72.

MT=456. $\bar{\nu}$ Prompt

Based on a fit to ^{240}Pu experimental data by Fr74 using systematics to infer delta $\bar{\nu}$ to ^{242}Pu , and renormalized to ^{252}Cf thermal $\bar{\nu}$ of 3.757.

MT=458. Energy of Fission

Based on work of Sh76.

File 2. Resonance Parameters (E_n=0-10 keV)

MT=151. (a) Resolved Resonances

The resolved resonance region covers the energy range 0-986 eV. One bound level and 67 resolved resonances describe the cross section data from zero to 986 eV. Except for the bound and 2.68 eV levels, parameters are from BNL-325 (Mu76). Parameters for the bound and 2.68 eV levels have been modified to preserve the cross section values and shapes in the thermal region as described by Yo70 and Yo71, along with the higher resonance capture integral suggested by integral and production experiments (Bu57, Ha64, and Be75).

(b) Unresolved Resonances

The unresolved resonance region covers the energy range from 986 eV to 10 keV. Average parameters obtained by averaging the resolved resonance data were used for the L=0 resonances. The remaining data were obtained from MAT 1161, ENDF/B-IV.

File 3. Neutron Cross Sections

General

Evaluation from 0.01 - 20 MeV described in Ma78. Statistical compound nucleus and direct reaction theory calculations performed with LASL versions of COMNUC (Du70, 3-29-78 version) and JUKARL (Re71). All calculations used LASL preliminary global actinide optical potential (Ma77). Complete set of calculations performed but elastic and fission cross section evaluations differ slightly (less than 5%) from calculations because of influence of fission measurements. (n,f), (n,nf), and (n,2nf) cross sections calculated subject to constraint that their sum equals measured (Be78) total fission cross section within 5%. Discrete fission channels (up to 12) and deformed level density continuum fission channels used.

MT=1. Total Cross Section

Spherical optical model calculation with nuclear deformation effects accounted for by coupled-channel calculations of up to 5 states of ground state band.

MT=2. Elastic Cross Section

Difference between MT=1 and MT=4, 16, 17, 18, and 102. Agrees with model calculation to within few per cent.

MT=4. Inelastic Scattering Cross Section

Sum of MT=51-69 and MT=91.

MT=16, 17 (n,2n) and (n,3n) Cross Sections

Based on compound nucleus statistical model calculations.

MT=18. Fission Cross Sections

Below 100 keV based on experimental data of Au71. From 0.1 to 20 MeV based on experimental data of Be78 (see Figs. 1 and 2).

MT=51-54. Discrete Inelastic Cross Sections

Based on Hauser-Feshbach compound nucleus calculation and coupled-channel calculation of direct inelastic scattering for first 5 levels of ground state rotational band using deformation parameters of Be73.

MT=55-69. Discrete Inelastic Cross Sections

Based on Hauser-Feshbach compound nucleus calculation.

MT=102. Capture Cross Sections

Based on compound nucleus statistical calculation with gamma strength function adjusted to agree with Ho75 measurements $2\pi T_\gamma/D = 0.01045$, Mu73). Above 4 MeV, semi-direct contribution added from preequilibrium cascade calculation with gamma-ray emission probability, calculated at each stage (Ar78). See Fig. 3 for comparison with measurements.

File 4. Neutron Angular Distributions

MT=2. Elastic Scattering Angular Distributions

Shape elastic component based on deformed optical model calculation. Compound nucleus component assumed isotropic. All distributions given in form of Legendre coefficients.

MT=16, 17, 18. (n,2n), (n,3n), and (n,f) Angular Distributions

Given as Legendre coefficients and assumed isotropic in the laboratory system.

MT=51-54. Discrete Inelastic Angular Distributions (A)

Direct component taken from deformed optical model calculation, and compound nucleus component assumed isotropic. Given in form of Legendre coefficients.

MT=55-69. Discrete Inelastic Angular Distributions (B).

Legendre coefficient representation assumed isotropic in the center-of-mass system.

MT=91. Continuum Inelastic Angular Distributions

Legendre coefficient representation assumed isotropic in the laboratory system.

File 5. Neutron Energy Distributions

MT=16, 17. (n,2n), (n,3n) Energy Distributions

Nuclear temperatures calculated from level density parameters used in model calculations (Gi65 and Co67).

MT=18. (n,f) Neutron Energy Distributions

Fission Maxwellian using energy-dependent temperatures from Terrell (Te65).

MT=91. Continuum Inelastic Neutron Energy Distributions

Nuclear temperatures calculated from level density parameters used in nuclear model calculations (Gi65 and Co67).

File 8. Fission-Product Yield and Nuclide Decay Data

MT=454. Fission Yield Data

Fission-product yields were obtained from the recommendations of the CSEWG Yields Subcommittee (T. R. England chairman).

MT=457. Decay Data

The Q (alpha) was obtained from the 1974 version of the Wapstra-Bos-Gove mass tables. Half-life values were taken from reference Va74, and other data were obtained from the Table of Isotopes (Le77) and Nuclear Data Sheets (El70). Note that the energies and intensities of the two highest energy alpha groups are those recommended by Rytz (Ry73).

All the decay data were translated into ENDF/B-V format by Mann & Schenter (HEDL, 6/76).

Files 12-15. Photon-Production Data

Files taken from the LLL evaluations of R. Howerton (Ho76). Files extended to the energy range 1.0^{-5} eV to 20 MeV and merged to this evaluation at BNL by R. Kinsey.

File 33. Neutron Cross Section Covariances (HEDL and LASL)

Approximate error files determined from estimated uncertainties in model calculations (MT=1, 2, 4, 16, 17, 102) and in experimental measurements (MT=18, 102).

REFERENCES

Ar78 E. D. Arthur, private communication (1978).
Au71 G. F. Auchampaugh, J. A. Farrell, and D. W. Bergen, Nucl. Phys. A171, 31 (1971).
Be73 C. E. Bemis et al., Phys. Rev. C8, 1466 (1973).
Be75 R. Benjamin et al., DP-1394 (1975).
Be78 J. W. Behrens et al., Nuc. Sci. Eng. 66, 433 (1978).
Bu57 J. Butler et al., Can. J. Phys. 35, 147 (1957).
Co67 J. L. Cook et al., Aust. J. Phys. 20, 477 (1967).
Du70 C. L. Dunford, AI-AEC-12931 (1970).
El70 Y. A. Ellis, Nucl. Data Sheets B4, #6, 683 (1970).
Fr74 J. Frehaut et al., CEA-R-4626 (1974).
Gi65 A. Gilbert and A. G. W. Cameron, Can. J. Phys. 43 1446 (1965).
Ha64 J. Halperin et al., ORNL-3679, 13 (1964).
Ho75 R. W. Hockenbury et al., NBS Special Publication 425, Vol. 2, p. 584, (1975).
Ho76 R. Howerton et al., UCRL-50400, Vol. 15, Part A (Methods, 1975) and Part B (Curves, 1976).
Kr70 M. S. Krick and A. E. Evans, Trans. Am. Nucl. Soc. 13, 746 (1970).
Le77 C. M. Lederer, Table of Isotopes, 7th Ed (preliminary data received in private communication, 1977).
Ma72 F. Manero and V. Konshin, At. En. Rev. 10, 637 (1972).
Ma77 D. Madland, LA-7066-PR, p. 12 (1977).
Ma78 D. G. Madland and P. G. Young, LA-7533-MS (1978).
Mu73 S. Mughabghab and D. Garber, BNL-325, 7th Ed., Vol. 1 (1973).
Re71 H. Rebel and G. W. Schweimer, KFK-133 (1971).
Ry73 A. Rytz, At. Data and Nucl. Data Tables 12, #5, 479 (1973).
Sh76 R. Sher, S. Fiarman, and C. Beck, private communication (Oct. 1976).
Va74 R. Vaninbroukx, Euratom report EUR-5194E (1974).
Wi78 K. Wissak and F. Käppeler, Nucl. Sci. Eng. 66, 363 (1978).
Yo70 T. Young and S. Reeder, Nucl. Sci. Eng. 40, 389 (1970).
Yo71 T. Young et al., Nucl. Sci. Eng. 43, 341 (1971).

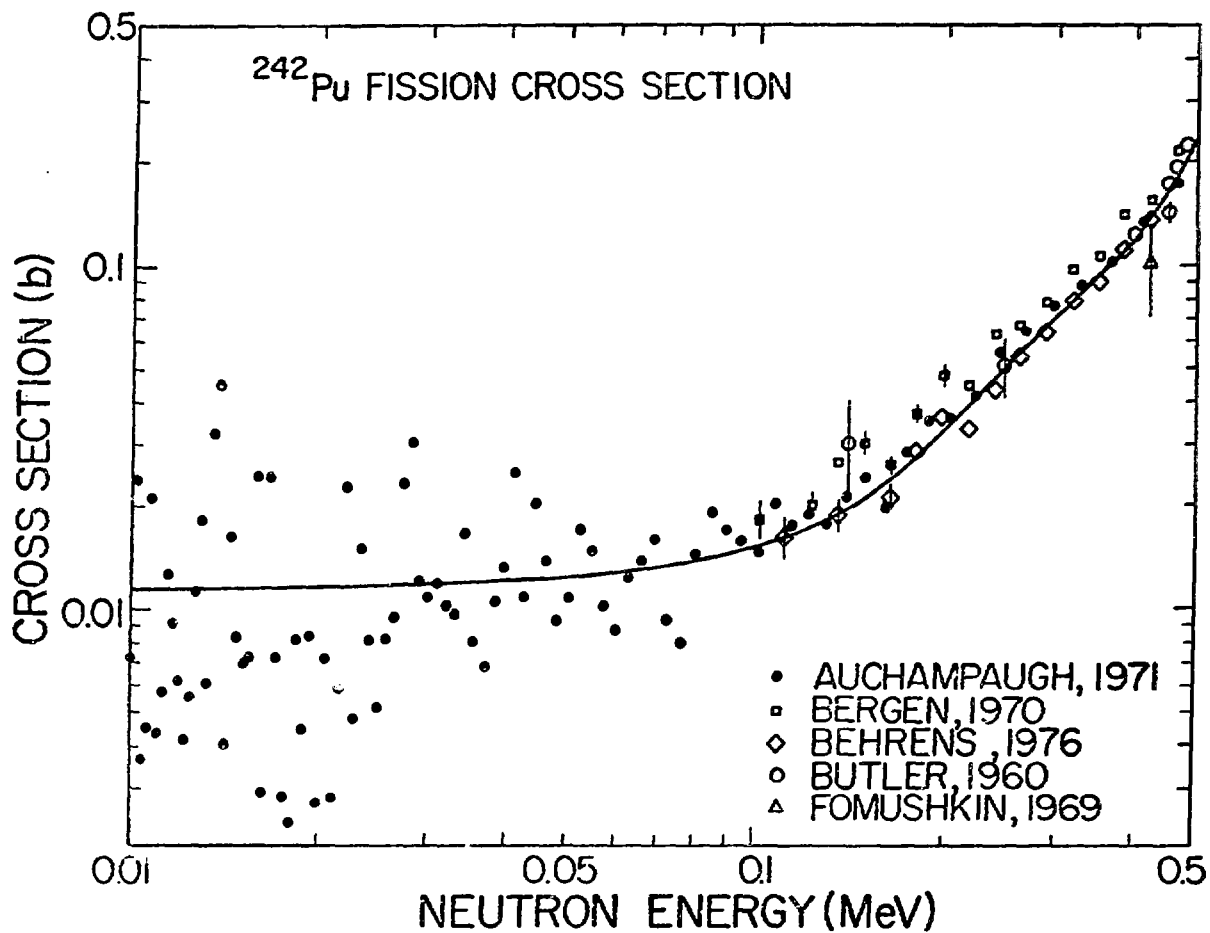


Fig. 1.

Experimental and evaluated cross sections for the $^{242}\text{Pu}(n,f)$ reaction from 10 keV to 0.5 MeV. The evaluated curve is based upon the Auchampaugh (Au71) and Behrens (Be76) ratio measurements relative to the $^{235}\text{U}(n,f)$ reaction. The values shown here were converted using a preliminary evaluation of the $^{235}\text{U}(n,f)$ cross section and will be adjusted by up to 4% in the final evaluation.

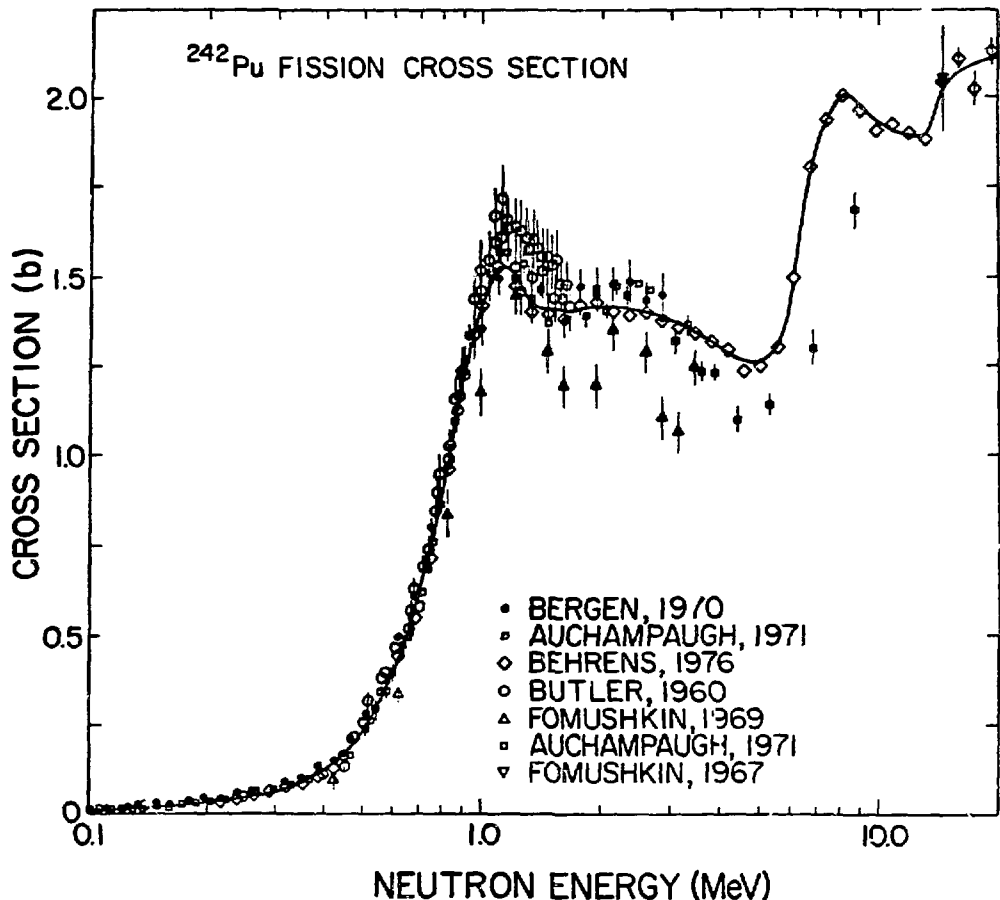


Fig. 2.

Experimental and evaluated cross sections for the $^{242}\text{Pu}(n,f)$ reaction from 0.1 to 20 MeV. See caption for Fig. 1.

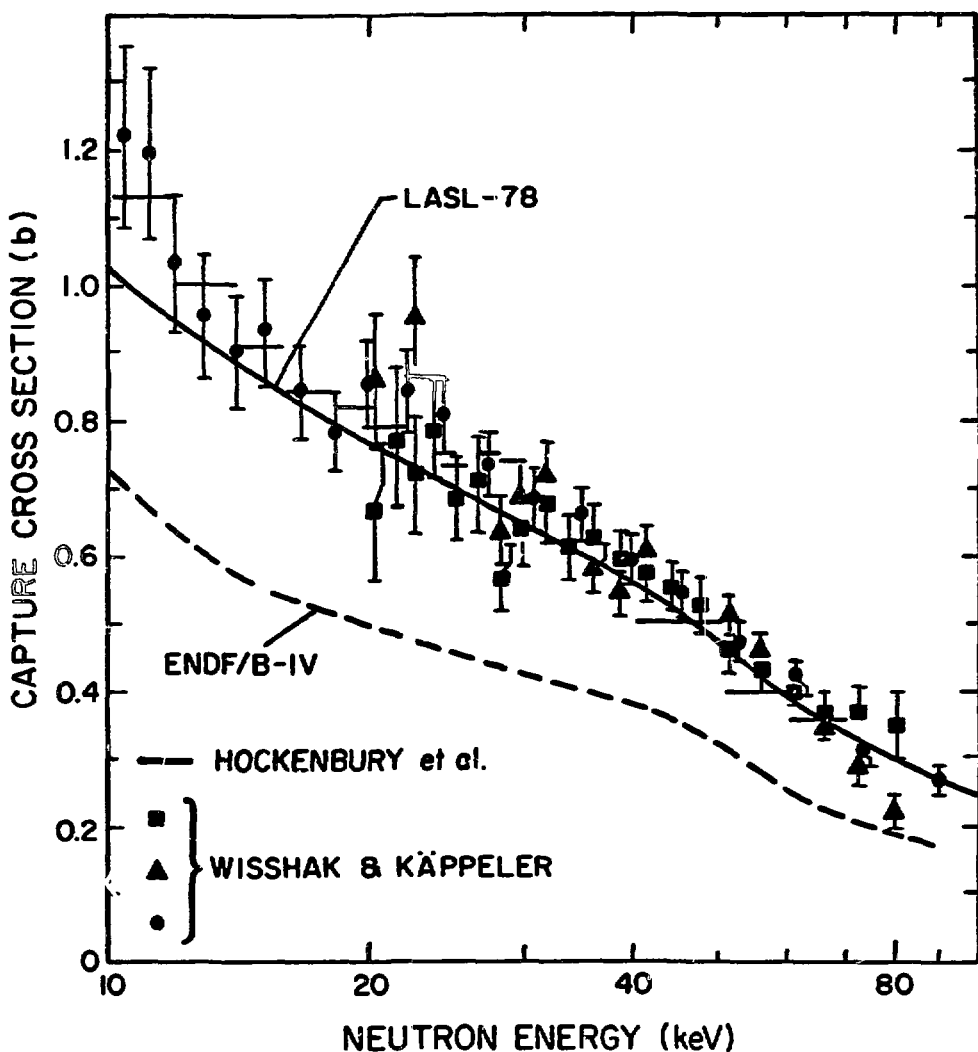


Fig. 3.

Experimental and evaluated cross section for the $^{242}\text{Pu}(n,\gamma)$ reaction between 10 and 100 keV. The experimental data are from Hockenbury (Ho75) and Wissak and Käppeler (Wi78).

APPENDIX B

**Summary Documentation of LASL Covariance
Data Evaluations for ENDF/B-V**

CROSS SECTION COVARIANCES FOR $^1_{\text{H}}$

by

D. G. Foster, Jr. and P. G. Young

I. Data Summary

Covariance data are included in MF = 33 for MT = 1, 2, and 102 of the $^1_{\text{H}}$ evaluation for the full energy range of 10^{-5} eV to 20 MeV. The covariances are developed mainly from two basic components: (1) a short range or locally correlated component resulting from statistical or localized errors in measurements, and (2) longer range correlated components resulting from systematic errors in the measurements used, or from the analysis procedure itself.

Covariance data are not provided for gamma-ray production data (MF = 12, 14) or for neutron angular distributions (MF = 4).

II. Methodology

a. MT = 2

The MT = 2 cross section is based upon a phase shift analysis of a large body of experimental data. The evaluated covariances are based upon quoted errors in the experimental data base, assuming a relatively high degree of correlation with energy due to the theoretical analysis. The standard deviations in the file range from 0.5 to 1%.

b. MT = 102

The MT = 102 cross section is based upon a very accurate thermal measurement, a 14-MeV measurement, numerous deuteron photodisintegration measurements, and a theoretical treatment of deuteron photodisintegration. Error estimates were based upon quoted standard deviations from the experimental measurements, which ranged from $\pm 0.6\%$ at thermal to $\pm 9\%$ near 20 MeV. Strong correlations with energy were assumed because of the use of a theoretical model to represent the experiments over most of the energy range. The covariances included in the file should be regarded as conservative since the use of deuteron photodisintegration theory probably reduces the uncertainty from the experimental values.

c. $MT = 1$

The $MT = 1$ covariances are given implicitly (NC-type subsection) over the entire energy range as derived from the sum of $MT = 2$ and $MT = 102$.

d. Correlations Across Reaction Types

Derivation of $MT = 1$ from $MT = 2$ and 102 leads to correlations of the type $MT = 1; MT1 = 2, 102$ over the entire energy range. These correlations are given implicitly in an NC-type subsection.

CROSS SECTION COVARIANCES FOR ${}^6\text{Li}$

by

G. M. Hale

I. Data Summary

Cross-section covariances intended for use at energies below 1 MeV have been supplied with the Version V ENDF/B evaluation for the reactions important at those energies. Specifically, File 33 data are given for the total, elastic and (n,t) cross sections (MF = 3; MT = 1, 2, and 105) for incident neutron energies between 10^{-5} eV and 20 MeV, although the values in the 1-20 MeV range are duplicates of those around 1 MeV, and are not intended for use. Covariances are not given at any energies for the neutron angular or energy distributions (MF = 4, 5), or for the gamma-ray production files (MF = 12, 14).

II. Methodology

The cross-section covariances are derived from covariances of the R-matrix parameters from which the evaluated cross sections are calculated, using first-order error propagation. The covariance between cross section X at energy E and cross section Y at energy E' is thus

$$\text{Cov} [X(E), Y(E')] = \sum_{ij} \frac{\partial X(E)}{\partial p_i} C_{ij} \frac{\partial Y(E')}{\partial p_j} \Big|_{p=\bar{p}} ,$$

where $\{p_i\}$ are the R-matrix parameters and C is the matrix of their covariances,

$$C_{ij} = \langle (p_i - \bar{p}_i)(p_j - \bar{p}_j) \rangle ,$$

which is known from the curvature of the χ^2 surface in the vicinity of the local minimum occurring at $p = \bar{p}$.

The relative covariances are entered directly (using the LB = 5 representation) in bins centered on a 15-point grid of energies between 0.1 and 1000 keV. For compactness, the relative covariances of the total cross section (MT = 1) are entered as NC-type sub-subsections, implying that they are to be constructed from those for the (n,n) (MT = 2) and (n,t) (MT = 105) reactions. This particular choice of "derived" cross section was necessary in order to avoid severe loss-of-significance problems in the derived covariances at low energies where $\sigma_T \approx \sigma_{n,t}$.

CROSS SECTION COVARIANCES FOR ^{10}B

by

G. M. Hale

I. Data Summary

Relative cross-section covariances are given for the total, elastic, (n,α_0) and (n,α_1) reactions (MF = 3; MT = 1, 2, 780, and 781), as well as for the total (n,α) reaction (MT = 107), for incident neutron energies between 10^{-5} and 1 MeV. Above 1 MeV, the covariances are set equal to zero, and are not intended for use. Covariances are not given at any energies for the neutron angular or energy distributions (MF = 4,5), or for the gamma-ray production files (MF = 12, 14).

II. Methodology

Cross-section covariances are derived from covariances of the R-matrix parameters from which the evaluated cross sections are calculated, using first-order propagation. The covariance between cross section X at energy E and cross section Y at energy E' is thus

$$\text{Cov} [X(E), Y(E')] = \sum_{ij} \frac{\partial X(E)}{\partial p_i} C_{ij} \frac{\partial Y(E')}{\partial p_j} \Big|_{p=\bar{p}} ,$$

where $\{p_i\}$ are the R-matrix parameters and C is the matrix of their covariances,

$$C_{ij} = \langle (p_i - \bar{p})(p_j - \bar{p}) \rangle ,$$

which is known from the curvature of the χ^2 surface in the vicinity of the local minimum occurring at $p = \bar{p}$.

The relative covariances are entered directly (using the LB = 5 representation) in bins centered on a 12-point grid of energies between 0.20 and 0.95 MeV. For compactness, the relative covariances of the tot. l cross section (MT = 1) and of the total (n,α) cross section (MT = 107) are entered as NC-type sub-subsections. The covariances for MT = 1 are thus constructed from those for MT = 2, 780, and 781, and those for MT = 107 are constructed from those for MT = 780 and 781. Choosing the total (MT = 1) as a "derived" cross section was necessary in order to avoid severe loss-of-significance problems in the derived covariances at low energies where $\sigma_T \approx \sigma_{n,\alpha_0} + \sigma_{n,\alpha_1}$.

CROSS SECTION COVARIANCES FOR ^{14}N

by

P. G. Young and D. G. Foster, Jr.

I. Data Summary

Covariance data are included in MF = 33 for MT = 1, 2, 4, 102, 103, and 107 of the ^{14}N evaluation for the full energy range of 10^{-5} eV to 20 MeV. In all instances, the covariances are developed from two basic components: (1) a short range or locally correlated component resulting from statistical or localized errors in measurements or knowledge of structure, and (2) longer range correlated components resulting from systematic errors in the measurements used, or from the analysis procedure itself.

Covariance data are not provided for MT = 51-82, 104, 105, 700-704, 720-723, 740-741, and 780-790, although discrete cross sections are given for these reactions in MF = 3. Similarly, there are no covariances for gamma-ray production data (MF = 12-15) or for angular and energy distributions (MF = 4,5).

II. Methodology

a. MT = 1

The total cross-section analysis was divided into three energy regions: below 10 keV, 10-500 keV, and 0.5-20 MeV. Both the low and high energy regions are based upon relatively few measurements. The data in the intermediate region is a composite of many measurements, and the normalization is influenced by the analysis in both the low and high energy regions. The covariances for the total cross section were estimated from the normalizations and shape adjustments that were required to bring the various measurements into agreement. The correlations with energy were estimated from the systematic errors in the measurements used for the three energy ranges. Weak linking correlations were assumed for the analyses in all three energy regions.

b. MT = 102, 103, and 107

Variances were obtained by roughly constructing $\pm 2\sigma$ curves bounding the experimental data. Correlations with energy were based upon estimates

of systematic errors in the measurements used for the evaluation. Near thresholds, progressively larger (fractional) uncertainties were assumed. Estimates of the covariances are probably poorest near the thresholds and where the cross sections are smallest, that is, where the variances are largest.

c. MT = 2, 4

Covariances for MT = 4 at energies below 10 MeV and for MT = 2 above 10 MeV were estimated as described above in Section II.b. In the case of MT = 4, uncertainties in the individual discrete inelastic reactions were combined to obtain the covariances.

The MT = 2 cross section was derived below 10 MeV by subtraction of the nonelastic from the total, and MT = 4 was similarly constructed above 10 MeV from the total, elastic, and reaction cross sections. This information was used to derive the MT = 2 covariances below 10 MeV and the MT = 4 covariances above 10 MeV, and these data are given explicitly in MF = 33. That is, the option to use NC-type subsections to represent derived quantities was not used.

d. Correlations Across Reaction Types

Below $E_n = 1$ keV, the MT = 1 and 2 cross sections were obtained by fitting the MT = 1 measurements with a constant plus $1/v$ expression, to represent elastic scattering and capture reactions (MT = 102, 103), respectively. The resulting correlations between MT = 1 and MT1 = 2, 102, 103 are given explicitly in the file. Similarly, the derivation of MT = 2 from the other reactions from 1 keV to 10 MeV leads to correlations between MT = 2 and MT1 = 1, 4, 102, 103, 107, and the derivation of MT = 4 above 10 MeV leads to correlations of the type MT = 4, MT1 = 1, 2, 102, 103, 107 from 10 to 20 MeV. These correlations are also given explicitly in the file, that is, NC-type subsections are not used to represent the derived quantities. Explicit representation of the derived covariances required extensive use of LB = 3 in the NI-type subsections.

CROSS SECTION COVARIANCES FOR ^{16}O

by

P. G. Young and D. G. Foster, Jr.

I. Data Summary

Covariance data are included in MF = 33 for MT = 1, 2, 4, 103, and 107 of the ^{16}O evaluation for the full energy range of 10^{-5} eV to 20 MeV. In all instances, the covariances are developed from two basic components: (1) a short range or locally correlated component resulting from statistical or localized errors in measurements or knowledge of structure, and (2) longer range correlated components resulting from systematic errors in the measurements used, or from the analysis procedure itself.

Covariance data are not provided for MT = 51-89, 102, 104, and 780-783, although discrete cross sections are given for these reactions in MF = 3. Similarly, there are no covariances for gamma-ray production data (MF = 12-14) or for angular and energy distributions (MF = 4,5).

II. Methodology

a. $E_n < 6$ MeV

In this energy range the evaluation of MT = 1, 2, 107 was based upon a coupled-channel R-matrix analysis of a composite of experimental data. Covariances were estimated from the normalizations and shape adjustments required to bring the various measurements into agreement, quoted errors for the experimental data, and estimates of the correlations introduced by the R-matrix analysis itself.

b. $E_n = 6-20$ MeV

1. MT = 1

The evaluated cross section in this region is based upon a composite of several measurements. Covariances were estimated from the normalizations and shape adjustments that were required to bring the various measurements into agreement. A weak, linking correlation with the energy region below 6 MeV was assumed.

2. MT = 103, 107

Variances were obtained by roughly constructing $\pm 2\sigma$ curves bounding the experimental data. Correlations with energy were based upon estimates of systematic errors in the measurements used for the evaluation. Near thresholds, progressively larger (fractional) uncertainties were assumed. Estimates of the covariances are probably poorest near the thresholds and where the cross sections are smallest, that is, where the variances are largest.

3. MT = 2,4

At energies below 13 MeV for MT = 4 and above 13 MeV for MT = 2, covariances were estimated as described in Sec. II.b.2. In the case of MT = 4, uncertainties in the individual discrete inelastic reactions were combined to obtain the covariances.

The MT = 2 cross section was derived below 13 MeV by subtraction of the nonelastic from the total, and MT = 4 was derived above 13 MeV from the total, elastic, and reaction cross sections. This information was used to derive the MT = 2 covariances below 13 MeV and the MT = 4 covariances above 13 MeV. These data are given explicitly in MF = 33, that is, the option to use NC-type subsections to represent derived quantities was not used.

c. Correlations Across Reaction Types

Derivation of the elastic cross section from the other reactions below 13 MeV leads to correlations of the type MT = 2; MT1 = 1, 4, 103, 107. Similarly, derivation of MT = 4 above 13 MeV results in correlations of the type MT = 4; MT1 = 1, 2, 103, 107. These correlations are also given explicitly in the file, that is, NC-type subsections are not used to represent the derived quantities. Explicit representation of the derived covariances required extensive use of LB = 3 in the NI-type subsections.

CROSS SECTION COVARIANCES FOR ^{27}Al

by

D. G. Foster, Jr. and D. W. Muir

I. Data Summary

Covariance data are included in MF = 33 for MT = 1, 2, 4, 16, 102, 103, and 107 of the ^{27}Al evaluation for the full energy range of 10^{-5} eV to 20 MeV. In all instances, the covariances are developed from two basic components: (1) a short range or locally correlated component resulting from statistical or localized errors in measurements or knowledge of structure, and (2) longer range correlated components resulting from systematic errors in the measurements used, or from the analysis procedure itself.

Covariance data are not provided for MT = 51-90, 104, and 105, although discrete cross sections are given for these reactions in MF = 3. Similarly, there are no covariances for gamma-ray production data (MF = 12-15) or for neutron angular and energy distributions (MF = 4,5).

II. Methodology

a. MT = 1

Diagonal elements of the covariance matrix are taken from running fits to the cross section data (single- or double-peaked Breit-Wigner shapes in the structured region and polynomial fits in the smooth regions). Correlations in the errors reflect: (1) dependence on particular time-of-flight measurements over broad ranges of energy; (2) energy-dependent normalization of the Columbia measurements to join smoothly to other measurements below 4.6 keV and above 189 keV; and, (3) correlations induced by the $1/v$ fit below 4.6 keV.

b. MT = 16, 102, 103, 107

Variances were estimated from dispersion of the experimental data and from quoted experimental errors. Correlations with energy were based upon estimates of systematic errors in the measurements used for the evaluation. Near thresholds, progressively larger (fractional) uncertainties were assumed. Es-

timates of the covariances are probably poorest near the thresholds and where the cross sections are smallest, that is, where the variances are largest.

c. $MT = 2$

From 10^{-5} eV to 9 MeV, the $MT = 2$ covariances are represented as derived from the other reaction types, using NC-type sub-subsections with $LYT = 0$. Similarly, from 17 to 20 MeV the covariances are derived from $MT = 1$. In the energy range 9 to 17 MeV, the covariances were obtained as described in Sec. II.b.

d. $MT = 4$

From threshold to 9 MeV, the $MT = 4$ covariances were obtained as described in Sec. II.b. From 9 to 20 MeV, the covariances are represented as derived from the other reaction types, using NC-type sub-subsections with $LYT = 0$.

e. Correlations Across Reaction Types

The derivation of $MT = 2$ from the other reactions below 9 MeV leads to correlations of the type $MT = 2$; $MT1 = 1, 4, 102, 103, 107$. Similarly, the derivation of $MT = 4$ above 9 MeV results in correlations of the type $MT = 4$; $MT1 = 1, 2, 16, 102, 103, 107$. Finally, correlations of the type $MT = 1$; $MT1 = 2$ occur from 17 to 20 MeV. In all cases, the correlations are given implicitly through use of NC-type, $LYT = 0$ sub-subsections.